THE INFLUENCE OF HUMAN UMBILICAL VEIN ENDOTHELIAL CELLS IN THE FORMATION OF GLIOBLASTOMA SPHEROIDS IN THREE-DIMENSIONAL MICROWELLS

A Dissertation

Presented to

the Faculty of the Department of Biomedical Engineering

University of Houston

In Partial Fulfillment

of the Requirements for the Degree

Doctor of Philosophy

in Biomedical Engineering

by

Naze Gul Avci

August 2015

THE INFLUENCE OF HUMAN UMBILICAL VEIN ENDOTHELIAL CELLS

IN THE FORMATION OF GLIOBLASTOMA SPHEROIDS

IN THREE-DIMENSIONAL MICROWELLS

Naze Gul Avci

Approved:

Chair Of The Committee
Dr. Metin Akay, Professor,
Biomedical Engineering Department

Committee Members:

Dr. Yasemin M Akay, Assistant Professor,
Biomedical Engineering Department

Dr. Ahmet Omurtag, Associate Professor,
Biomedical Engineering Department

Dr. Ting Chen, Assistant Professor,
Biomedical Engineering Department

Dr. David Gorenstein, Professor,
Department of NanoMedicine and
Biomedical Engineering
The University of Texas

Dr. Suresh K. Khator,
Associate Dean,
Cullen College of Engineering

Dr. Metin Akay, Founding Chair,
John S. Dunn Cullen Endowed Professor,
Department of Biomedical Engineering

Acknowledgements

I would like to thank my advisor Dr. Metin Akay for giving me the opportunity to work in his laboratory. I would like to offer my sincere thanks to Dr. Yasemin Akay for her kind help during my research. I am grateful for their guidance, confidence and support they have provided me during my studies at University of Houston.

I would like to express my appreciation to Dr. David Gorenstein, Dr. Ahmet Omurtag, and Dr. Ting Chen, for serving as my committee members. I would like also to thank our lab members Dr. Andrei Dragomir and Dr. Yantao Fan, for their helpful scientific discussion, and advise to improve my research. I wish to express my warm thanks to my lab mates Leon Duong Nguyen and especially Renee Keller for her help with the language of my dissertation. It has been a pleasure to work with you.

I would like to express my sincere gratitude to Dr. Tianfu Wu for his valuable support and guidance while I was a TA of his class. It has been an honor for me to work with you. I would like to acknowledge the assistance of Dr. Juan Fueyo and Dr. Candelaria Gomez-Manzano for the experimental training while I was a graduate student intern in Neuro-Oncology Department at The University of Texas MD Anderson Cancer Center.

My most sincere thanks go to Hasan Onur Keles. You have been a great support and you were always there when I needed it. Always stay around Dr. HOK! Additionally, to all my friends that I have met along the way in Houston for all the fun trips and good times, especially my old lab mate and roommate Pinar Kanlikilicer Unaldi. Thank you for your friendship.

Last but not least, I owe my deepest gratitude to my best friends and my family. Words cannot express how grateful I am to have you. To Merve Oney and Ozberk Saygun, my closest and dearest friends since forever. I know you are always there for me no matter what. To Kaan Saadetlioglu, for his never-ending encouragement, patience and love during the most stressful times of my life for all these years. To my brother, Can Avci and my sister, Ipek Kocoglu for always being there for me and kept me laughing through the hardest time. You are my only ones, without you I would be lost. To my parents; my mother, Gamze Gul Avci and my father, Resat Avci, I know you always believe in me. You are the best parents I could ever image. I will always treasure your never-ending trust, support and love. My grandmother, Sureyya Hepgul, thank you for constantly loving me as your own daughter, and dedicating your life to your grandchildren. I am so lucky to have you and I would not be where I am today without you! If this work has sometimes prevented us from sharing important moments of life, know that I never stopped thinking about you. I dedicated my dissertation work to you.

THE INFLUENCE OF HUMAN UMBILICAL VEIN ENDOTHELIAL CELLS IN THE FORMATION OF GLIOBLASTOMA SPHEROIDS IN THREE-DIMENSIONAL MICROWELLS

An Abstract

of a

Dissertation

Presented to

the Faculty of the Department of Biomedical Engineering

University of Houston

In Partial Fulfillment

of the Requirements for the Degree

Doctor of Philosophy

in Biomedical Engineering

by

Naze Gul Avci

August 2015

Abstract

Glioblastoma multiforme (GBM) is the most malignant primary brain tumor with a high infiltrative capacity and increased vascularity. Despite current therapies overall patient survival rate is still poor. Therefore, alternative therapies have been considered for GBM treatment such as oncolytic viruses (OVs).

The studies with two-dimensional (2D) cell cultures have been used as physiological models for understanding the cellular and molecular behavior of the GBM tumors. They are also highly desirable for virus studies. However they may not provide three-dimensional (3D) characteristics of the tumors. Therefore, there is an increasing need in 3D cell culture models to investigate cell growth and cell-cell interactions.

In this thesis, we hypothesized that culturing GBM cells with endothelial cells in the hydrogel microwells would mimic the *in vivo* microenvironment of tumor cells. Thus, we could provide beneficial 3D *in vitro* co-culture models for GBM treatment with oncolytic adenovirus, Delta-24-RGD (Δ24RGD). Therefore, in the first part of this study, we used our recently designed 3D PEGDA hydrogel microwell platform to co-culture GBM and HUVEC. We investigated the gene expression differences to gain further insight into molecular mechanism of 3D *in vitro* co-culture. Our gene expression data suggested the relative up-regulation of tumor angiogenesis markers PECAM-1/CD31 and VEGFR2, in co-cultures. Finally, we treated GBM tumors using Δ24RGD. Our results showed a significant cell lysis in 3D spheroids. The cell viability was decreased approximately 37%, 54% and 65% with 10, 50 and 100 MOIs, respectively. The infection of the Δ24RGD was found more effective on 3D spheroids when compared to 2D monolayer cell culture. These results implicate that our hydrogel microwell platform could

contribute to mimic *in vivo* microenvironment of the GBM tumors and provide a promising 3D model to investigate the oncolytic potential of the viruses *in vitro*.

Table Of Contents

List Of Figures

List Of Tables

List Of Abbreviations

Ad	Adenovirus
Ad5	Adenovirus class C serotype 5
Ad-Δ24	Adenovirus Delta 24
ANOVA	Analysis Of Variance
ATCC	American Type Culture Collection
BBB	Blood–Brain Barrier
bFGF	Basic Fibroblast Growth Factor
bp	Base pair
Δ24RGD	Delta-24-RGD
ΔE1	E1-deleted adenovirus
E1A	Early 1 A
CAD	Computer-Aided Design
CAM	Cell-Adhesion Molecule
CAR	Coxsackie adenovirus receptor
CBTRUS	Central Brain Tumor Registry Of The United States
cDNA	Complementary Dna
CNS	Central Nervous System
Ct	Cycle Threshold
DAPI	6-Diamidino-2-Phenylindole
DMEM	Dulbecco's Modified Eagle Medium
DTT	Dithiothreitol
DUV	Deep Ultraviolet
EB	Embryoid Bodies
ES	Embryonic Stem Cell
EC	Endothelial Cell
ECM	Extracellular Matrix
EGF	Epidermal Growth Factor
EGFR	Epidermal Growth Factor Receptor
EGM-2	Endothelial Cell Medium

FBS	Fetal Bovine Serum
FDA	Food And Drug Administration
FGF	Fibroblast Growth Factor
GAPDH	Glyceraldehyde 3-Phosphate Dehydrogenase
GBM	Glioblastoma
GelMA	Gelatin Methacrylate
GFP	Green Fluorescence Protein
GIC	Glioma-Initiating Cells
HA	Hyaluronic Acid
HIF-1	Hypoxia-Inducible Factor 1
HUVEC	Human Umbilical Vein Endothelial Cells
Kbp	Kilo-base pair
MGMT	O6- Methylguanine-DNA Methyltransferase
MOI	Multiplicity of infection
MW	Molecular Weight
NaOH	Sodium Hydroxide
OD	Optical Density
OV	Oncolyic viruses
PBS	Phosphate Buffered Saline
PDGF	Platelet-Derived Growth Factor
PDMS	Polydimethylsiloxane
PECAM-1/CD31	Platelet Endothelial Cell Adhesion Molecule 1
PEG	Poly (Ethylene Glycol)
PEGDA	Poly (Ethylene Glycol) Diacrylate
PEGDMA	Poly (Ethylene Glycol) Dimethacrylate
Pfu	Plaque forming units

PGA	Polyglycolide
PI	Photoinitiator
PI3K	Phosphatidylinositol 3-Kinase
PIK3R1	Phosphatidylinositol 3-Kinase Regulatory Subunit Alpha
PMMA	Polymethylmethacrylate
PLG	Poly (L-Lactide-Co-Glycolide)
PTEN	Phosphatase And Tensin Homolog Deleted On Chromosome 10
Rem	Replica Molding
Rb	Retinoblastoma
Rpm	Revolutions Per Minute
RTKS	Receptor Tyrosine Kinases
RTOG	Radiation Therapy Oncology Group
TBS	Tris-buffered saline
TKIS	Tyrosine Kinase Inhibitors
TMSPMA	3-(Trimethoxysilyl)Propyl Methacrylate
TMZ	Temozolomide
qPCR	Quantitative Real Time Polymerase Chain Reaction
UV	Ultraviolet
VEGF	Vascular Endothelial Growth Factor
VEGFR2	Vascular Endothelial Growth Factor Receptor 2
WHO	World Health Organization
µcp	Microcontact Printing
µflp	Microfluidic Patterning
2D	Two-Dimensional
3D	Three-Dimensional

Chapter 1. Background information and significance

1.1. Glioblastoma

A glioma, a type of tumor that arises from glial cells is mostly found in the brain or spine and accounts for approximately 30% of all brain and central nervous system tumors and 80% of all malignant brain tumors [1, 2]. It includes astrocytoma, glioblastoma multiforme (GBM), oligodendroglioma, ependymoma, mixed glioma such as oligoastrocytomas and a few more rare histologies [3] (**Figure 1.1**).

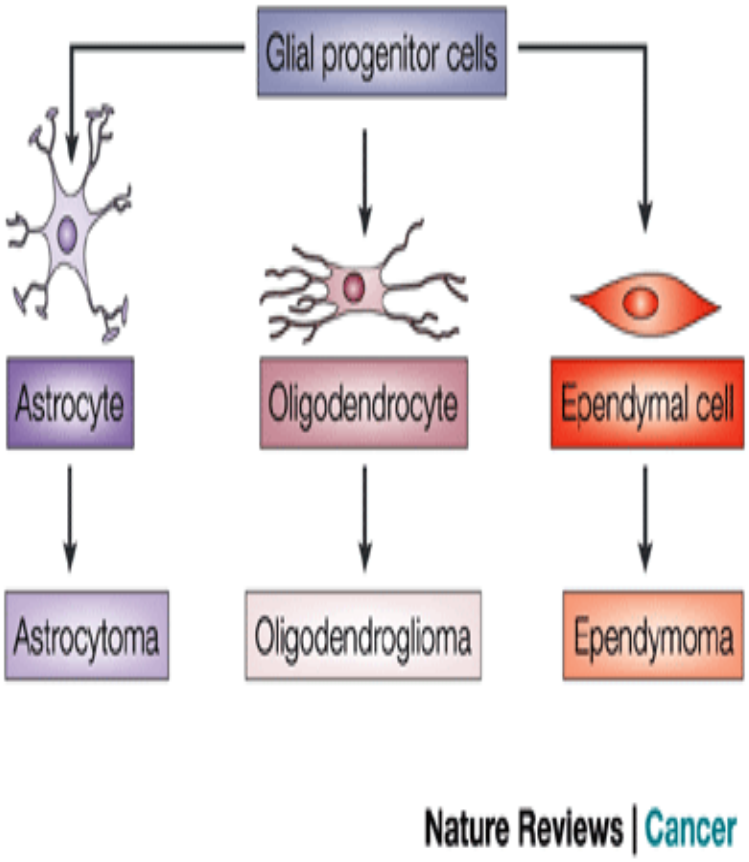

Figure 1. 1. Schematic classification of gliomas. Glial cells from the central nervous system constitute several cell types that arise to several tumor types classified as gliomas [4].

The World Health Organization (WHO) classifies the different types of gliomas based on a malignancy scale ranging from I to IV [5, 6]. Astrocytomas are categorized into four grades, which show higher lethality with a higher grade. Grade I is known as pilocytic astrocytoma, Grade II as low-grade astrocytoma, Grade III as anaplastic astrocytoma and Grade IV as glioblastoma multiforme [7]. A WHO Grade IV GBM tumor is specifically characterized by increased cellularity and mitotic activity, distinct nuclear atypia and vascular proliferation [5, 8].

GBM occurs with an incidence of 5 in 100,000 and constitutes more than 50 % of all gliomas [9, 10]. It is the most aggressive and invasive tumor among all brain tumors and is characterized by high mortality rates [11].

It is estimated there are annually 9000 new cases of GBM cancer diagnosed in the United States, with a median survival rate of 12-15 months and a 5-year relative survival rate of only 34% [12, 13]. GBM tumors may occur at any age, but advanced age is an important factor that affects the survival. A study led by the Radiation Therapy Oncology Group (RTOG) presented that median survival of GBM patients with an age 60 or older was 7.5 months while it was 16.2 months in patients younger than 40 years old [14]. However, it remains unclear whether age is a negative prognostic factor in patients or not [15].

Patients with a GBM tumor may have different symptoms such as headaches caused by an increase in intracranial pressure due to the growth of the tumor, as well as nausea and vomiting. Patients may also suffer from seizures, impaired vision, confusion, memory loss, and even in some cases personality changes [12].

Current therapies often involve treating GBM tumors via surgical removal followed by radiotherapy and/or chemotherapy to kill malignant cells that may have survived the surgery and to treat any metastasis that may have occurred [16]. Radiation used in clinical practice is low energy transfer ionizing radiation to defeat cancer cells by indirect damage of the free radicals at a specific site [17]. However, GBM patients who receive radiotherapy may experience neurological side effects that are often impossible to determine whether they are caused by radiotherapy [18].

For effective targeting, chemotherapy drugs should have low molecular weight (MW < 500 Da), lipophilic features, and low protein binding capacity to effectively cross the blood brain barrier [19]. Drugs primarily used in the treatment of GBM are Temozolomide (TMZ), CPT-11 (ironotecan), bis-chloroethyl-nitrosurea (BCNU) [20]. Currently, TMZ is the drug of choice following surgery and in combination with radiotherapy [21]. Methylation of DNA by TMZ was shown to induce the cytotoxicity of tumor cells, which leads to damage to the DNA of tumor cells [22]. The discovery of the role of O-6- methylguanine-DNA methyltransferase (MGMT) in GBM tumor resistance has improved patient survival [23]. MGMT is a DNA repair gene and studies showed that when MGMT was silenced, GBM patient survival was improved after treatment with TMZ compared to patients with active MGMT [24, 25]. Thus, poor treatment efficacy for GBM has been related to tumor cellular and genetic heterogeneity and limited delivery of therapy to the tumor site [26]. However, chemotherapy also has some disadvantages. Between treatments, it has been shown that there is re-growth of vascular endothelial cells that support the tumor growth, consequently resulting in more aggressive tumor resistance to the drugs [27]. Moreover, most chemotherapeutics are highly toxic and lack

specificity in the differentiation between normal and cancer cells, leading to side effects throughout the patient's body [27]. Therefore, current treatments do not significantly increase the poor prognosis [24, 25].

Glioblastoma can either be primary or secondary. Secondary GBM that is slowly developed from grade II astrocytoma or grade III anaplastic astrocytoma is mostly found in younger patients around age 40 and can be diagnosed using neuroimaging techniques and/or histological (bioptic) evidence [28].

However, the incidence of the GBMs to show de novo growth (primary GBM) without any previous symptoms increases with old ages [3]. Both primary and secondary GBMs are identical histologically, but they have different genetic and epigenetic profiles [29–31] that are considered hallmarks of GBM. Mutations of the tumor suppressor gene p53 on chromosome 9 play a role in poor response to therapy and occur with a high incidence in secondary GBMs [32]. In about one third of all GBMs, it was shown that the amplification of the epidermal growth factor receptor (EGFR) gene leads to increased cell proliferation in primary GBMs [33]. Also, the changes in the expression of tumor suppressor phosphatase and tensin homolog (PTEN) result in activation of the phosphatidylinositol 3-kinase (PI3K) survival pathway [34, 35]. All of these genetic alterations have different effects on cell protein expression and thus may result in tumor formation.

Pathologically, GBM tumors are also characterized by microvascular proliferation and necrosis, which cause them to be highly vascular tumors [36]. The mechanism that triggers the vascularity in most of the solid tumors is hypoxia, which induces the transcription factor hypoxia-inducible factor 1 (HIF-1). In hypoxic conditions, tumor

vascular system is unable to supply an adequate amount of oxygen, which consequently causes oxygen and nutrient deprivation in the tumor cells. This contributes to rapid and abnormal tumor growth [37]. HIF-1 overexpression regulates cell cycle arrest and activates expression of vascular endothelial growth factor (VEGF) [38], thus stimulating angiogenesis, the formation of the new blood vessels from pre-existing ones [39].

1.1.1. Angiogenesis in Glioblastoma Tumor

Angiogenesis, the development of new vessels from pre-existing blood vessels, involves endothelial cell (EC) proliferation, migration, and basement membrane degradation [40]. The process called 'angiogenic switch' coordinates the initiation of angiogenesis by promoting cell tumorigenicity, activating oncogenes and suppressing anti-oncogenes [41].

Nutrients and oxygen are provided to cells by blood vessels. Angiogenesis in GBM tumors is provoked when tumor tissues need more nutrients and oxygen. Several steps are involved in the angiogenesis. Dilation of the blood vessels starts the process. By the production of proteolytic enzymes, the extracellular matrix is degraded which causes hypoxia and promotes the migration of the endothelial cells. This allows for the differentiation of new vessels. When tumors start to exponentially grow, they cause the angiogenic switch that basically initiates angiogenesis by changing the balance between proangiogenic and antiangiogenic factors [41]. Tumor growth and metastasis depends on angiogenesis and is triggered by soluble angiogenic factors secreted from tumor cells such as VEGF, epidermal growth factor (EGF) and platelet-derived growth factor (PDGF) [42]. Finally, in the maturation stage, mesenchymal cells join to the vessel wall thus providing structural support [43]. Vessel destabilization, endothelial cell

proliferation and migration, tubular formation, and vessel maturation regulate angiogenesis. Soluble growth factors are key regulators of the process [44, 45] **(Figure 1.2).** Tumor blood vessels are composed of both endothelial cells and tumor cells, as shown in **Figure 1.2A** where green cells represent normal tumor cells; black cells represent necrotic tumor cells. Endothelial fenestrae make vessels semipermeable to soluble growth factors. Initially, avascular tumors can regulate the expression of angiogenic factors such as VEGF, FGF, or interleukin (IL)-8 as shown in **Figure 1.2B (i)** or they can develop on an existing blood vessel where it induces the expression of angiogenic factors as shown in **Figure 1.2B (ii)** [44, 46].

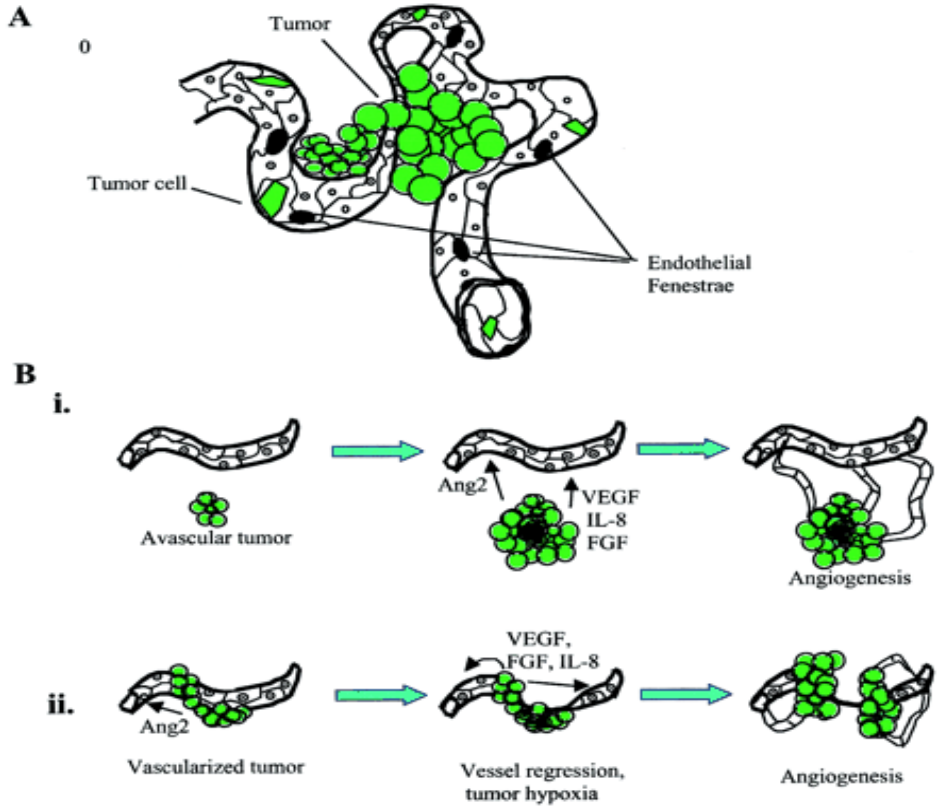

Figure 1. 2. Mechanism of tumor angiogenesis. (A) Schematic of tumor blood vessel. (B) Model of tumor-induced neovascularization [44].

Vascular endothelial growth factors (VEGF) and its homologues (VEGF-B, VEGF-C, VEGF-D and placental growth factor) are the main factors of vascular endothelial cell sprouting [47]. VEGFR1, VEGFR2, and VEGFR3 are receptor tyrosine kinases (RTKs) that are expressed on the surface of endothelial cells and bind to VEGFs. These RTKs play important roles in different physiological processes of VEGF on endothelial cells including proliferation, signal transduction and cellular functions [47–49].

VEGF signaling promotes GBM growth through its endothelial receptors VEGFR2 (also known as KDR/VEGFR2) and a number of pathways including PI3-Kinases [50], PTEN/pI3-kinase/Akt [51], EGF [52] and PDGF [53]. VEGF is stimulated mostly by hypoxia and found to be abnormally elevated. Thus it increases permeability in the tumor vasculature and causes the leaky vessels [54].

Besides VEGF, there are other pro-angiogenic growth factors that promote angiogenesis either in combination with VEGF or alone, such as angiopoietins, fibroblast growth factor (FGF) and EGF [55–57]. The mechanism of activation of angiogenesis is given in **Figure 1.3**. Under hypoxic conditions, VEGF and basic fibroblast growth factor (bFGF) expressions are upregulated by GBM and thus the transcription of VEGFR1 and VEGFR2 in endothelial cells is increased. The activation of VEGF also promotes the activation of the PDGF pathway [58].

1.2. Targeting Tumor Microenvironment

Previously, cancer had been believed to be a genetic disease with abnormal genetic alterations and malignant cells in tumors; consequently, primary anticancer strategies have been focused on targeting these malignant cells [59]. However, it is now indubitable

that tumors are also formed of numerous types of normal cells and extracellular matrix (ECM).

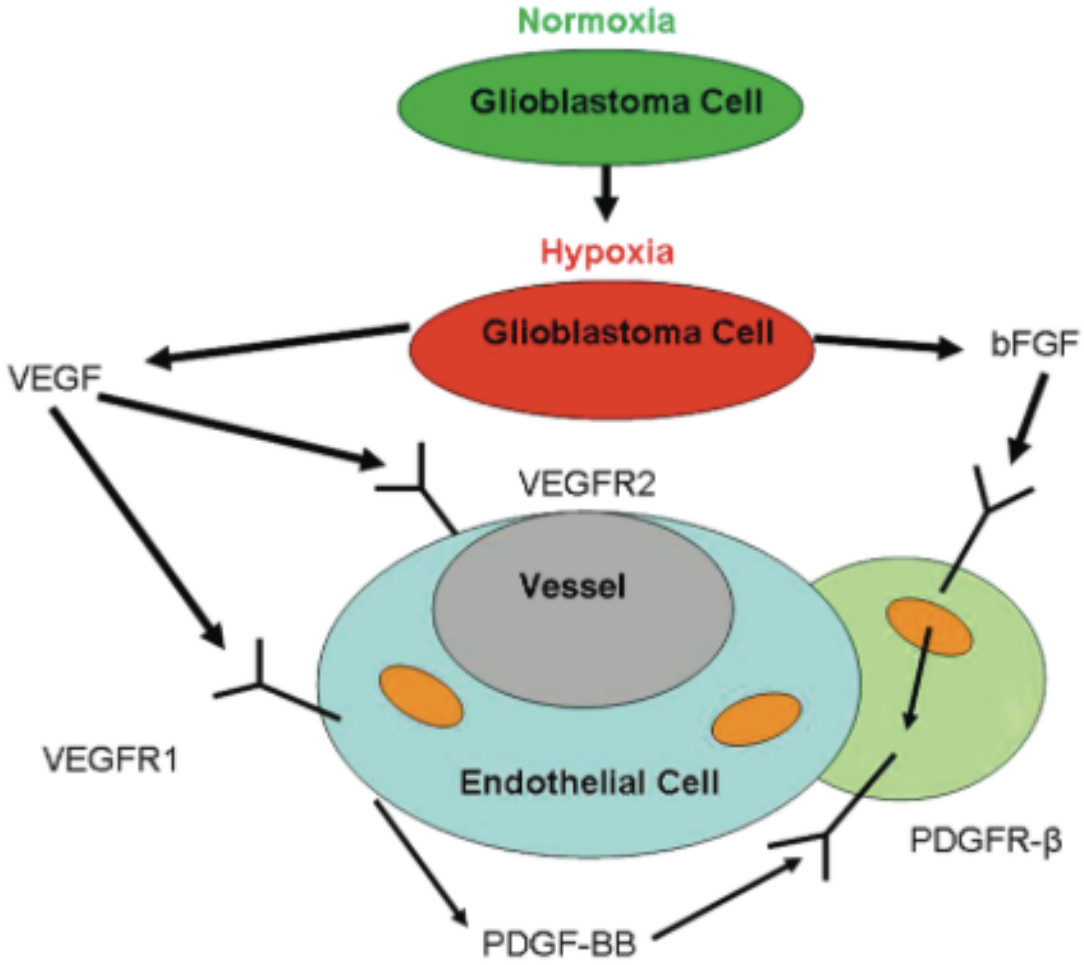

Figure 1. 3. Paracrine mechanism between glioblastoma and endothelial cells [58].

However, it is now indubitable that tumors are also formed of numerous types of normal cells and extracellular matrix (ECM). Interactions between cells and their microenvironment is crucial for both normal regulation of cellular behavior and for tumor growth through processes such as angiogenesis and immunosuppression [60, 61]. The complexity of the tumor microenvironment illustrated in **Figure 1.4** shows the importance of the microenvironment during tumorigenesis, which was originally

proposed by Joyce and Pollard [62]. Much attention has been placed on understanding the mechanisms that occur in the tumor microenvironment for tumor proliferation and tumorigenesis [63]. In particular, communication between tumor cells and the endothelial cells shows a tight relationship that influences tumor initiation and progression [64, 65].

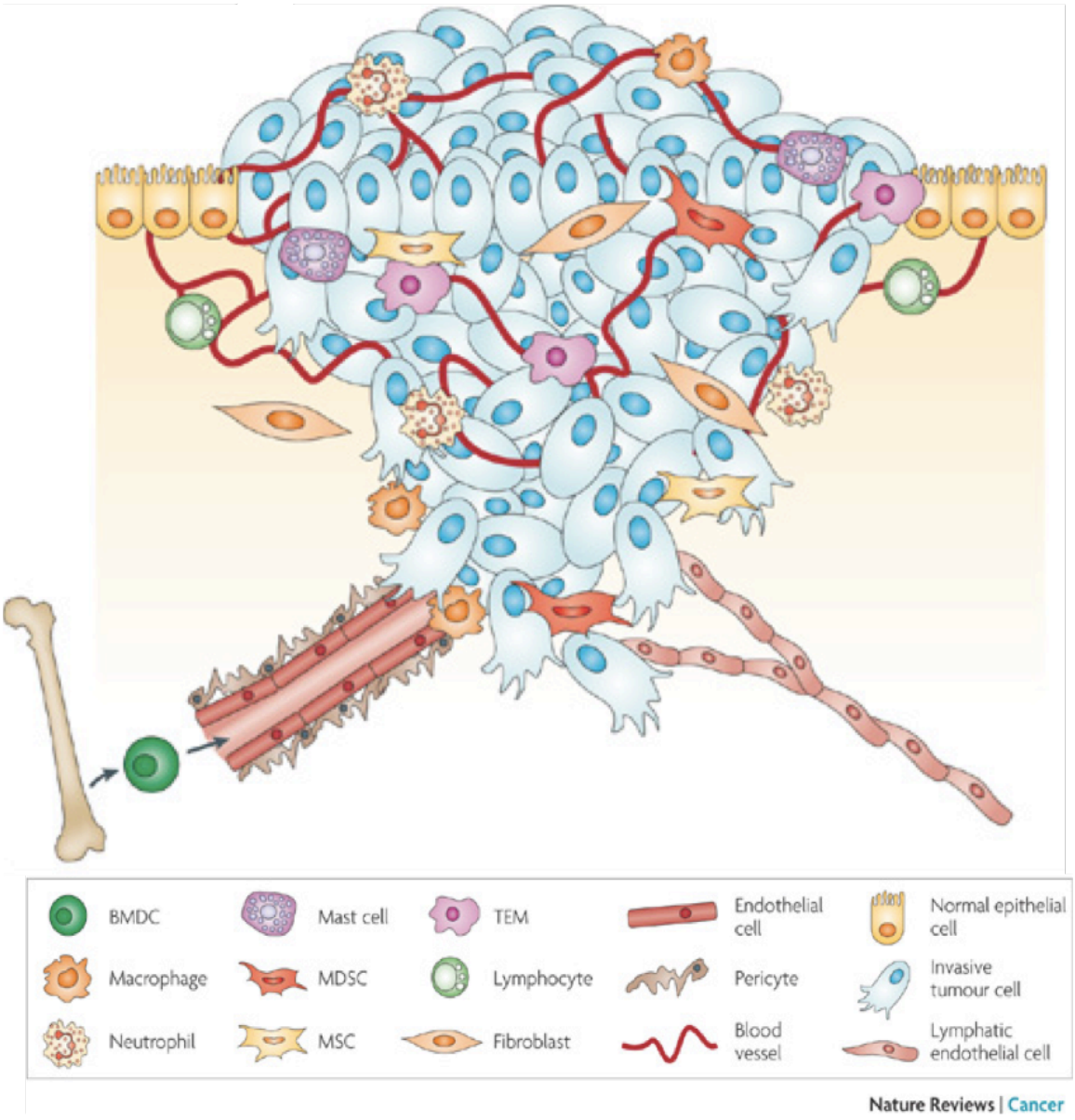

Figure 1. 4. Complex microenvironment of tumors cells including endothelial cells, stromal fibroblasts and a variety of bone marrow-derived cells [62].

It has been shown that endothelial cells can actively promote tumor initiation, progression, angiogenesis and affect the therapeutic response by providing the oxygen and nutrients for tumor survival [66–68]. Therefore, the experimental cancer models using tumor-associated endothelial cells to create *in vivo* like tumor microenvironment conditions have become attractive targets.

1.2.1. Endothelial Cells

The endothelium, viewed as inert cellophane-like membrane that maintains the permeability of the vessel-walls, has been shown to actually be a dynamic organ that controls vital secretory, metabolic and immunologic functions [69]. Despite the fact that ECs have been defined to have common functional and morphological characteristics, they also show notable heterogeneity in different organs. They may even present with significant heterogeneity in the same organ [70]. Researchers are still trying to solve the question of how ECs acquire different phenotypic and functional properties within the same organ. One hypothesis is that their interactions with surrounding cells through the release of soluble mediators and cell-to-cell adhesion can change their functions upon activation [70]. In the brain, ECs have continuous endothelium connected by tight junctions that control the flow of nutrient substances and help to maintain the blood-brain barrier [71]. They also regulate hemostasis, vascular growth, and the inflammatory response by cell-adhesion molecules (CAMs), expressed both on endothelial and blood cells [72].

Endothelial cells can acquire malignant properties and form tumors. Several studies showed that these cells proliferate faster than normal ECs [73, 74]. Currently, three hypotheses have been suggested about the development and origin of tumor ECs. The

first one states that tumor ECs can develop from normal ECs recruited into the tumor site and occurs as a result of angiogenic growth factors derived from the tumor [74]. The second hypothesis is that an endothelial progenitor cell, which has migrated to the tumor site and differentiated into vessels can cause the development of tumor ECs [74]. Due to some tumor-induced properties of the tumor ECs, it was also hypothesized that they might be developed from dedifferentiated tumor cells [74].

1.2.1.1. Endothelial Cell Markers

Endothelial cells derived from a variety of tumors express different markers compared to normal ECs. Several reports have shown ECs can be identified *in vivo* and *in vitro* by the specific markers that they express. Although, most of the markers have been found on both ECs and mature blood cells, some of them are induced and expressed only after activation by inflammatory cytokines or growth factors **(Table 1.1)**. As an example tumor EC lines derived from brain tumors express typical markers such as CD31 (also known as platelet endothelial cell adhesion molecule 1, PECAM-1) and VE-cadherin, which is a tight junction protein that controls the integrity of the blood–brain barrier (BBB), similarly to control ECs [75]. Studies showed that GBM-derived ECs have altered expressions of CD31 and VE-cadherins. Therefore, it has been suggested that decreased expression of these markers may provide a breakdown in tumor blood vessels [75, 76]. Charalambous and colleagues presented in their studies that in GBM-derived ECs, the distribution of CD31 was different. CD31 was present in the cytoplasm, whereas in control cells this receptor was predominantly expressed on the cell surface. This funding may show angiogenic mechanism by specific CD31 interactions between glial and endothelial cells [77].

Table 1. 1. Endothelial Markers present in human in all types of endothelium and Inducible EC Markers. Adapted by Garlanda and Dejana [70]

Endothelial Markers

	Cell Type[1]
PECAM-1/CD31	ECs, platelets, B and T lymphocyte subsets, monocytes, neutrophils [78]
Angiotensin-converting enzyme	ECs, epithelial cells, T lymphocytes [79]
Vascular endothelial cadherin	ECs [80]
CD34	ECs [81]

Inducible Endothelial Markers

	Cell Type	Stimulus
KDR/Flk-11 (VEGFR-2)	ECs	Neoangiogenesis, vascular tumors [82]
Flt-1 (VEGFR-1)	ECs	Neoangiogenesis [83]
Tie-1	ECs	Neoangiogenesis [84]
Tie-2/Tek	ECs	Neoangiogenesis [85]

[1] For some markers, tissue distribution analysis is incomplete; only the most common expression pattern has been considered.

1.2.2 Potential Targets for Anti-Angiogenic Therapy in Glioblastoma

Tumor endothelial cells have a specific proliferation characteristic compared to normal endothelial cells. Targeting tumor vessels to prevent new blood vessel formation and to deprive the tumor of oxygen and nutrients would be a specific approach for anticancer therapies since the tumor vasculature lead by angiogenesis is needed for tumor growth. Therefore, the common idea is to lead tumors to starvation and causing them to shrink to death.

Using the inhibition of tumor angiogenesis for the treatment of solid tumors was proposed in 1971 [42]. Due to the proliferative and abnormal vasculature, GBM tumors are ideal targets for anti-angiogenesis inhibitors to repress the tumor growth [86]. The anti-VEGF therapies aim to inhibit new blood vessel formation, provoke endothelial cell apoptosis and restrict the incorporation of hematopoietic and endothelial progenitor cells [87]. They can also cause contractions in the blood vessels and affect their functioning [87]. One of the FDA approved anti-angiogenesis agents is bevacizumab (Avastin® developed by Genentech/Roche), a humanized monoclonal antibody which works against VEGF by preventing its interaction with VEGFR [88].

1.3. *In Vivo* and *In Vitro* Models of Glioblastoma

Several *in vivo* and *in vitro* models of GBM have been proposed for tumor studies. To understand the underlying mechanism of tumor generation, growth, angiogenesis, invasion, and metastasis and to provide evidence of therapeutic efficacy during drug development, *in vivo* and *in vitro* models of GBM will be discussed in the following sections.

1.3.1. *In Vivo* Glioblastoma Models

One of animal models that is widely used is the xenograft model in which tumor development occurs after implantation of primary or immortalized human glioblastoma cells into nude mice [89]. Other GBM models include transgenic or spontaneous animal models; however, they are not preferred due to low reproducibility rates, latency of tumor development and low cost-efficiency [90, 91]. The U87 xenogeneic mouse model originally established by Ponten and colleagues from a female patient with GBM [92] is the most well-characterized tumor model. It has received significant attention for

assessing tumor angiogenesis and anti-angiogenic therapies [93, 94] as well as for the gene expression profile differences between differing *in vivo* growth conditions (e.g., subcutaneous and intracranial) [95]. It shows highly cellular characteristics with irregular nucleoli and unrestrained neovascularization [93], which is characterized by leaky vessels that could provide higher targeting by systemic drugs, in contrast with GBM [94]. At the molecular level, U87 models show some resemblance to human GBM such as a mutant PTEN [96] and up-regulation of the PI3K/Akt pathway as a result of high Akt expression [11].

Other models commonly used for *in vivo* GBM models are U251, GL261, and CNS-1. Among them, U251 displays an aggressive invasion into normal brain and exhibits similarities at the genetic level to human GBM [11, 36]. However, U251 xenogeneic mouse models are known for not reproducing the tumor–host immune response [97].

The GL261 mouse model was induced originally by intracranial injection of 3-methylcholantrene into C57BL/6 mice that do not require a deficient immune system [98]. It shows invasive features into normal brain and has similar markers and mutations with human GBM. However, because of these serial passages, it may lack important glial differentiation markers, such as glial fibrillary acidic protein [99]. A hallmark of the central nervous system (CNS)-1 model is its infiltrative and invasive characteristics of *in vivo* growth. CNS-1 model has been used to investigate the relationship between tumor cells and their microenvironment; however, a comprehensive study in the cellular mechanism of CNS-1 model needs to be carried out at molecular level [100]. However, animal models are usually expensive, time consuming, and too frequently fail to reflect human tumor biology [101–103].

1.3.2. *In vitro* Glioblastoma Models

In vitro GBM models are mostly used to understand tumor biology and inhibit its growth as well as investigate tumor response to chemotherapy and radiation through mimicking the *in vivo* tumor microenvironment. Due to a lack of suitable animal models, *in vitro* models are important for preclinical toxicity tests. *In vitro* cancer models consist of either primary cells and/or tissue explants taken from the patient or immortalized cells. However because phenotypic and genotypic features of the tumors can be lost during cell passaging and culturing, immortalized cells are the most preferred cells for cancer research [104]. The most commonly used immortalized GBM cell line is U87 [105, 106]. As an immortalized cell line, U87 cells have been cultured for decades in medium containing 10% fetal bovine serum (FBS) and it has been shown that it maintains the cellular and nuclear characteristic of the original tumor; it can express tumor markers such as EGFR and retain its tumorigenic features [104].

A convenient *in vitro* tumor model should provide *in vitro* sustainability, reproducibility, restate *in vivo* features of the GBM such as angiogenesis, and withstand genetic manipulation. Although U87 is a standard preclinical model for screening therapeutic agents [105], genomic alterations are known to occur and two-dimensional (2D) *in vitro* models in the tissue culture flasks or Petri dishes may not be an accurate representation of GBM tumors. The lack of cell-cell and cell-extracellular matrix interactions in 2D conventional monolayer models can alter cell metabolism, reduce functionality [107, 108], and affect drug testing results. Monolayer cultures when comparing to 3D *in vitro* cultures has been shown that they cannot mimic the tumor microenvironment. They lack the differences in the cellular organization of tumors and

characteristics of the tumor cells such as hypoxia [109]. These two culture methods have significant differences in terms of cell proliferation, and tumor vascularization [110], and tumor treatment responses [111, 112]. Comparative studies between 2D and 3D cell culture models also showed that the expression of genes changed depending on the cell culture architecture [59, 113]. Therefore, 2D cell culture results cannot be translated directly into *in vivo* settings [114, 115]. There have been close similarities between 3D *in vitro* studies and *in vivo* studies of cell characteristics in morphology, phenotype and gene expression profiles [107, 116]. To effectively study the gene expression profiles as well as the functional and microenvironmental features of the GBM tumors, there is an increasing need for 3D *in vitro* tumor models that strongly mimic the tumor *in vivo* microenvironment.

1.3.3. Three-Dimensional *in vitro* Glioblastoma Models

In the central nervous system, there is a complex 3D environment that shows regional organization and specificity and maintains a high degree of inter-regional connectivity between different cell types through both physical and biochemical mechanisms [117]. At the cellular level, glial, neuronal, vascular and immune cells are interacting to form a well regulated environment [118].

The complex organization in the CNS and the interactions between brain cells make tumor studies and drug therapy studies challenging. Tight junctions between endothelial cells, specialized transport mechanisms, and cellular metabolism of endothelial and glial cells determine interactions between neural and vascular endothelial cells. They form a specialized barrier that prevents therapeutic agents from entering brain tissues and thus prevents treatments from being effective [119–121].

3D cell cultures provide a higher degree of cellular organization and greater control of the cell growth environment which is influenced by regulatory interactions from other cells via signal transduction and the ECM [122]. Therefore, 3D cultures yield more realistic cell metabolism, diffusion, transport and kinetic properties and promote biological functions that are not observed in 2D monolayer cell cultures. This approach has been found to be effective in the study of tumor morphology, differentiation, migration and functionality [122–124].

3D GBM spheroid model were first grown as multicellular spheroids from conventional monolayer cultures by the aggregation of GBM cells to form 3D spheroids [125]. Then this model is ameliorated by growing spheroids from single cells obtained from primary GBM tissue [126]. In the 1990's, to mimic the *in vivo* characteristic of the GBM tumors, organotypic spheroids that were isolated from GBM tissue and preserved the characteristics of the original tissue were introduced [127]. They have been shown to be valid tumor models to simulate *in vivo* GBM models.

To build an *in vitro* 3D spheroid capable of modeling GBM tissues, it is important to design biomaterials that are nontoxic, mechanically stable, do not provoke inflammatory responses and permit cell attachment and growth. New approaches have been revolutionized by the integration of microfabrication techniques and cell culture technologies for the design of new cell culture platforms that mimic the 3D characteristics of the *in vivo* environment [128–133]. The new approaches incorporate multiple signaling pathways and genetic expression profiles and aim to facilitate the understanding of the cellular complexities [134–137].

Microfabrication technologies have the potential to conduct experiments on the micrometer scale (0.1 – 100 μm), thus to expanding the capabilities of biologic and drug screening systems [138, 139]. Cells can be designed as standardized spheroids with mechanical and biochemical mechanisms similar to those found in the ECM through the control of surface architecture, topography and size in which cells are cultivated and manipulated *in vitro* [140].

Technologies for fabricating 3D scaffolds are mainly derived from 3D printing [141]. Typical 3D printing processes include lithography techniques, which involve the process of drawing specific patterns featured on the wafer such as soft lithography and photolithography. Radiation sensitive materials are used to obtain the pattern. The process can be performed by wet chemical etching, dry plasma etching or the conversion to volatile compounds through the exposure to radiation. Radiation may be visible, like deep ultraviolet or X-ray photons. Two important lithographic process, soft lithography and photolithography, are described in detail below.

Soft lithography, first developed and characterized by Whitesides and his group [142–144] is based on the use of soft elastomeric membranes to design platforms with surface patterns that simulate fiber- and conduit-like microstructures related to tumor growth [145]. Soft lithography does not describe one specific technique but a group of methods such as replica molding (REM) [142], microfluidic patterning (μFLP) [146] or microcontact printing (μCP) [147] with the common feature that a polymeric material is used to design the chemical structure **(Figure 1.5)** [148]. A liquid pre-polymer is cast on the structured master surface (I). After curing (II), the elastomeric stamp is ready for use (III) **(Figure 1.5A)**. In μCP, the stamp is inked with the solution containing the molecules

to be printed (I). The molecules are transferred by printing onto the substrate (II). Following the removal of the stamp (III) the surface is backfilled with the second molecular solution for passivating (IV) **(Figure 1.5B)**. In μFLP, the stamp is first brought into tight contact with the substrate (I). Using capillary forces, the patterning solution is afterwards introduced into the channels (II). After adsorption of the molecules of interest, the stamp is removed (III) and the remaining area backfilled with a passivating solution (IV) **(Figure 1.5C)**.

Polymeric materials such as polymethylmethacrylate (PMMA), polydimethylsiloxane (PDMS), and poly-para-xylylene (Parylene) offer many advantages in microfabrication applications. PDMS, the most commonly used material in microfabrication platforms, can provide an interface between the mesoscale and microscale devices, resists cell adhesion, enables spheroid formation and outlines the cell migration within microsized channels that mimic *in vivo* conditions [145, 149, 150].

In recent reports, a tissue culture polystyrene platform, fabricated using soft lithography was used to study the migratory behavior of primary GBM cells. The results showed that GBM cells performed a more directionally determined motion pattern compared to metastatic lung and colon tumor cells [145].

Fujioka et al., used a microfluidic device made of PDMS, which was fabricated using soft lithography to analyze the interaction between the glioma-initiating cells (GIC) and human umbilical vein endothelial cells (HUVEC). Their results showed that glioma invasiveness was higher in co-culture with HUVEC than in mono-culture regardless of culture medium, the differentiation and stem cell media. They concluded that the secreted factors from HUVEC enhanced the invasion of GIC [151]. The study concluded that the

simulation of GBM tumor microenvironments and cell manipulation along with the study of the molecular mechanisms behind such behaviors might be facilitated by using PDMS models [145].

Models fabricated by using soft lithography technique are biocompatible and simple. They do not require a clean room resulting in cheaper fabrication compared to other microfabrication techniques. They are thermally stable and permeable to solvent and gases [152]. Despite these advantages, there are several disadvantages to be solved for soft lithographic techniques. The high hydrophobicity of PDMS makes it difficult to introduce water-based materials into devices. PDMS's high permeability to solvent and gases allows water vapor and organic solvents to infuse easily into PDMS, and thus cause unwanted evaporation and changes in solution osmolality [153]. Also the long-term stability of PDMS micropatterns under the pressure needs improvement [142].

Photolithography is a mainstream technology due to its high wafer throughput. The platform generally consists of an illuminator, a photomask, and a wafer also called substrate that can be silicon or glass due to their semiconductor properties. Transparent substrates such as glass, quartz or Pyrex are mostly used for cell culture applications. Polymerization can occur by different mechanisms, including UV photopolymerization, redox initiation, ionic crosslinking, temperature change, or pH change.

In the photolithography patterning process, geometrical designs drawn on a photomask are transferred onto a substrate by a light source with wavelengths between 436 nm and 365 nm in the ultraviolet (UV) range, between 248 nm and 193 nm in the deep UV (DUV) range, and 13 nm and below settled in the extreme UV (EUV) [128,

154]. The photomask that contains the pattern to be printed is made using computer-aided design (CAD) tools to pattern geometrical features [128].

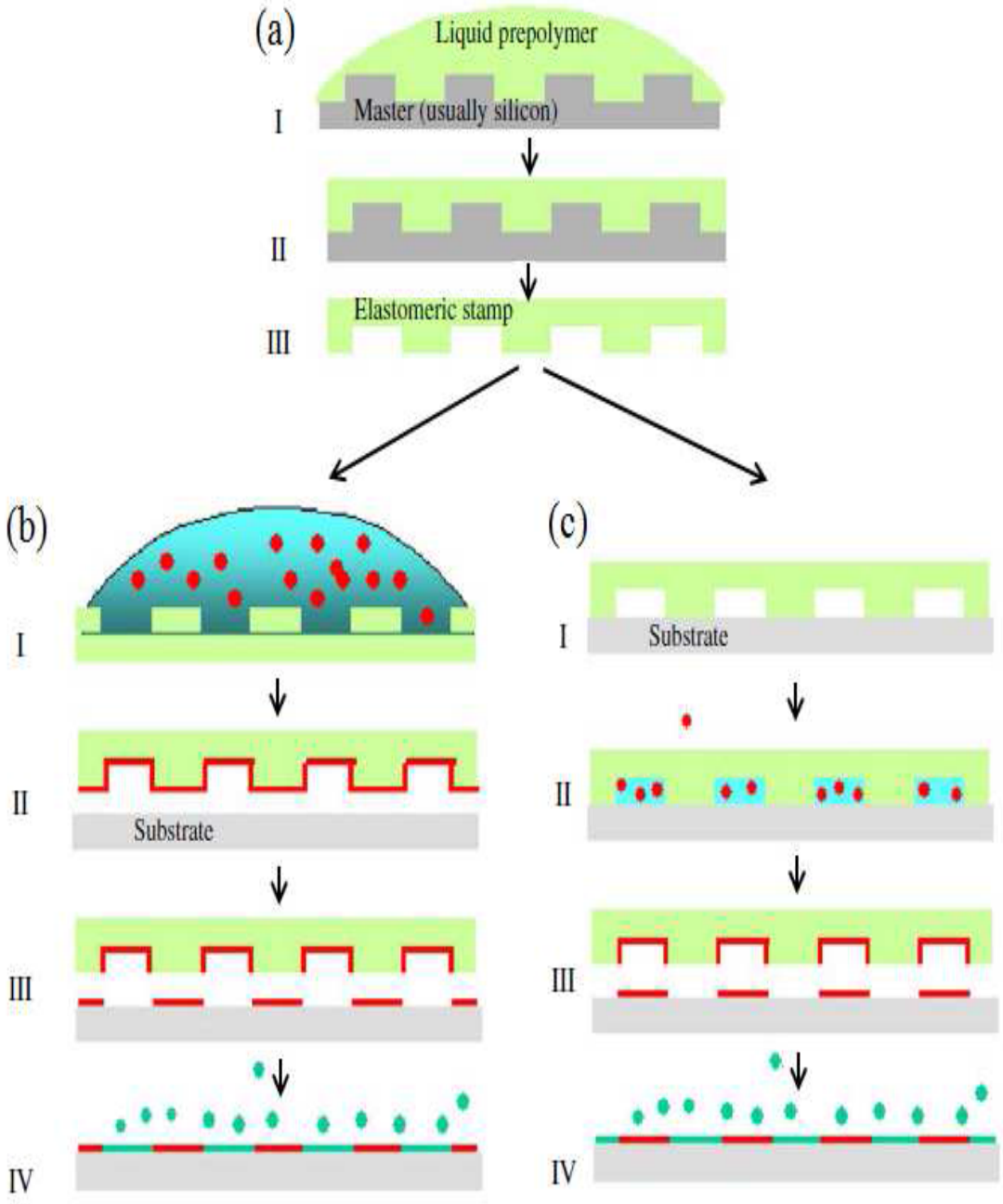

Figure 1. 5. Schematic images of microcontact printing (μCP) and microfluidic patterning (μFLP) methods. Adapted from Falconnet, D. et al., [148].

Before starting the photolithography process, the substrate's surface is coated with thin, uniform, and UV-sensitive films of photo-sensitive polymers, by either spinning the substrate at low speed or not spinning at all. After coating, the substrate is placed under UV source and covered with the photomask. UV light is applied to the substrate to pattern the UV sensitive polymer by passing through the transparent regions of the polymer as shown in **Figures 1.6-1** and **1.6-2**. Depending on the experimental purposes, positive-tone polymers are obtained when UV exposed regions of the polymer turn into soluble form. A negative-tone polymer is exposed to UV to become insoluble and thus negative images with reference to photomask can be produced. The polymerization steps are summarized in **Figures 1.6-3** and **1.6-4.**

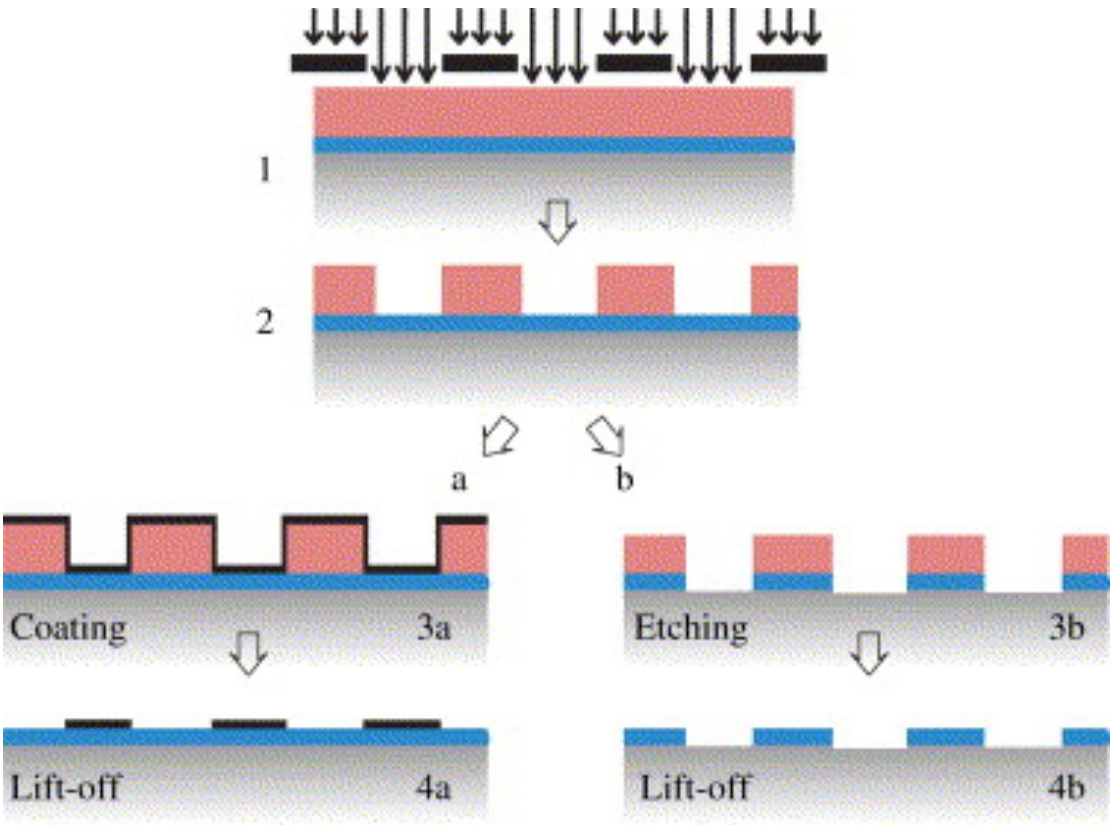

Figure 1. 6. The schematic representation of photolithographic process. Adapted from Falconnet, D. et al., [148].

The photoinitiators (PI) that impact the polymerization reaction are one of most important factors for the UV sensitive polymers. They establish the polymerization rate, the resistance to the UV light and storage stability of the hydrogel [155]. Wang and Heath studied how cellular interactions in GBM cancer cells affect cellular architectures. They used a standard photolithographic method to fabricate hard PDMS molds with 3D microchannels. They showed that cells that adhered to the collagen-coated PDMS surface secreted VEGF and EGFR proteins. This model could help to establish cellular signaling pathways that play a role in cellular structures in GBM models [156].

Revzin and his colleagues developed a microfabrication method using photolithography to develop PEG microstructures with diameters ranging from 7 μm to 600 μm. Using a photomask, they generated microwells on both silicon surfaces and glass surfaces so that they could predict the degree of hydrogel swelling. Thus the stability of the microwells could be based on the MW of the PEG hydrogel [128]. Using the same generation method, mammalian cells were encapsulated in the PEG-based hydrogel microwells produced via photolithography which led the cell-cell interaction studies in tissue engineering [129].

Due to the lack of soft lithographic techniques to pattern PEG hydrogels directly on the surface, Suh et al., introduced a patterning method that incorporated two techniques; photopatterned PEGDMA microstructures to provide a physical barrier and the PDMS substrate exposed to capillary force lithography to promote protein or cell adsorption. To investigate the effectiveness of the method, they prepared bovine serum albumin dissolved in PBS, cultured murine embryonic fibroblasts, and treated the PEGDMA patterns with the cells. Because of the cell-repellent characteristic of the PEG hydrogel

that prevent cell and protein adsorption, the substrate showed protein resistance and the cells deposited only on the exposed substrate, not on a PEG surface [157].

Similar technique was used by Karp and his colleagues to investigate the formation of embryonic stem (ES) cell aggregates, called embryoid bodies (EBs), and homogenously controlled their differentiation [131]. They utilized the cell repellant feature of the PEG hydrogel to generate ES cells within the microwells, with controlled sizes and shapes. They fabricated a PDMS mold placed directly onto an evenly distributed PEG polymer layer. After the hydrogel was photocrosslinked with UV, they removed the PDMS mold to get the microwell arrays. They evaluated the time course and the viability of ES cells within PEG microstructures of different sizes and demonstrated constant time course diameter of the EBs for over 10 days within all sizes of microwells as well as viable cells with the dimensions of the microwells regardless of microwell diameter (40–150 mm). Thus, they concluded that this microwell fabrication technique could potentially be used to control the size and shape of the EBs and direct ES cell differentiation.

Contact Liquid Photolithography was also used as a microfabrication method that promotes surface modification of device components. This method has three features: (i) the liquid photoresists, which are polymer solutions consisting of the polymer, the photoinitiator, and the solvent to adjust the viscosity in contact with the photomask; (ii) the photomask; (iii) and the living radical processes that facilitate multiple polymeric chemistries and mechanical properties of 3D patterns. The advantage of having polymer solution in contact with the photomask enables the control of the layer thickness as well as surface geometries [158].

PEG-based microwells were designed with the ability of controlling the well dimensions and the layer thickness to promote mouse insulinoma 6 (MIN6) cell-cell interactions, aggregations and encapsulations (**Figure 1.7**). Photocrosslinkable polymer solution (red) composed of PEGDA, photoinitiator, and Rhodamine B in Hank's balanced salt solution was placed between a glass slide and a photomask separated by spacers with defined thickness **(Figure 1.7A)**. Microwells formed after ultraviolet light exposure (350–450 nm) for 60 s were covalently attached to the functionalized glass slide **(Figure 1.7B)**. Representative confocal image of a microwell device (width and height=100 μm) in both the x-y plane (top) and x-z plane (bottom) was given in **Figure 1.7C**. PEG microwells yielded uniform β-cell aggregates from a single-cell suspension of MIN6, which preserved functional expression during seeding, culture, and encapsulation and the aggregates with controllable sizes could be removed from the microwells for macroencapsulation, implantation, or other biological assays [159].

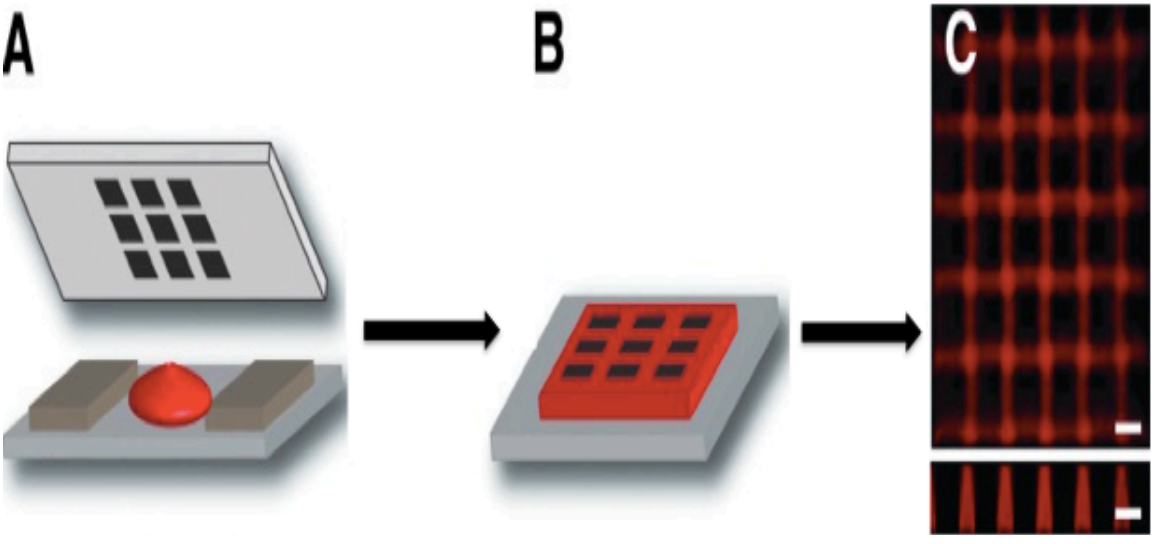

Figure 1. 7. Formation of hydrogel microwell devices. Scale bars represent 100 μm [159].

The ability of PEG to be conjugated with different substances makes it advantageous over other polymers. Recently, PEGDMA was used incorporated with gelatin methacrylate (GelMA) monomer. The incorporation of GelMA with PEG yielded a biodegradable PEG-based copolymer and allowed the cell attachment by using UV-assisted capillary force lithography approach [160]. The mixture of GelMA and PEGDMA was photocrosslinked under UV light (365 nm) for 5 minutes in the presence of a photoinitiator and yielded PEG-GelMA copolymer. The mixture dropped onto treated cover glass, which was covered with master mold and polymerized with UV-assisted capillary force lithography to obtain patterns (**Figure 1.8**). HUVECs cultured on patterned PEG–GelMA substrates showed increased cell attachment compared with those cultured on unpatterned PEG–GelMA substrates. Moreover, the PEG–GelMA platform helped to increase the cellular migration speed such that this model could be used in the vascular modeling for drug screening [160].

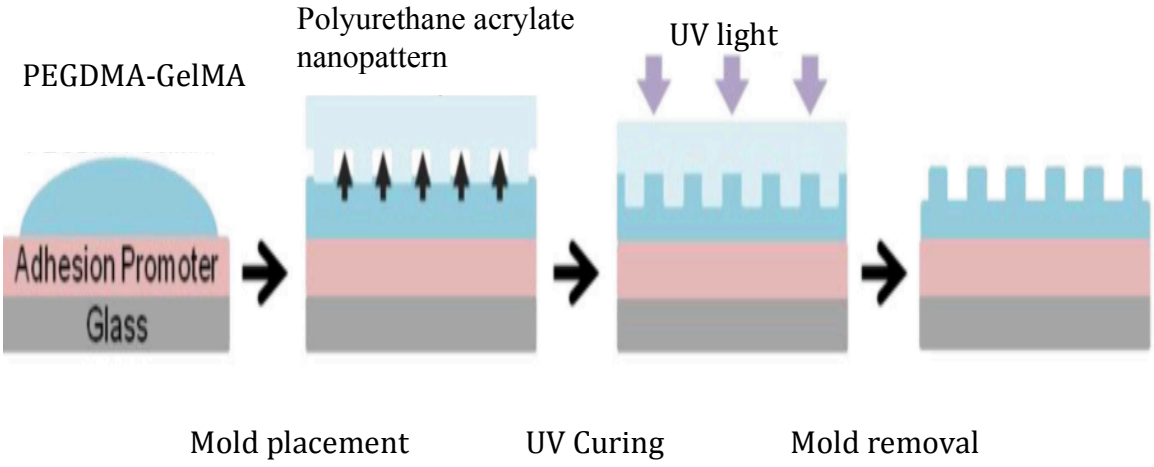

Figure 1. 8. Schematic illustration of the fabrication of process of nanostructures [160].

The PEG-based hydrogels can also be incorporated with biomolecules such as protease-degradable sites, adhesive ligands, and growth factors [161] and the incorporation of these sequences can induce cell behaviors. Moon and colleagues immobilized Arg-Gly-Asp-Ser (RGDS) molecules on the surface of PEGDA hydrogels with photolithography and investigated the effect of patterned RGDS concentration on endothelial tube formation. They showed that endothelial cell adhesion, migration and angiogenic responses can be manipulated by PEGDA hydrogels micropatterned with bioactive ligands [162]. Lutolf et al., demonstrated that the intricate interactions between cells and ECM can be mimicked in synthetic systems by using a PEG hydrogel cross-linked with oligo peptides, which simulated the development and regeneration of natural ECM protein, collagen; and they validated the high cell survival rate in their network [163]. However, most of these approaches could not be effectively translated into clinical use [164].

Recently, our group designed 3D PEGDA hydrogel microwells using photolithography to control the development of GBM cells, generate 3D GBM models and provide a novel *in vitro* platform for cancer studies [133]. GBM cells for 21 days in the PEGDA microwells using their cell-repellant properties to generate cell spheroids. We evaluated the viability of the cell spheroids using live/dead assay, which showed an improvement over 21 days as shown in **Figure 1.9** [133]. The shape and thickness of the cell spheroids were observed by fluorescence microscopy. By the characterization of the cell spheroids, we concluded that 3D GBM spheroids were successfully constructed in the PEGDA microwells, which can control the spheroid's size and shape. This *in vitro* platform could be used as an ideal building unit for 3D GBM spheroid formation and could serve as a

reliable *in vitro* model for *in vivo* studies in terms of time for the preclinical brain tumor growth studies [133]. All these patterning method where PEG limits the attachment of the cells to the surface contribute to formation of aggregates in a given barrier that could lead to the fabrication of high-throughput cell screening devices.

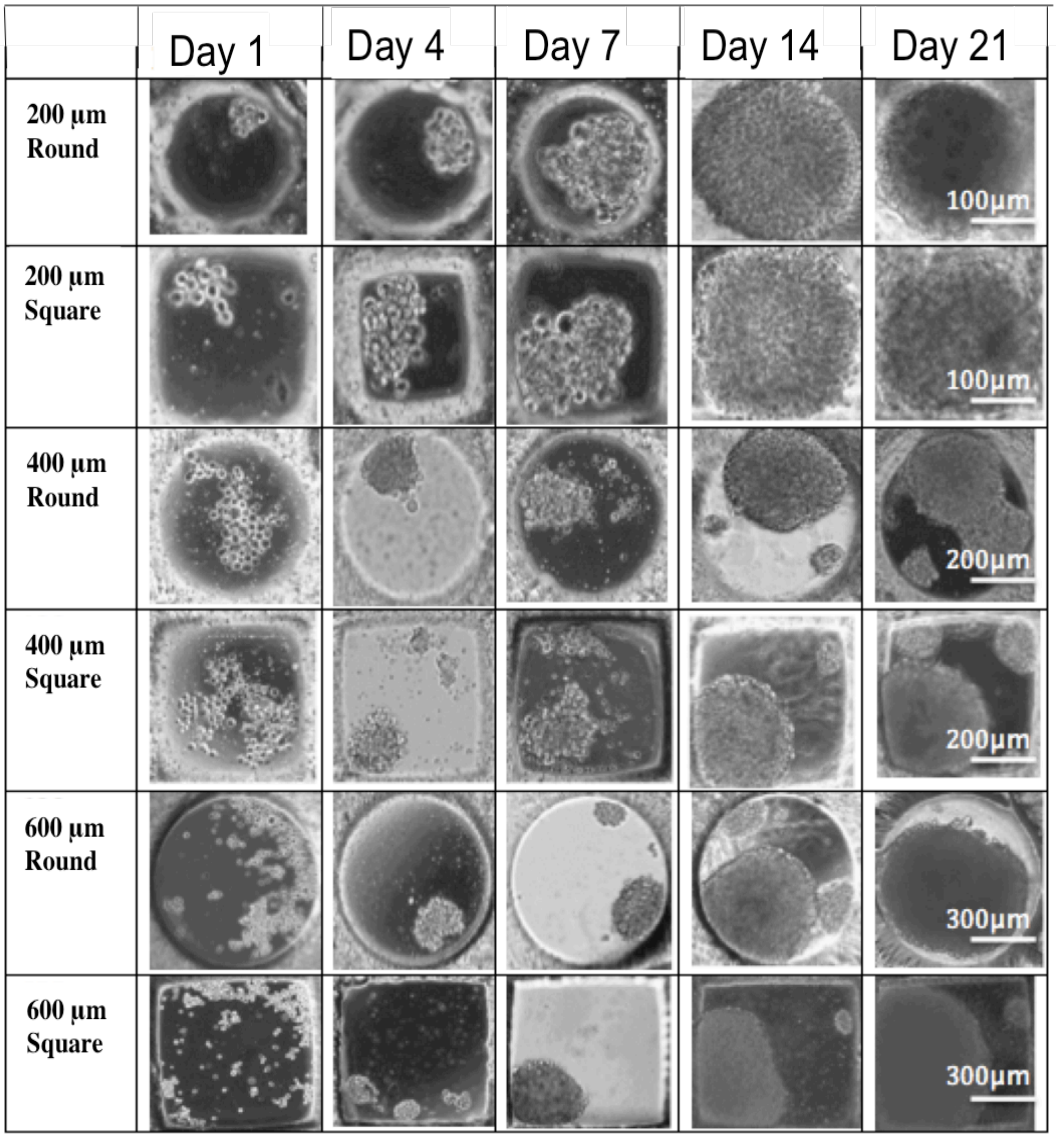

Figure 1. 9. Time course of GBM cells within PEGDA-750 microwells of different sizes over a period of 21 days [133].

1.4. Hypothesis and Objectives

Accumulating evidence indicates that GBM tumors are the most malignant brain tumors with a poor prognosis. The failure to provide effective treatments causes very low survival rates with a median patient survival approximately 1 year. Cell models have an important role in cell and molecular biology studies, drug development and tumor targeting studies. *In vitro* models based on 2D cell culture have been used to study tumor growth, metastasis, and resistance to antitumor agents. Studies showed that 3D models resemble the *in vivo* characteristics at both cellular and molecular levels. For an effective tumor treatment, accurate 3D *in vitro* tumor models that can mimic *in vivo* features of the GBM tumor are required. Despite the advances in cell culture models and cancer research, there is still an urgent need for the development of more accurate *in vitro* models. Previous studies encouraged us to develop a 3D *in vitro* tumor model to study GBM spheroid formation kinetics and a possible treatment method using a more realistic model. Therefore, we recently built a novel 3D cell culture platform based on hydrogel microwells that could mimic *in vivo* tumor microenvironment. We applied the 3D photopatterning technique to GBM (U87) cells using the photolithography method to generate 3D tumor spheroids with controlled shape and size. Our preliminary results suggested that uniform GBM spheroids can be formed in 3D, and the size of these GBM spheroids depends on the size of microwells [133]. However, the use of the GBM tumor by itself may not exactly represent the *in vivo* microenvironment of the tumor since tumor cell growth and development are supported by interactions of endothelial cells and growth factors, that led to receive other critical signals from their environment.

Therefore, we undertook this study to design a 3D hydrogel microwell platform for the co-culture of 3D *in vitro* GBM tumors with endothelial cells in order to closely mimic the *in vivo* behaviors of GBM tumors and to treat them, which could present new avenues in the precise studies of the GBM tumor spheroid structures, tumor targeting and its treatment. Our hypothesis is that GBM tumor cells co-cultured with endothelial cells in 3D PEG-based hydrogel models simulate more *in vivo* behaviors that can be identified and characterized. One prediction of this hypothesis is that cell-repellent characteristics of the PEG-based hydrogels allow cells to grow in space without attaching to the hydrogel, which facilitates 3D spheroid formation. Our other prediction is that the co-culture of U87 cells with HUVECs allows for the recreation of the *in vivo* microenvironment and the signaling pathways of the GBM tumor cells. To test our hypothesis, we fabricated a 3D *in vitro* microwells by using FDA approved, cost-effective PEG-based hydrogel and used HUVEC cells to co-culture with GBM cells. We examined the progression of GBM spheroids in our 3D platform at a molecular level by investigating important markers such as CD31 and VEGFR2, which are expressed in tumor cells. Lastly, we targeted 3D tumor spheroids with an oncolytic adenovirus, which is selective for GBM tumors and is currently being used in clinical trials. This novel platform could meet the need for cost-effective cell culture technologies that enable formation of controllable and uniformly sized spheroids and has the potential to improve current tumor models for the screening of 3D other solid tumors and assessment of treatment responses.

Chapter 2. Materials And Methods

2.1. Chemicals

Poly(ethylene glycol) dimethyl acrylate (PEGDA) (MW 750 Da and MW 1000 Da), 3-(Trimethoxysilyl)propyl methacrylate 98% (TMSPMA), 2-hydroxy-2-methyl propiophenone photoinitiator (PI) were purchased from Sigma-Aldrich Chemical Company (St. Louis, MO). Dulbecco's modified Eagle's medium (DMEM), phosphate buffered saline (PBS), fetal bovine serum (FBS), Calcein AM, ethidium homodimer, 4', 6-diamidino-2-phenylindole (DAPI) and Trypan Blue (0.4%) were obtained from Life Technologies (Grand Island, NY). Penicilin and streptomycin antibiotics were purchased from Corning Cellgro (Mediatech, Inc., Manassas, VA). Mouse monoclonal adenovirus 5 E1A (M58) and β-actin mouse monoclonal antibodies (8H10D10) were obtained from Santa Cruz Biotechnology (CA, USA) and Cell Signaling Technology (Danvers, MA, USA), respectively.

2.2. Methods

2.2.1. PEG Hydrogel-Based Microwell Preparation

As we described in our previous studies, we dissolved PEGDA 750 and PEGDA 1000 at 10 – 80% w/w concentration in PBS and prepared fresh for each experiment [133]. The PI was dissolved in PEGDA solution to have a final working concentration of 0.05% w/v. Solutions were thoroughly mixed before the polymerization.

The surface of cover glasses (18 x 18 mm cover glasses purchased from Corning Incorporated) was covered by the first layer of PEGDA hydrogel in order to prevent cellular interaction with the underlying glass substrate. For this first layer of the hydrogel, 10 µl of the solution was dropped on the cover glass and exposed UV for 30 seconds at a

working distance of 6 inches. The UV exposed cover glass with a first layer was turned upside down and put on top of the 50 to 100 µl of PEGDA hydrogel that was dropped on a new petri dish with spacers, which are used to adjust the depth of the microwells, then finally, the photomask with square or round patterns was placed on top. The second layer was exposed to UV. After the exposure, the cover glass with the microwells was washed with PBS to remove any uncrosslinked polymer solution.

The desired patterns were prepared using AutoCAD (Autodesk Inc) and the printed photomasks (purchased from CADart Washington, USA) were placed on the cover glass for UV exposure. Related data was given in **Table 2.1**. We used photomasks with different sizes i.e., 200 µm, 400 µm, and 600 µm and geometries i.e., round and square as shown **Figure 2.1**. Photopolymerization was carried out with an Omnicure S2000 (320-500 nm, EXFO, Ontario, Canada) lamp at 100 mW/cm^2 (measured for 365 nm) to yield solid hydrogels.

2.2.2. Stability Testing of PEGDA Hydrogel on Treated and Untreated Cover Glasses

We also used TMSPMA to generate an adhesive surface to PEGDA hydrogels on the cover glass. A glass beaker was put in a bucket of ice; 50 g of sodium hydroxide (NaOH) pellets was weighed, 450 ml of distilled water was slowly added and all pellets were dissolved by mixing. In the same beaker, all cover glasses slides were placed in a staggered manner to make contact with NaOH solution. The beaker was covered with a pyrex and kept overnight in the fume hood. 10% NaOH solution was discarded then with gloves; each cover glass slide was thoroughly rinsed and rubbed under distilled water.

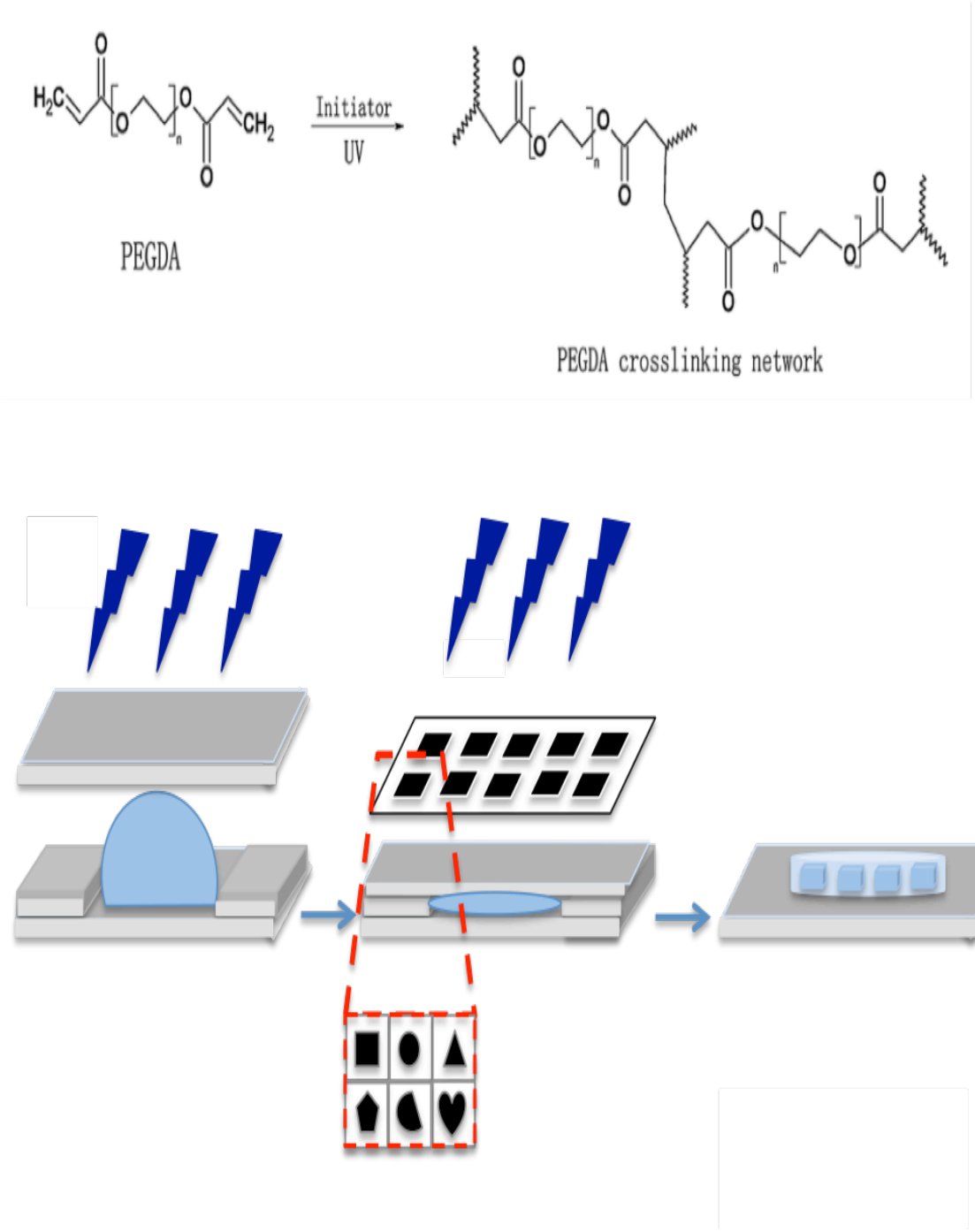

Figure 2. 1. Schematic of the formation of the controlled-size GBM cancer spheroids using PEGDA hydrogel microwells.

Table 2. 1. The optimization of UV exposure time for PEGDA-750. (A) PEGDA-750 with a concentration of 10% (B) 20% of PEGDA-750, (C) 40% of PEGDA-750 [133]

(A)	10% PEGDA-750									
Time (s) / Size (μm)	80	85	90	100	105	110	120	130	135	140
200	x	✔	x							
400					x	✔	x			
600								x	✔	x

(B)	20% PEGDA-750					
Time (s) / Size (μm)	45	55	65	75	85	95
200	x	✔	x			
400				x	✔	
600					x	✔

(C)	40% PEGDA-750								
Time (s) / Size (μm)	10	12	15	18	20	22	30	32	35
200	x	✔	x						
400				x	✔	x			
600							x	✔	x

They were dipped in 3 distinct 100% reagent alcohol baths and let air-dry. The glass slides were wrapped with aluminum foil and baked for 1 hour at 80 °C. Cover slides were stacked vertically and 3ml of TMSPMA was poured on top of the stack using a syringe. After 30 minutes, the stack was flipped upside down to get even coating. The whole

assembly was baked in the beaker overnight at 80 °C. The cover slides were cleaned in 100% reagent alcohol with 3 baths and air-dried. They were wrapped with aluminum foil and baked for 1-2 hours at 80 °C. They were stored wrapped in aluminum foil at room temperature. All the cover glass slides were used within 7 days after TMSPMS surface treatment [133].

A series of concentrations of PEGDA hydrogels, i.e., 10%, 20%, 40%, 60% and 80%, were prepared on TMSPMA treated glasses that were prepared as previously described in Hydrogel-Based Microwell Preparation step as shown in **Figure 2.1**. The same samples of PEGDA hydrogels were fabricated on the untreated cover glasses as a control group. These PEGDA hydrogels were immersed in PBS and kept in the incubator for 21 days. These samples were observed daily under microscopy (Olympus, IX51). A cover glass was marked "unstable" when any part of the PEGDA hydrogel was detached from the cover glass's surface as shown in **Figure 2.2**. Stability testing and optimization studies showed that treated cover glasses with PEGDA-750 hydrogels required less preparation and fabrication time compared to PEGDA-1000. Therefore, studies were carried out with PEGDA-750 hydrogel with a concentration of 40% that yielded accurate polymerization time (**Table 2.1**).

2.2.3. Cell Lines And Culture Conditions

Human glioma cells U87 and HUVECs were both obtained from American Type Culture Collection (ATCC). U87 cells were cultured in Dulbecco's modified Eagle's medium (DMEM) supplemented with 10% (v/v) fetal bovine serum (FBS), 100 U/ml penicillin and 100 μg/ml streptomycin.

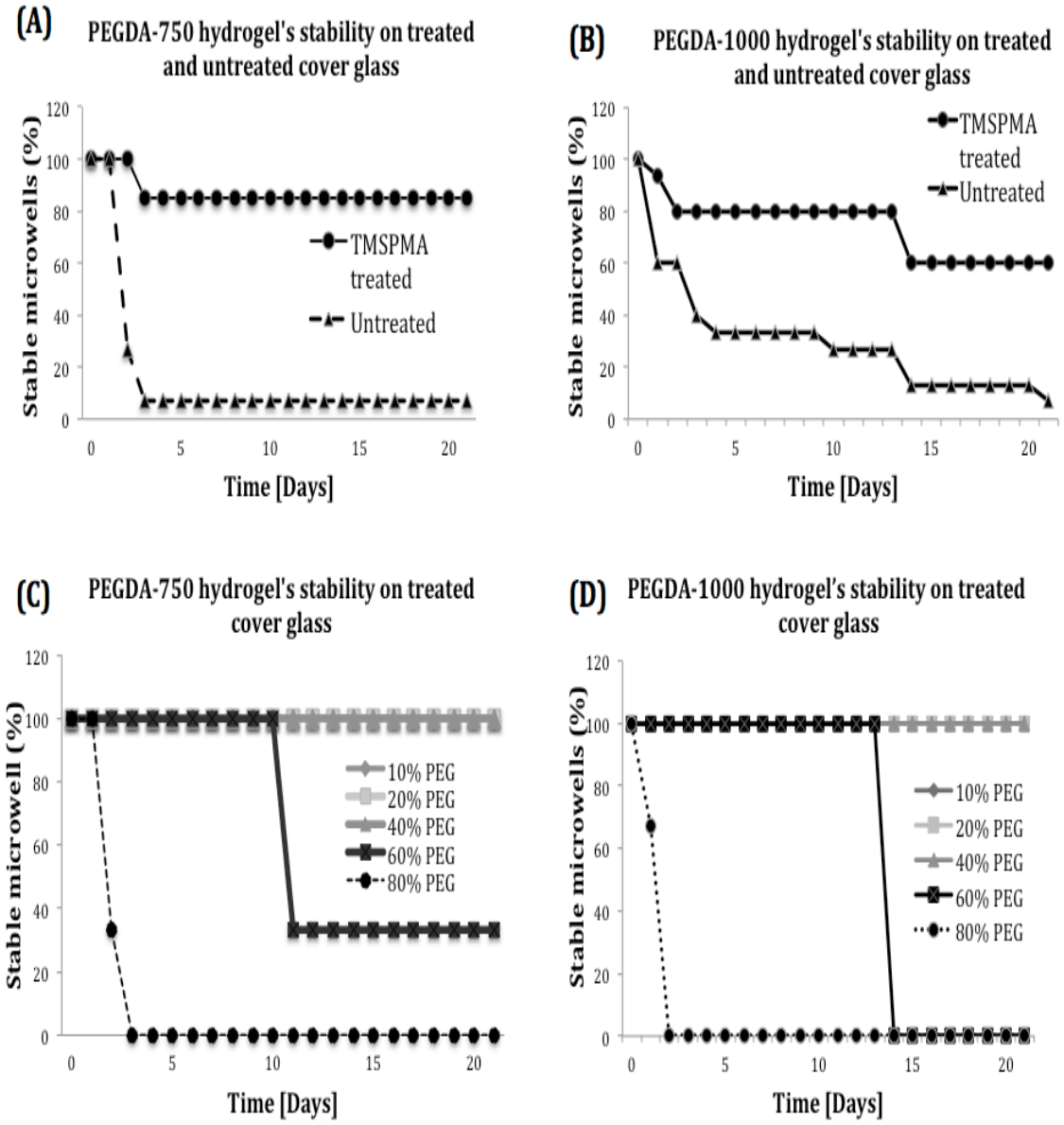

Figure 2. 2. Stability of PEGDA hydrogel. (A and B) Percentage of stable microwells on TMSPMA treated and untreated cover glasses. (C and D) Stability of different concentration of PEGDA-750 and 1000 [133].

HUVECs were grown and maintained in endothelial cell medium, EGM-2 (Lonza), which contains EBM-2 medium (serum free, growth-factor free), supplemented with 2% fetal bovine serum (FBS), human fibroblast growth factor-B (hFGF-B), human epidermal

growth factor (hEGF), human vascular endothelial cell growth factor (hVEGF), long R insulin-like growth factor-1 (R3-IGF-1), ascorbic acid, hydrocortisone, and heparin.

Frozen cells in the vial were thawed by gentle agitation in a 37 °C water bath for approximately 2 minutes. The vial content was transferred to a centrifuge tube containing 9 ml appropriate medium and centrifuge for 3 minutes at 1200 revolutions per minute (rpm). The pellet was resuspended with appropriate medium and dispensed in a new culture dish for monolayer cell culture. The cells were plated at a concentration of 1.0 x 10^6 cells/ml (10 ml total volume) in 100 mm diameter tissue culture dishes and were passaged every 3 days at a subculture ratio of 1:4. All cells were manipulated under sterile tissue culture hoods and maintained in a 95% air – 5% CO_2 humidified incubator at 37 °C. Monolayer cells were cultured between 70% and 90% confluence.

2.2.4. Optimization of U87 Cell Seeding Concentrations

As described in Fan et al., for the optimization of U87 cells' seeding concentration in the microwells, the DMEM medium was removed from dish by aspiration and the monolayers were washed by PBS to remove all traces of medium. Trypsin-EDTA solution was used to completely cover the monolayer of cells and place in 37 °C incubator for approximately 2 minutes to dissociate cells. DMEM medium was added to the cell suspensions to inhibit the trypsin that was present in the dish. The cells were collected by gently pipetting in the tube and centrifuged for 3 minutes at 1200 rpm. The supernatant was removed and the pellet was suspended in PEGDA precursor solution. They were seeded in the microwells at five different concentrations, i.e., 0.05 x 10^6 cells/ml, 0.20 x 10^6 cells/ml, 0.70 x 10^6 cells/ml, 1.0 x 10^6 cells/ml and 2.0 x 10^6 cells/ml as shown in **Figure 2.3**. Cells in the microwells were cultured in 37 °C incubator for 21

days to observe cell growth. The optimization studies showed that 0.2 x 10^6 cell/ml allowed the formation of proper sized U87 spheroids in all size of microwells over 3 weeks of culture.

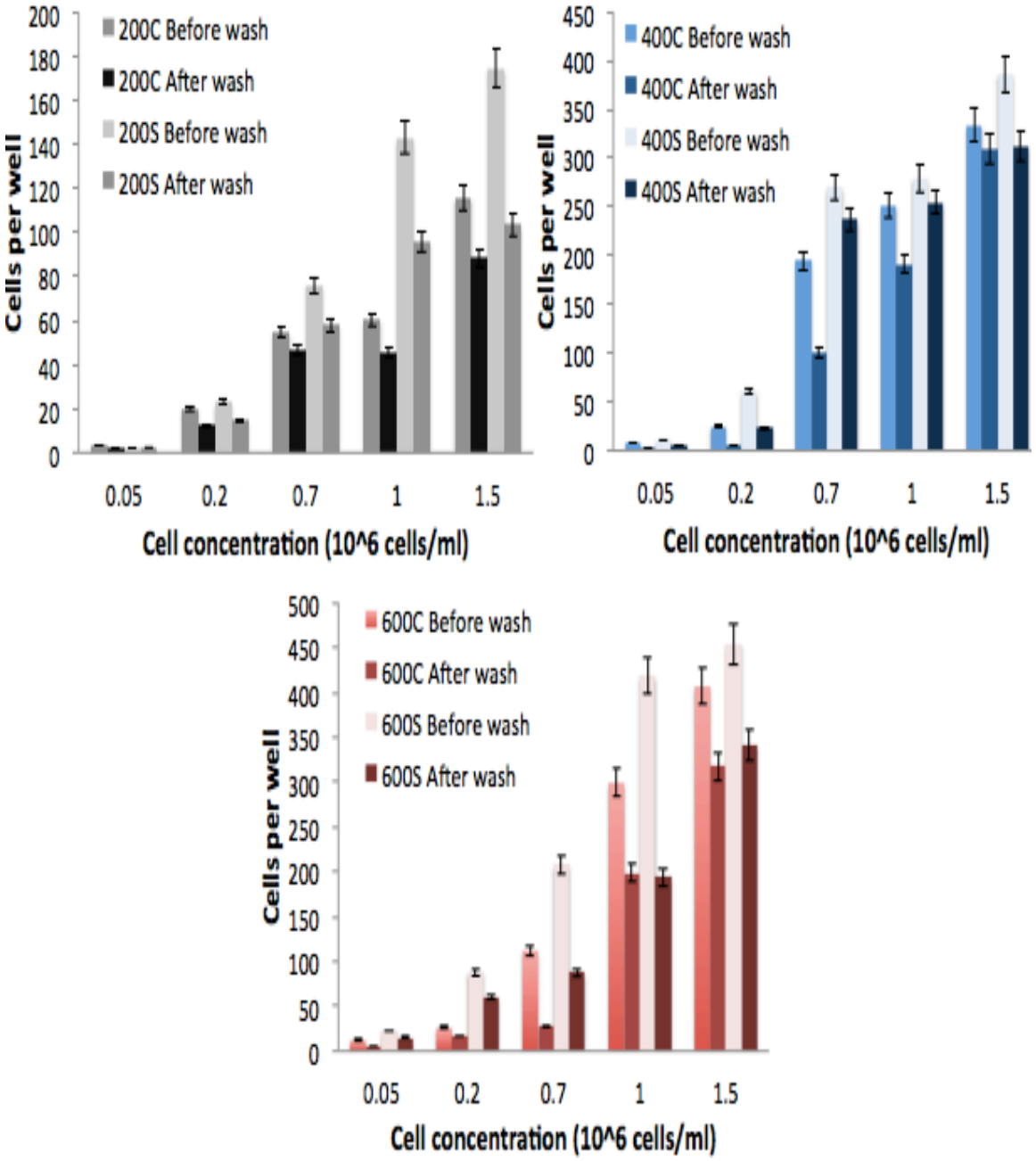

Figure 2. 3. Optimization of seeding concentration of U87 cells into the microwells [133].

2.2.5. Three-Dimensional Co-culture of Glioblastoma Cells and HUVEC cells

Cells were cultured at 37 °C between 70% and 90% confluence in monolayer T75 flasks prior to use. Cells were prepared by washing in PBS buffer followed by the treatment with trypsin for the dissociation from the flask surface. They were collected and centrifuged at 1200 rpm for 3 minutes. They were resuspended in appropriate medium and initial cell concentration was calculated using a hemocytometer (Hausser Scientific, 1483). To distinguish between U87 cells and HUVECs in co-culture experiments, U87 cells were stained with 15 µM of CellTracker™ Blue CMAC (7-amino-4-chloromethylcoumarin) fluorescence dye while HUVECs were stained with 15 µM of CellTracker™ Red CMTPX fluorescence dye as shown in **Figure 2.4**. Cell suspensions were diluted with the cell medium to prepare the exact concentrations. They were seeded in the microwells with U87:HUVEC 1:1 and 3:1 ratios at a concentration of 0.2 x 10^6. As control groups, stained U87 cells and HUVECs were mono-cultured and incubated in the same culture conditions. HUVECs used for these experiments were between passage 3 and 5.

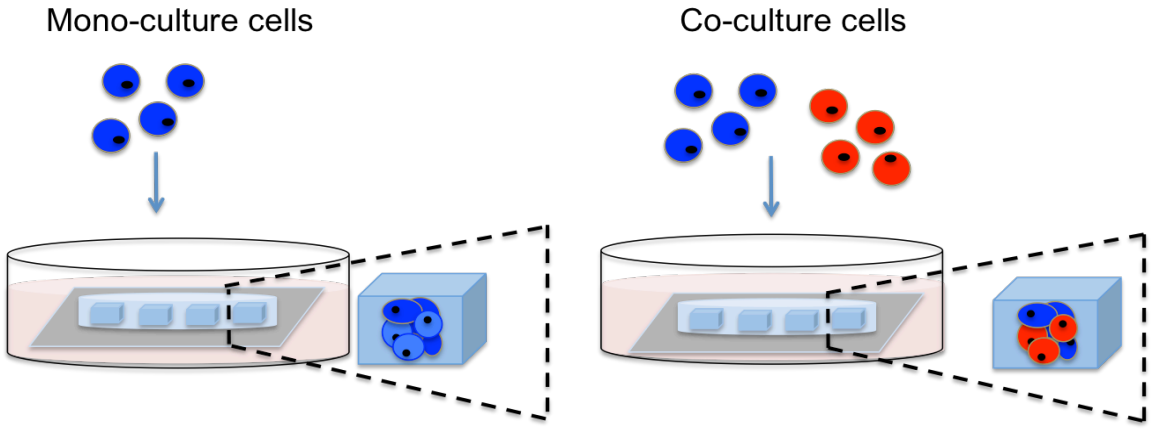

Figure 2. 4. Schematic of the formation of U87 and U87-HUVEC mono-culture and co-culture spheroids, respectively, within the microwells. U87 cells were tracked with blue and HUVECs with red cell trackers.

2.2.6. Cell Viability Assay

Cell viability was determined using Live/Dead Cell Viability Assay Kit. The Live/Dead Assay kit contains calcein AM (2 μg/ml, in PBS) and ethidium homodimer (4 μg/ml in PBS) reagents. U87 cells were cultured in the DMEM medium in the microwells for 1, 4, 7, 14 and 21 days. 5 μL calcein AM (Component A) and 20 μL ethidium homodimer (Component B) were added to 10 ml PBS to create a staining solution. DMEM medium was removed form the cells and cells were washed with PBS to remove the cells that were not in the microwells. 100 - 150 μL of the staining solution was added directly to the microwells. The plates were incubated for 30 minutes at 37° C and the images were captured. Green fluorescence was measured because of the calcein AM reaction from viable cells and damaged cell membranes stained red because of their reaction with ethidium homodimer. The cell aggregates were monitored for 21 days using an Olympus fluorescence microscope. The fluorescence intensity was quantified using ImageJ (National Institutes of Health). The green and the red fluorescence images from viable and non-viable cells, respectively, were merged to one image and the intensity was evaluated. Eight images from each different microwell were taken to count the fluorescence intensity. For each microwell, the boundaries were chosen as a region of interest and the fluorescence intensity was calculated.

2.2.7. Total RNA extraction

Total RNA of GBM, HUVECs and GBM-HUVEC co-culture cells were extracted using RNeasy Mini Kit (Qiagen). Maximum of 1 x 10^7 cells were disrupted and homogenized in 600 μl of Buffer RLT. The lysate was centrifuged for 3 minutes at 14,000 rpm and the supernatant was carefully removed. 1 ml of 70% ethanol was added

to the supernatant by pipetting. 700 µl of the sample was transferred to a 2 ml collection tube with an RNeasy Mini spin column and centrifuged for 15 seconds at 10,000 rpm. The flow-through was discarded. 350 µl Buffer RW1 was added to RNeasy column, and centrifuged for 15 seconds at 10,000 rpm. The flow-through was discarded. 10 µl DNase I solution was added to 70 µl Buffer RDD, mixed gently and centrifuged briefly. 80 µl DNase I incubation mix was directly added to RNeasy column membrane and placed in benchtop (20-30 °C) for 15 minutes. 350 µl Buffer RW1 was added to Rneasy column, the tube was centrifuged for 15 seconds at 10,000 rpm and the flow-through was discarded. 500 µl Buffer RPE was added to the spin column and centrifuged for 15 seconds at 10,000 rpm. The flow-through was discarded. 500 µl of Buffer RPE was added to the spin column and the tube was centrifuged for 2 minutes at 10,000 rpm. The RNeasy spin column was placed in a new 2 ml collection tube and centrifuged at 14,000 rpm to dry the membrane. The RNeasy spin column was placed in a new 1.5 ml collection tube, 50 µl RNase-free water was directly added to spin column membrane, the tube was centrifuged for 1 minute at 10,000 rpm to elute the RNA. The quality and quantity of the RNA was established by reading the optical density (OD) of each sample at 260 nm and 280 nm using a Nanodrop (2000 series).

2.2.8. Primer Design

Primer3 was used to design primers (Sigma-Aldrich) for quantitative real-time polymerase chain reaction (qPCR) assay [165]. To reduce the possibility of amplifying genomic DNA, each pair of primers was designed to target a short (90–120 bp) segment of the mRNA sequence expanding adjacent exons. Therefore, the genomic sequence of each gene was obtained from the ENSEMBL genome database, and the mRNA sequence

of the corresponding gene was obtained from GenBank. The sequences of two consecutive exons were used in Primer3 for primer selection. Primer sequences of tested genes are listed in **Table 2.2**.

Table 2. 2. Primer Sequences Used in qPCR

Gene	Forward primer	Reverse primer
PIK3R1	AAGTGCCAGAGTGAAGTGGC	TGGATTTCCTGGGATGTGCG
PECAM-1/CD31	TCCGGATCTATGACTCAGGG	ACAGTTGACCCTCACGATCC
VEGFR2	GCAGGGGACAGAGGGACTTG	GAGGCCATCGCTGCACTCA
GAPDH	CTCTGCTCCTCCTGTTCGAC	AAATGAGCCCCAGCCTTCTC

2.2.9. Gene Expression Analysis by Quantitative PCR

cDNA was generated from isolated total RNA using Superscript II reverse transcriptase (Invitrogen Life Technologies, Carlsbad, CA). 1 µl Oligo-dT(20) primers (500 µg/ml) (Invitrogen), 10 ng/µl total RNA, 1 µl dNTP Mix (10 mM each) were added into a eppendorf tube and adjusted to 12 µl with sterile, distilled water. The mixture was heated to 65 °C for 5 minutes and quick chilled on ice. The content from the tube was collected by brief centrifugation. 4 µl first-strand buffer (5X), and 2 µl 0.1 M DTT were added. 1 µl RnaseOUT (40 Units/µl) was required if the starting RNA concentration was lower than 50 ng. Contents of the tube was mixed gently and incubated at 42 °C for 2 minutes. 1 µl (200units) of SuperScript II RT was added to the mixture and pipetted gently up and down. The tube was incubated at 42 °C for 50 minutes followed by heating at 70 °C for 15 minutes for the inactivation of the reaction. Quantitative PCR was performed on a Stratagene Mx3005P qPCR System (Agilent Technologies, CA) using

PerfeCTa® SYBR® Green SuperMix (Quanta BioSciences, Inc., MD) in a 25 µl reaction mixture containing 12.5 µl SYBR Green PCR Mix, 0.5 µl 10 mM primers, 4 µl of the 1:6 diluted cDNA synthesis reaction product. PCR was performed for 40 cycles at 95 °C for 15 seconds and 53 °C for 45 seconds after initial incubations at 95 °C for 10 minutes.

PCR product specificity and purity were confirmed by generating a dissociation curve. Sample cycle threshold (Ct) values were normalized to values for Glyceraldehyde 3-phosphate dehydrogenase (GAPDH), all of which were calculated from duplicate or triplicate reactions. Relative changes in gene expression were expressed as fold changes calculated by the following formula: fold change = 2^DDCt, where DDCt = (Ct of gene of interest, co-culture – Ct of housekeeping gene, co-culture) – (Ct of gene of interest, mono-culture – Ct of housekeeping gene, mono-culture), and Ct is the threshold cycle number. The qPCR products were also run on a 3% of agarose gel and the intensities were quantified to the intensities of housekeeping genes GAPDH.

2.2.10. Protein Isolation and Quantitation

Cell culture plates with the microwells were placed on ice and cells were washed with ice-cold Tris-buffered saline (TBS). TBS was aspirated and 1 ml per 100 mm well ice-cold RIPA buffer supplemented with fresh protease inhibitor cocktail at 1:100 dilution was added to the plates and cells were incubated with RIPA buffer for 15 minutes. Using a cold plastic cell scraper, cells in the microwells were gently transferred into a pre-cooled microcentrifuge tube. The microcentrifuge tubes were maintained for 30 minute at 4 °C with a constant agitation. Cells were spinned at 14,000 rpm for 20 minutes in a 4 °C pre-cooled centrifuge. The microcentrifuge tubes were gently removed and placed on ice. Supernatant was transferred to a new ice-cold tube and pellet was discarded. 10 to 20

µl of lysates were removed to determine the protein concentration for each cell lysates. To prepare the protein standards in triplicate using a 0.5 mg/ml BSA stock solution was used (**Table 2.3**).

Table 2. 3. Preparation of BSA protein standard

Standard Solution	Volume 0.5 mg/ml BSA (µl)	Volume 0.15 M NaCl (ml) (µl)	Final BSA Concentration (µg/ml)
Blank	0	100	0
S1	5	95	250
S2	10	90	500
S3	15	85	750
S4	20	80	1000

Bradford reagent was gently mixed and then the required volume was transferred to a plastic tube to equilibrate to room temperature before use. 10 µl of each standard was pipetted into the wells of a 96-well plate. 200 µl of Bradford reagent was added to each standard dilution, mixed by pipetting and allowed to stand at room temperature for 2 minutes. The absorbance was read at 595 nm using a NanoDrop reader (Thermo Scientific, USA) A standard curve was generated by plotting absorbance at 595 nm versus protein concentration. For the unknown GBM, HUVEC and co-culture samples 10 µl, the steps were repeated using the unknown samples in place of the BSA. The standard curve was used as a reference to determine the concentration of the unknown samples.

2.2.11. Western Blotting

After the protein concentration was determined, 100 µg of protein lysates were mixed with an equal volume of 2X Laemmli sample buffer and boiled at 95° C for 5 minutes. Equal amounts of protein were loaded into the 4 – 20% SDS polyacrylamide gel

electrophoresis (SDS-PAGE) along with molecular marker. The gel was run for 10 minutes at 80 V and the voltage was increased to 120 V to finish the run in about 1 hour. The gel was placed in 1X transfer buffer for 10 – 15 minutes. The transfer sandwich was assembled and the cassette was placed in the transfer tank with an ice block. The transfer was done at 100 V for 1 hour. The blot was rinsed in water and membrane was blocked in 3% BSA in TBST at room temperature for 1 hour. The membranes were incubated with the primary antibody solutions CD31 (1:1000), VEGFR2 (1:1000) and β-actin (1:1000) diluted in 3% skim milk. The blots were rinsed 3 times for 5 minutes with TBST. Membranes were then incubated with the HRP-conjugated secondary antibodies (1:2000) diluted in 3% skim milk for 1 hour at room temperature. The blots were rinsed 3 times for 5 minutes with TBST. The chemiluminescent substrate reagents (ECL) at a ratio of 1:1 were applied to the blots. The protein bands were detected by using a CCD camera-based imager. The loading control protein β-actin was used to normalize the target protein levels.

2.2.12. Adenovirus Infection

Δ24RGD-GFP virus was kindly provided by our collaborator Dr. Juan Fueyo (The University of Texas MD Anderson Cancer Center, Department of Neuro-Oncology). For 3D spheroid culture, cells were allowed to grow for 14 days after seeding. Then, without removing the spheroids from the microwells, they were infected with the replication-competent Δ24RGD-GFP, which expresses green fluorescence protein (GFP), at a multiplicity of infections (MOI) of 10, 50 and 100 plaque-forming units per cell as shown **Figure 2.5** or uninfected. Subsequently, fresh medium was added. Green fluorescence

was assessed by fluorescence microscopy on days 3 and 10 post infection. Uninfected cells with EGM-2 medium were used as a control.

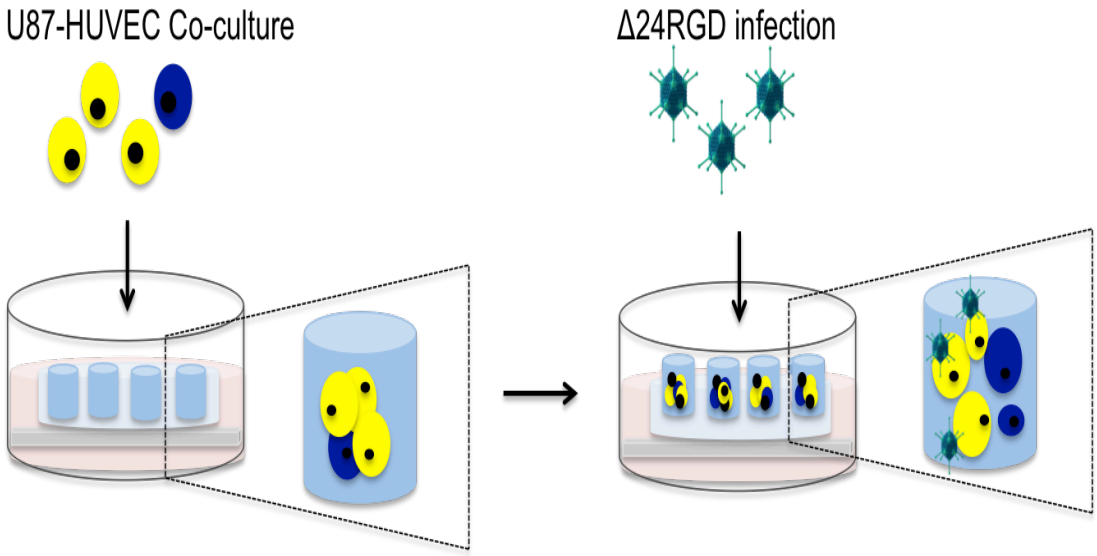

Figure 2. 5. Schematic representation of 3D tumor infection. Co-cultured U87-HUVEC spheroids were treated with Δ24RGD-GFP.

2.2.13. Quantification of cell lysis

Lysed cells were accessed by trypan blue exclusion assay. Briefly, trypan blue solution (0.4%) was prepared in PBS. Both type of cultures were suspended in PBS and 0.1 ml of trypan blue stock solution was added to 1 mL of cells. The unstained (viable) and stained (dead) cells were counted with a hemocytometer within 3 to 5 minutes. Viability is expressed as a percentage of control uninfected cells. The number of viable cells per mL of culture was calculated as shown

$$\%\ viable\ cell = \left[1.00 - \left(\frac{Number\ of\ blue\ cells}{Number\ of\ total\ cells}\right)\right] \times DF \times 10. \quad (1)$$

2.2.14. Validation of GFP expression by Δ24RGD-GFP

To analyze the GFP-expressing characteristics of Δ24RGD-GFP, we compared the GFP expression with uninfected cells. Monolayer and 3D spheroid co-cultures of GBM-HUVEC cells were cultured. Three days after monolayers were seeded and 10 days after

spheroids were seeded, GFP intensity was quantified using ImageJ (National Institutes of Health). Eight images from each different microwell were taken to count the fluorescence intensity. For each microwell, the boundaries were chosen as a region of interest and the fluorescence intensity was calculated.

2.2.15. E1A expression analysis

Cells seeded in monolayer 2D cultures were cultured for 3 days and infected at MOIs of 10, 50, and 100 or uninfected. Control and infected cells were lysed after 72 hours post infection by incubating cells in RIPA lysis buffer supplemented with a protease inhibitor cocktail (1:100). Cells cultured in the 3D microwells for 14 days were infected with Δ24RGD expressing GFP at MOIs of 10, 50, 100, or uninfected, then were collected 10 days after infection. The 3D cells spheroids were collected from the microwells and spheroids were lysed with RIPA buffer for 15 minutes as explained in Materials and Methods of Chapter III. After centrifugation at 14,000 rpm, all supernatant proteins determined by Bradford assay were electrophoretically separated by 4 – 20% SDS-PAGE and transferred to nitro-cellulose membrane. They were probed with antibodies against adenovirus 5 E1A (13 S-5) (1:1000), or β-actin (1:1000) (Santa Cruz Biotechnology, Santa Cruz, CA) overnight. The secondary antibodies were HRP-conjugated secondary anti-mouse and anti-rabbit IgGs (1:2000) (Santa Cruz Biotechnology, Santa Cruz, CA). Uninfected groups were used as controls. Membranes were developed according to Amersham's Enhanced chemioluminiscent protocol with an ECL system (Amersham, Arlington Heights, IL).

2.2.16. Image Acquisition

Microwells and nuclei of the cells were stained with DAPI. The DAPI stock solution was diluted to 300 nM on PBS. 300 µl of this dilute DAPI staining solution was added on top of the cover glass with microwells. The samples were incubated for 5 minutes protected from light. The stain solution was removed and the microwells were rinsed 3 times in PBS. The morphology of the microwells and cells were observed using fluorescence microscope (Olympus, IX51, Melville, NY) and confocal microscopy (Nikon Instruments Inc.).

2.2.17. Statistical Analysis

Data were compared using one-way and the effects of time, days and cell type were evaluated using two-way analysis of variance (ANOVA) followed by Tukey's post-hoc comparisons for repeated measures. A statistical significance threshold was set at 0.05 for all tests (with $p<0.05$). Error bars in the figures represent mean ± standard deviation.

For virus study, infection differences in tumor cell monolayer and 3D spheroids were compared at three doses by Student’s t-test. Two-way ANOVA analysis was fit to the data to examine the effect of serial viral replication with different doses and culture groups (monolayer vs. spheroid) as a treatment effect followed by Student’s t-test.

Chapter 3. The Influence of Human Umbilical Vein Endothelial Cells in The Formation of Glioblastoma Spheroids in Three-Dimensional Microwells

3.1. Introduction

The aggressiveness of the GBM solid tumor is characterized by its rapid vascularization and invasive growth with a high capability for inducing angiogenesis through the secretion of a large quantity of tumor angiogenic factors [3]. As GBM tumor cells experience irregular proliferation beyond the support capacity of the tumor vasculature, growth factors involved in angiogenesis regulation are secreted, which is an essential mechanism for tumor proliferation and metastatic spread [166]. The levels of both vasculature density and expression of angiogenic factors tend to reflect an aggressive tumor phenotype [59]. Therefore, these angiogenic factors released from tumor cells are important for understanding cell abnormalities [66]. Among the several regulators, VEGF has been shown to play an important role in the activation of tumor angiogenesis and the secretion of VEGF by tumor cells increases the expression of certain endothelial cell genes as well as other molecules such as PECAM-1 [167, 77]. VEGF receptors (VEGFRs) such as VEGFR2 were also shown to regulate functions including proliferation, migration, and differentiation that are inherent to endothelial cells [49, 168]. Therefore, it is critical to develop new and robust *in vitro* cell models so that we can better understand the complex behavior of GBM tumors and overcome the limitations of GBM research. Different 2D and 3D models have been used to study GBM angiogenesis and the microenvironmental contributions to cell behaviors. Brown et al., investigated the influence of tumor cells on the expression of endothelial cells by co-culturing U87 glioblastoma cells with HUVEC. They demonstrated that HUVECs co-

cultured with GBM cells in 2D showed resistance to radiation-mediated cell death. The expression of HUVEC genes were affected by the VEGF secreted from U87 GBM cells [167]. A 3D *in vitro* angiogenesis model by co-culturing human glioma cells U87, T98 and human teratocarcinoma cells NT2 with HUVECs in a fibrin gel system were characterized [169]. This model used to study the role of VEGF in vascular sprout formation and restate the relationship between VEGF and angiogenesis in GBM cultures. They suggested that VEGF is the only factor that regulates HUVEC growth under the co-culture conditions. Khodarev et al., found that when U87 GBM was co-cultured with HUVECs, tumor cells stimulated the formation of the paracrine loops via soluble growth factors as well as the formation of autocrine loops in endothelial cells [170]. These results support the idea that multiple factors play roles in the stimulation of growth and differentiation of endothelial cells when co-cultured with glioma cells.

In this study, we introduced a 3D *in vitro* tumor model with an increased complexity by co-culturing GBM cells with HUVEC in a 3D PEGDA hydrogel microwell platform to mimic the *in vivo* GBM tumors microenvironment. We investigated whether endothelial cells influence GBM tumor growth and progression. To gain further insight into the signaling pathways, we studied the gene expression profiles of the 3D *in vitro* co-culture, by using qPCR and quantified PECAM-1/CD31, KDR/VEGFR2 and Phosphatidylinositol 3-kinase regulatory subunit alpha (PIK3R1). Our fluorescence intensity and gene expression data suggested that 3D co-culture spheroids generated in the hydrogel microwell platform could mimic the tumor microenvironment. We believe that our 3D co-culture spheroids could be effective for 3D *in vitro* angiogenesis, gene expression profiles and high throughput drug screening studies.

3.2. Results

3.2.1. Cell Culture Studies

In this study, mono and co-culture spheroid growths were monitored over 21 days using the fluorescence microscope; the effect of the cell-seeding ratios on the cell spheroids' formation was observed. To assess the uniformity and formation of spheroids, we tracked the GBM and HUVEC cells using blue and red cell trackers, respectively. At a ratio of GBM:HUVEC 1:1, mono-culture GBM cells formed tight 3D spheroids in PEGDA hydrogel microwells within 21 days of culture. We observed that the GBM spheroid's size was controlled by the size of the microwell regardless the culturing time as shown in **Figure 3.1A**, GBM column. HUVEC mono-culture showed that the cell-cell contact was not as confluent as GBM tumor cells (**Figure 3.1A**, HUVEC column). GBM-HUVEC co-culture was also relatively uniform in spheroid shape (**Figure 3.1A**, co-culture column). When we increased the seeding ratio to 3:1, the ratio-dependent behavior of the GBM cells was observed as expected (**Figure 3.1B**, GBM column). Cells growth and formation of the spheroids were higher than 1:1 ratio as observed in **Figures 3.1A** and **B**, GBM columns. At 3:1 ratio, GBM mono-culture and GBM-HUVEC co-culture showed relatively uniform spheroid shapes compared to HUVEC mono-culture as we can see in **Figure 3.1B**. The side view images of the GBM-HUVEC co-culture also showed that cells were able to grow as 3D cell spheroids as shown in **Figure 3.1C**.

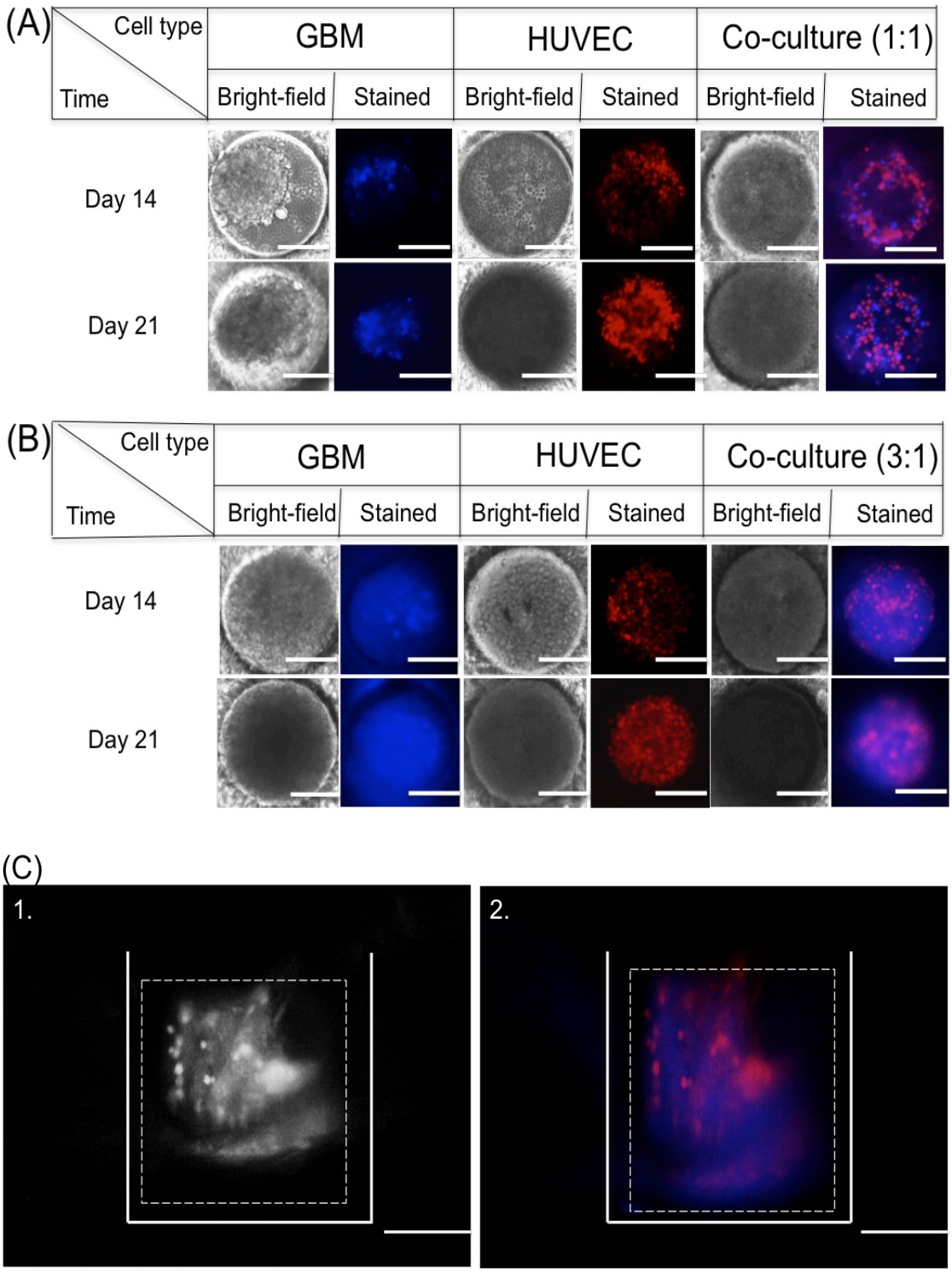

Figure 3. 1. Fluorescence microscopy images of cells within microwells (A-B) Mono and co-cultured cells at a ratio of 1:1 and 3:1. (C) Fluorescence side view image at a ratio of 3:1. Scale bars represent 200 μm.

When GBM was co-cultured with HUVECs with the ratio of 1:1, there is statistically significant difference in the observed fluorescence intensity both for time (days) $p<10^{-12}$ and cell types (GBM vs. HUVEC vs. GBM+HUVEC) $p<10^{-8}$ with two-way ANOVA. A significant increase in HUVEC mono-culture growth was observed starting from day 7 and a decrease was observed at day 21. When comparing day 21 data, t-test showed that GBM and HUVEC are different with $p<10^{-3}$, GBM and GBM + HUVEC are different with $p<10^{-3}$ and no significant differences were observed between HUVEC and GBM + HUVEC.

When GBM was co-cultured with HUVECs with the ratio of 3:1, we observed that there is statistically significant difference both for time (days), as well as for cell types (GBM vs. HUVEC vs. GBM+HUVEC) $p<10^{-30}$. For day 21, we have statistically significant difference for all 3 cases (GBM vs. HUVEC $p<10^{-3}$, GBM vs. GBM + HUVEC $p<0.01$ and HUVEC vs. GBM+HUVEC $p<10^{-8}$, t-test) **(Figure 3.2).** We observed a significant increase ($p<10^{-30}$) (two-way ANOVA) in cell growth when the ratio was increased however when the GBM cells and HUVECs were co-cultured in the ratio of 3:1 in the microwells, there was a decrease in the cellular growth at day 21.

The 3D spheroid formation of the co-cultured cells was observed with confocal imaging. We stained the cells with calcein AM to asses cell viability and the high green fluorescence determined the living cells with high viability in the microwells. The merged blue and red fluorescence from the cell trackers of GBM and HUVEC respectively, also showed that the cells were able to grow together to form 3D spheroids (**Figure 3.3**).

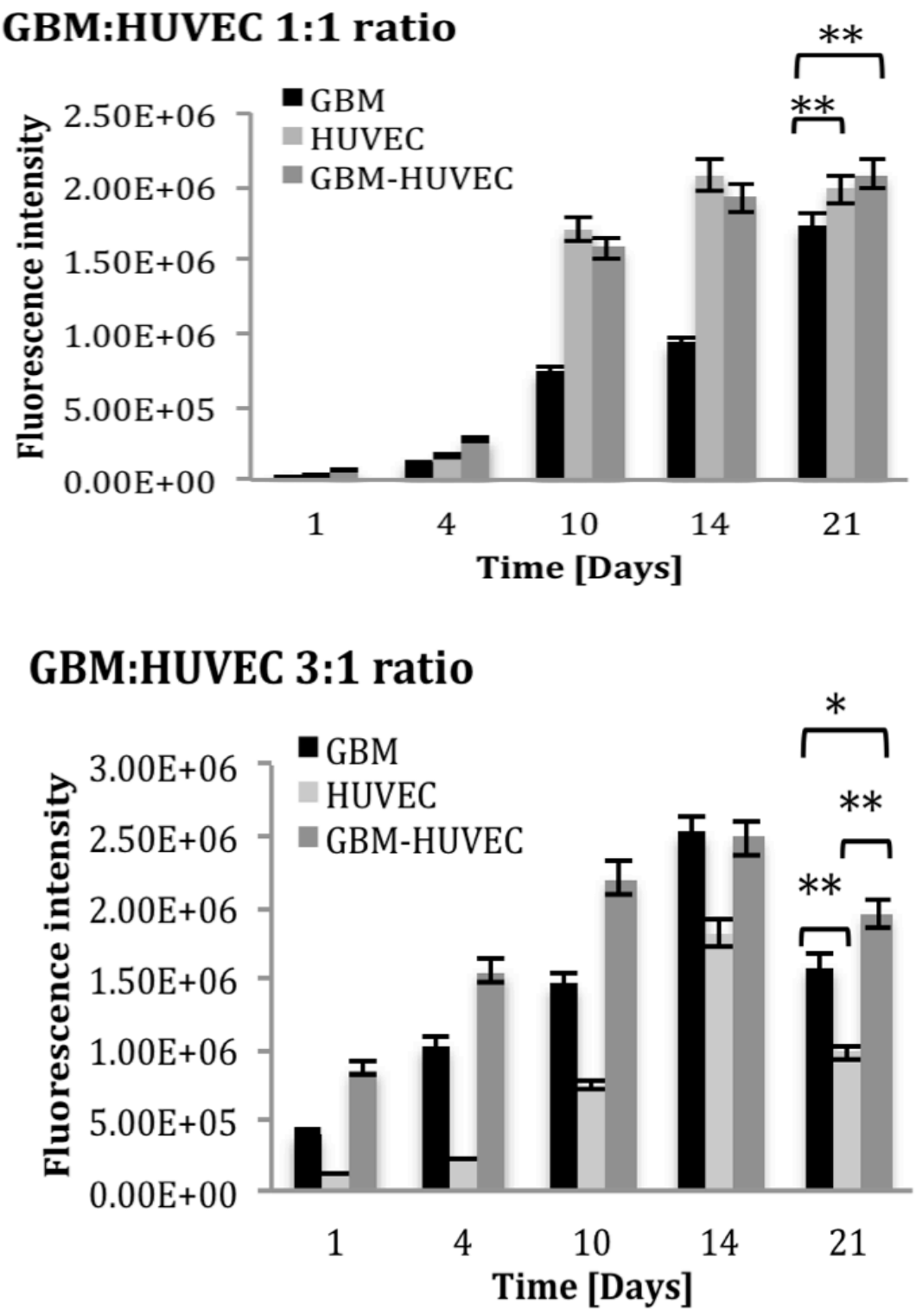

Figure 3. 2. Cellular growth of GBM and HUVEC spheroids over a period of 21 days in the microwells (* denotes $p < 0.05$, ** denotes $p < 0.01$, sample size n=16).

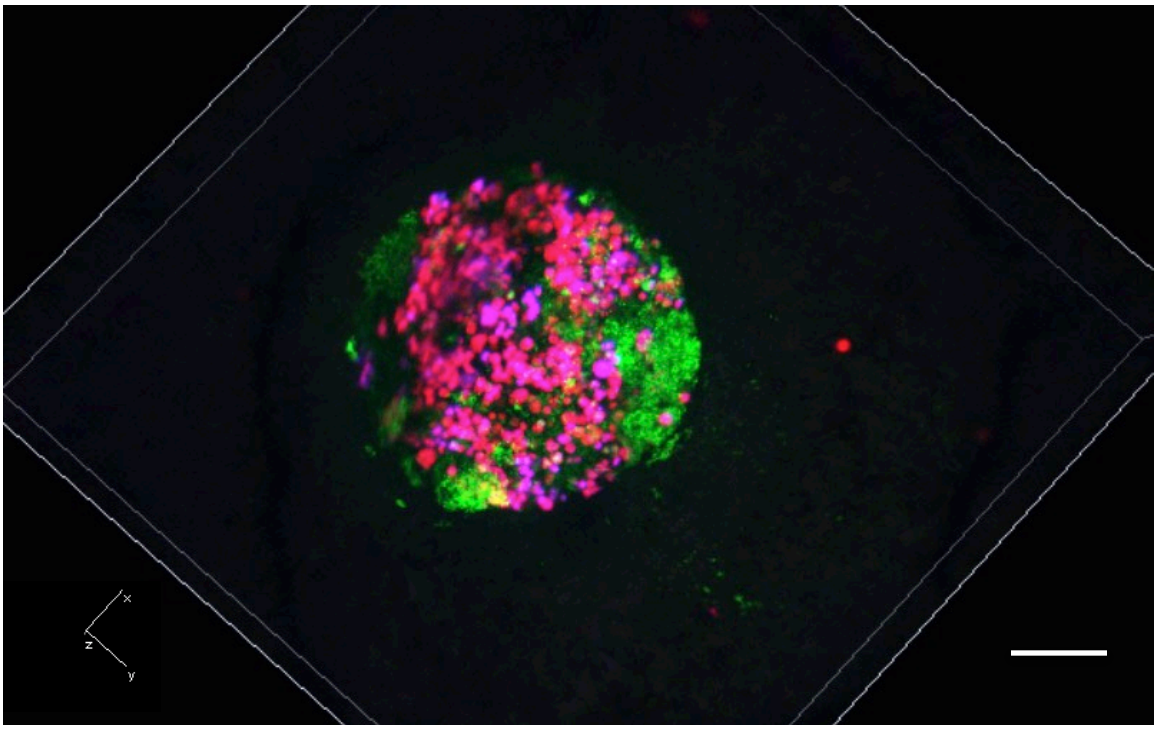

Figure 3. 3. Confocal images of 3D GBM-HUVEC co-culture spheroids tracked with blue and red Cell Trackers, respectively, within the microwell. Scale bar corresponds to 100 μm.

3.2.2. Gene Expression Studies

To further test the viability of our PEGDA hydrogel platform we investigated the molecular characteristics of the tumor spheroids resulting from GBM and HUVEC co-culture. Our results indicate that co-culture significantly upregulated CD31 expression by 14.9-fold when compared to HUVEC mono-culture ($p<0.05$) as shown in **Figure 3.4**. At the same time, the relative change in the expression of CD31 in co-culture when compared to GBM mono-culture was only 1.36-fold.

To extent gene expression analysis, we investigated the expression of VEGFR2 in GBM-HUVEC co-culture. In **Figure 3.4,** although the results did not reach statistical significance, gene expression analysis showed a relative 2.8-fold up-regulation in VEGFR2 expression in co-culture, when compared to HUVEC mono-culture.

Additionally, lower levels of expression of the gene (only 1.28 fold change up-regulation) were detected in co-culture when compared to GBM cells. We noticed that PIK3R1 showed an up-regulation trend in co-culture spheroids, with a relative fold change of 3.07 when compared to GBM mono-culture. A lower level of up-regulation with a relative 1.87 fold change was identified when comparing the GBM-HUVEC co-culture with HUVEC mono-culture as shown in **Figure 3.4.**

We performed western blotting to analyze the expression of VEGFR2 and CD31 endothelial cell markers. Both cell lines U87 and HUVEC expressed VEGFR2. VEGFR2 expression in co-culture was upregulated than the mono-cultures. Contrary to HUVEC that express a CD31, interestingly, GBM cells did not express endothelial cell marker CD31 although the gene expression results showed CD31 to be expressed to a certain degree in U87 cells. Co-culture of GBM and HUVEC cells displayed high expression of CD31 (**Figure 3.5**).

3.3. Discussion

In this study, we co-cultured GBM and endothelial cells in order to investigate the progression of GBM cells co-cultured with endothelial cells in 3D microwells and better simulate the *in vivo* GBM tumor microenvironment. GBM cells and HUVECs were mono and co-cultured with 1:1 and 3:1 ratios, respectively and the spheroid growth was monitored over 21 days using the fluorescence microscope. We have previously concluded that the cell seeding concentration was important to get cell spheroids because the cancer spheroid's growth was mostly controlled by the size of the microwells [133], which is also confirmed in the results of GBM:HUVEC 1:1 culturing ratio in **Figure 3.1A**.

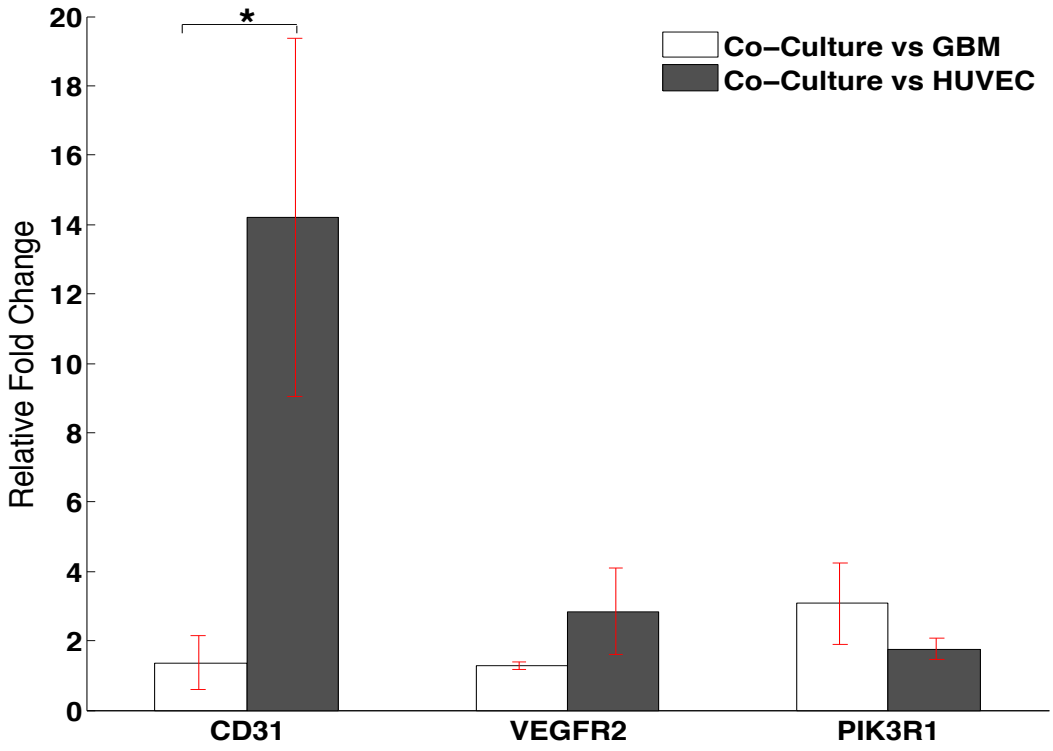

Figure 3. 4. Quantitative analysis of CD31, VEGFR2 and PIK3R1 genes using 2^ΔΔCt method. Results correspond to 3:1 co-culture ratios (* denotes p< 0.05).

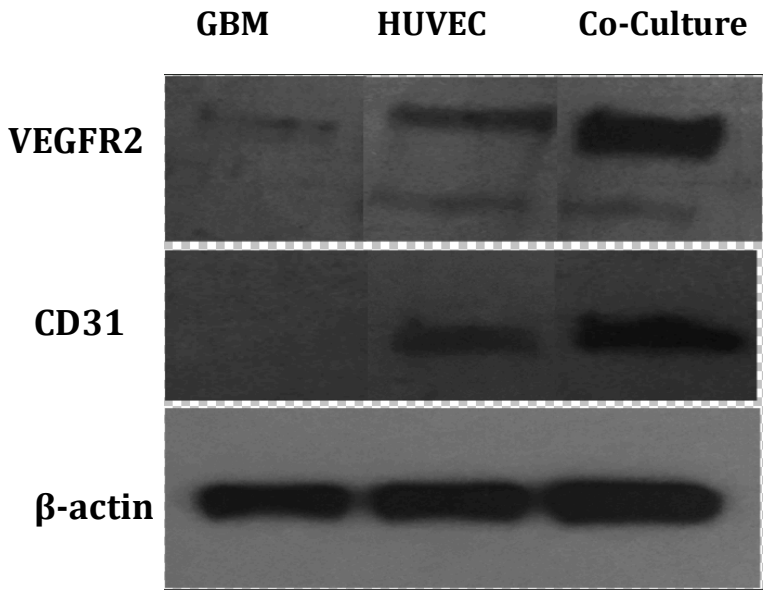

Figure 3. 5. Western blot analysis against VEGFR2 and CD31. β-actin expression was used as a loading control. Western blots are representative of three independent experiments.

Consistent with our previous results [133], in this study, we observed the GBM spheroid formation in the microwells, the GBM and HUVEC co-culture studies also showed that, the co-cultured cells were able to form cell spheroids in the hydrogel microwells as shown in **Figures 3.1A** and **B**. When we compare the GBM:HUVEC co-culturing ratios 1:1 and 3:1, mono-cultured tumor cells continued to grow for 21 days at both ratios, however a decrease in the HUVEC mono-cultures were observed at day 21, which could support the idea of stimulation of endothelial cells by tumor cells as the initial stages of the angiogenesis [170]. When comparing GBM:HUVEC 1:1 and 3:1 culturing ratios, a significant increase in the cell growth was observed when the ratio was increased however when the GBM cells and HUVECs were co-cultured in the ratio of 3:1 in the microwells, there was a decrease in the cellular growth at day 21. Fluorescence intensity measured by Live/Dead cell assay showed a decrease at day 21. This decrease could be due to the size of the microwells that constrains the growth of the cell spheroids or the lack of enough oxygen and nutrients in the core of the spheroids could result hypoxia in the tumor [171] (**Figure 3.2**). These finding suggest that tumor spheroid formation was ratio dependent as we expected. When two types of cells were co-cultured, our results showed that the 3:1 ratio was mimicking the *in vivo* environment of the cells better than 1:1 ratio. Our results are consistent with the literature since GBM tumor cells show continual unregulated proliferation [172], and invade HUVEC cells, as we can observe in the GBM-HUVEC stained image from Day 21 at a ratio of 3:1, in **Figure 3.1**. Also with this ratio, we were able to easily distinguish living cells by the enzymatic conversion of calcein AM to fluorescent calcein. As shown in **Figures 3.1** and **3.2**, we observed continuous tumor growth in our PEGDA hydrogel platform. For 14 days, which

is extended culture time, the co-cultured cells were able to keep their high viability and their structures; they also showed an increased growth and development starting from day 4 for both ratios.

To assess the reliability of our 3D *in vitro* co-culture platform, we investigated the *in vitro* gene expression differences between mono and co-cultures that mimic direct and indirect interactions of tumor and endothelial cells. We selected 3 genes (PECAM-1/CD31, KDR/VEGFR2, PIK3R1) that have been shown to play important role in the tumor angiogenesis. Because of the role of CD31 (a cellular adhesion receptor) to initiate the cell-cell contacts *in vitro* experiments [173], CD31 is evaluated as one of the important gene for angiogenic process [177]. Our gene expression data showed a significant increase in the relative expression of CD31, when comparing co-culture samples with GBM and HUVEC mono-cultures. We hypothesized that the relative down-regulation of CD31 in HUVEC cells might be related to the reduced cell-cell contact we observed in our HUVEC mono-cultures, as a result of decreased cell viability at this stage. Similar observations have been reported in sub-confluent HUVEC cell cultures with reduced cell-cell contact [174–176]. At the same time, the expression of CD31 in co-culture was slightly upregulated when compared to GBM mono-culture. This result might be explained with previous observations, which showed CD31 to be expressed to a certain degree in GBM cells [77].

3D *in vitro* co-culture models can restate fundamentals of the angiogenic process, including endothelial cell proliferation. Angiogenesis is regulated by growth factors and their receptors. As a growth factor receptor, VEGFR2 have shown to be directly correlated with angiogenesis and malignancy of GBM which is highly angiogenic tumor

and overexpress VEGFR2 [178]. Therefore, we also demonstrated VEGFR2 expression differences in mono and co-cultures. We observed a relative fold increase in VEGFR2 expression in co-culture when comparing co-cultures with mono-cultures that confirmed the role of VEGFR2 as marker for tumor angiogenesis in our 3D *in vitro* co-culture model. Moreover, when compared to GBM mono-culture, we observed relatively similar levels of expression of the VEGFR2 which suggests that it is expressed in cancer cells, as previously reported [168, 179–181].

Phosphatidylinositol 3-kinases (PI3Ks) are lipid kinases and they are involved in several important regulatory pathways such as regulation of cell cycle, apoptosis, DNA repair, angiogenesis, and cellular metabolism and in endothelial cell migration during angiogenesis through VEGF signaling [182]. It has been reported that the phosphatidylinositol-3-OH kinase complex and the regulatory subunit gene (PIK3R1) can be mutated either by deletion of PTEN (phosphatase and tensin homologue, located on chromosome TEN) and/or amplification of VEGFR and their alteration is involved in tumorigenesis in several cancer types including glioblastoma [58, 183, 184]. Previous studies highlighted PIK3R1 to be among the genes significantly mutated in GBM [185–187]. VEGFR2 has binding sites for p85 regulatory subunit of PI3K and its binding result in increased PI3K activity *in vitro*, which is responsible for endothelial cell proliferation [188]. However in terms of gene expression, the regulatory subunit gene PIK3R1 was neither amplified nor overexpressed in GBM [189]. To ascertain whether our 3D *in vitro* microwell co-culture model influences the expression of PIK3R1 gene and check the contribution of PIK3R1 gene in GBM and HUVEC culture, we also investigated regulatory subunit gene PIK3R1. We observed PIK3R1 to be upregulated in co-culture

spheroids when compared to GBM mono-culture and a lower level of up-regulation was noticed when comparing co-culture with HUVEC mono-culture.

To test the hypothesis that HUVEC cells act on GBM cells, we investigated the mono and co-cultured cells. We performed western blotting to analyze the expression of VEGFR2 and CD31 endothelial cell markers. Although VEGFR2 is known as an endothelial cell protein, evidence suggests that it may be expressed by cancer cells [190]. Our results showed that both cell lines GBM and HUVEC expressed VEGFR2, whereas GBM cells expressed VEGFR2 less than HUVECs. Co-culture of GBM-HUVEC expressed stronger VEGFR2 than the mono-cultures (**Figure 3.4**). Western blots results for CD31 endothelial cells marker showed that HUVEC expresses CD31. However, GBM cells did not express endothelial cell marker CD31 showing that GBM cells were distinct from endothelial cells, consistent with previous reports [191].

Although, the qPCR results of co-culture vs. GBM displayed higher expression of CD31 than mono-cultures, studies showed that gene expression is controlled at many different stages between transcription and translation and changes in gene expression level may not be frequently reflected at the protein level [192–195]. The higher expressions of VEGFR2 and CD31 in both co-cultures suggest that the interaction of endothelial cells with tumor cells could effect the expression of cell markers.

Chapter 4. Delta-24-RGD Induced Cytotoxicity Of Glioblastoma Spheroids In Three Dimensional PEG Microwells

4.1. Introduction

For several decades, oncolytic viruses (OV) have been used as a promising approach for cancer therapy in both preclinical models and clinical trials with human patients because OVs are able to replicate selectively in cancer cells after genetic mutations. OVs show multiple cancer killing mechanism including (i) direct oncolysis of cancer cells by the virus (e.g., apoptosis, necrosis and autophagic cell death) [196], (ii) necrotic death of the uninfected cells induced by anti-angiogenesis and anti-vasculature of OVs [197] and (iii) activation of innate and tumor-specific immune cells resulting in a cytotoxic effect on cancer and stromal cells [198]. They can infect both normal and cancer cells, but replication can only occur in cancer cells. When the cancer cell is lysed, infective viral progeny is released into remaining tumor tissue and infects other neighboring cancer cells [199]. As the most commonly used vectors, adenoviruses (Ad) (24%) and retroviruses (20%) have been reported to be the most effectives (**Figure 4.1**)

4.1.1. Adenoviruses

The adenovirus belongs to the family *Adenoviridae*, which is divided into four established genera: *Mastadenovirus* originating from mammals, *Aviadenovirus* from birds and the two smaller genera, *Atadenoviruses* and *Siadenovirus*, originating from a broad range of hosts including reptiles and ruminants [200]. The various types of human *Mastadenovirus* are divided into six species (A–F) based on DNA homology and hemagglutination patterns [201]. Adenovirus class C serotype 5 (Ad5) is the most well-described serotype, with a genome of approximately 36 Kbp [202].

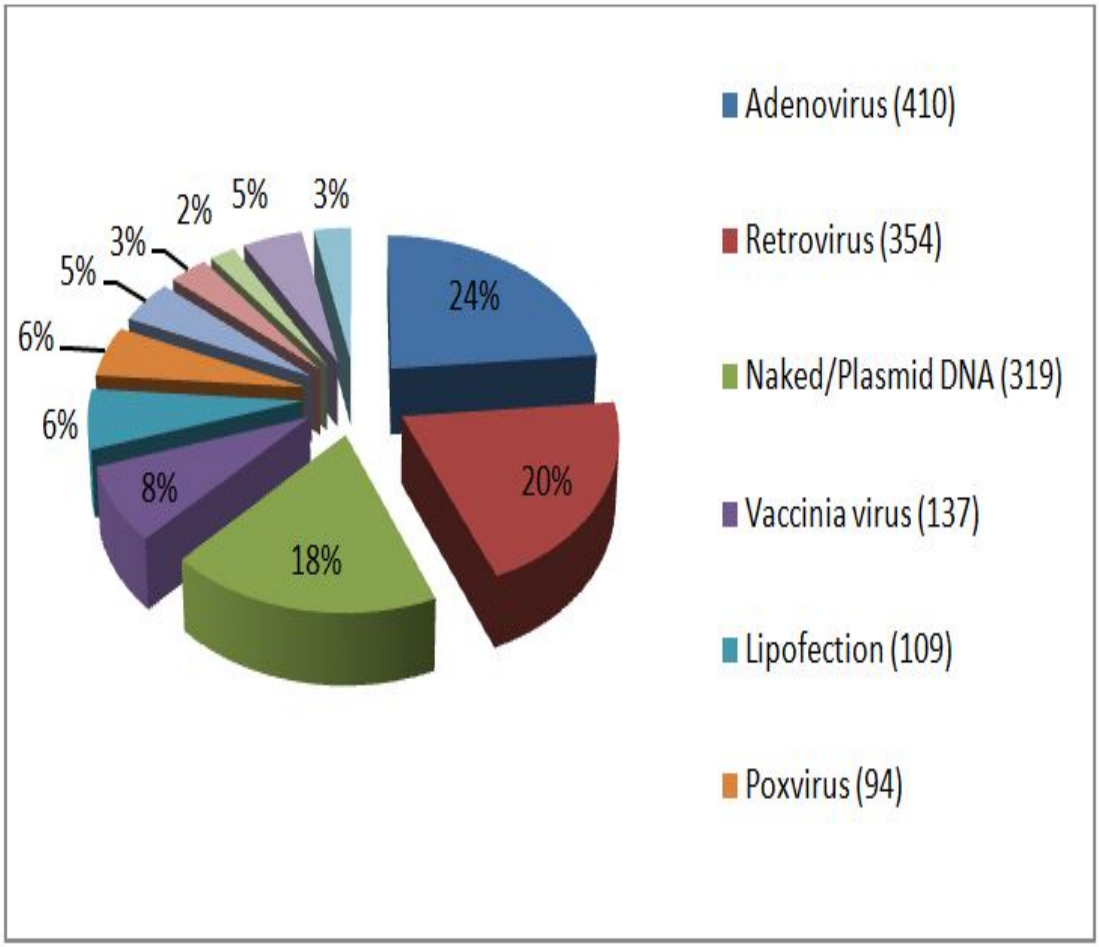

Figure 4. 1. Graphical representation of transfer vectors used in clinical settings provided by Wirth and Ylä-Herttuala [203].

Ads were first characterized by Rowe and colleagues in the 1950s from tonsils and adenoid tissues of children with acute respiratory infections; epithelial cells are the primary targets for adenovirus pathology [204]. They are considered to have low-pathogenicity due to the self-limiting infections [205].

Ads are non-enveloped, DNA viruses. The mature adenovirus particle is ~70–100 nm in diameter and consists of an icosahedral-shaped capsid with a double stranded DNA genome. The protein capsid of the adenovirus promotes virus attachment and internalization. Initially, the fiber knob domain containing a Coxsackie and Adenovirus receptor (CAR) cell receptor serves as the principal attachment receptor and the Arg-Gly-

Asp (RGD) motif in the penton-based capsid promotes the internalization through αv integrins [206] (**Figure 4.2**). Then, the virion is released from the endosomes.

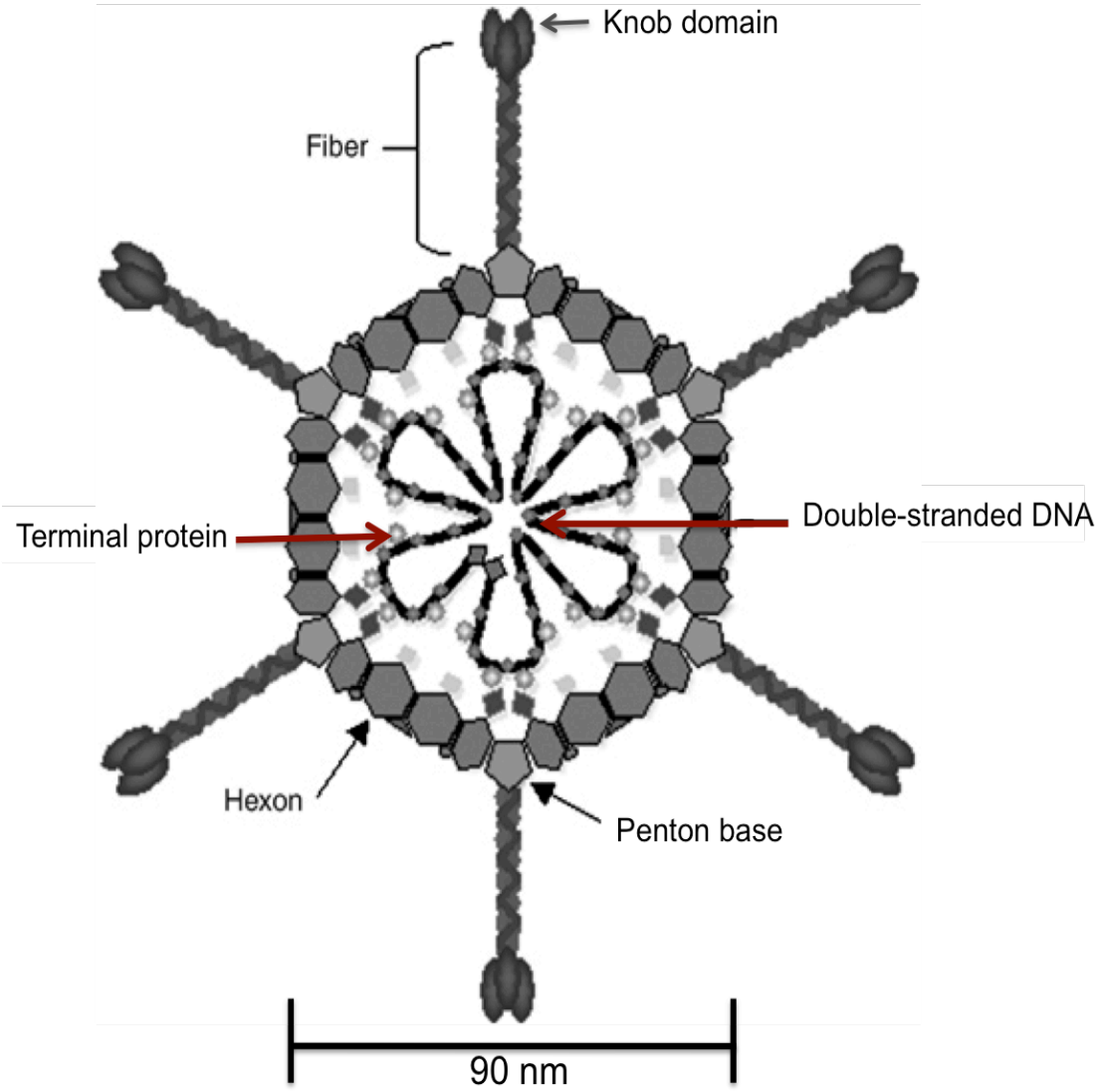

Figure 4. 2. Schematic representation of the adenovirus structure [207].

Adenovirus transcription can be divided into two phases: Early and Late Phases. The Ad5 genome is made up of four early genes (*E1–E4*) and five late genes (*L1–L5*) as shown in **Figure 4.3**. The proteins of the early phase are expressed from six different transcription units: E1A, E1B, E2A, E2B, E3 and E4. Among the E-genes, E1 and E4 are involved in virus replication and cell cycle control; E2 gene products, E2A and E2B, are

involved in DNA replication; while E3 is involved in virus specific immune responses [208–211]. The E1 gene products, E1A and E1B, are regulatory factors that are necessary for transcriptional activation of the E-genes. E1A regulates the tumor suppressor protein, p53, and mediates cell cycle arrest or apoptosis upon DNA damage [212]. The late genes (L-genes) transcribed later than E-genes are from the same major late promoter (MLP) [213]. From a single transcript, at least 18 different late mRNAs are produced by splicing and grouped from L1 to L5. They encode structural proteins used for viral assembly. The signals responsible for the packaging of the adenovirus DNA into the capsid are the inverted terminal repeats (ITRs), which are present on the 5' and 3' ends. Upon assembly, adenoviruses express the adenovirus death protein (E3, which is 11.6K long) to lyse the cells allowing for their release and dissemination [214] (**Figure 4.4**).

4.1.2. Adenoviruses As Cancer-Therapeutics

Clinical trials with adenoviruses have been conducted due to their potential as anti-cancer therapeutics since their discovery in the 1950s [216]. Several approaches, which include the combination of viruses with cytotoxic drugs and radiation therapy, have been proposed to improve the oncolytic therapy. Most of the trials involve mutations or deletions of certain viral genes that can be complemented in tumor cells, but not in normal cells (**Table 4.1**).

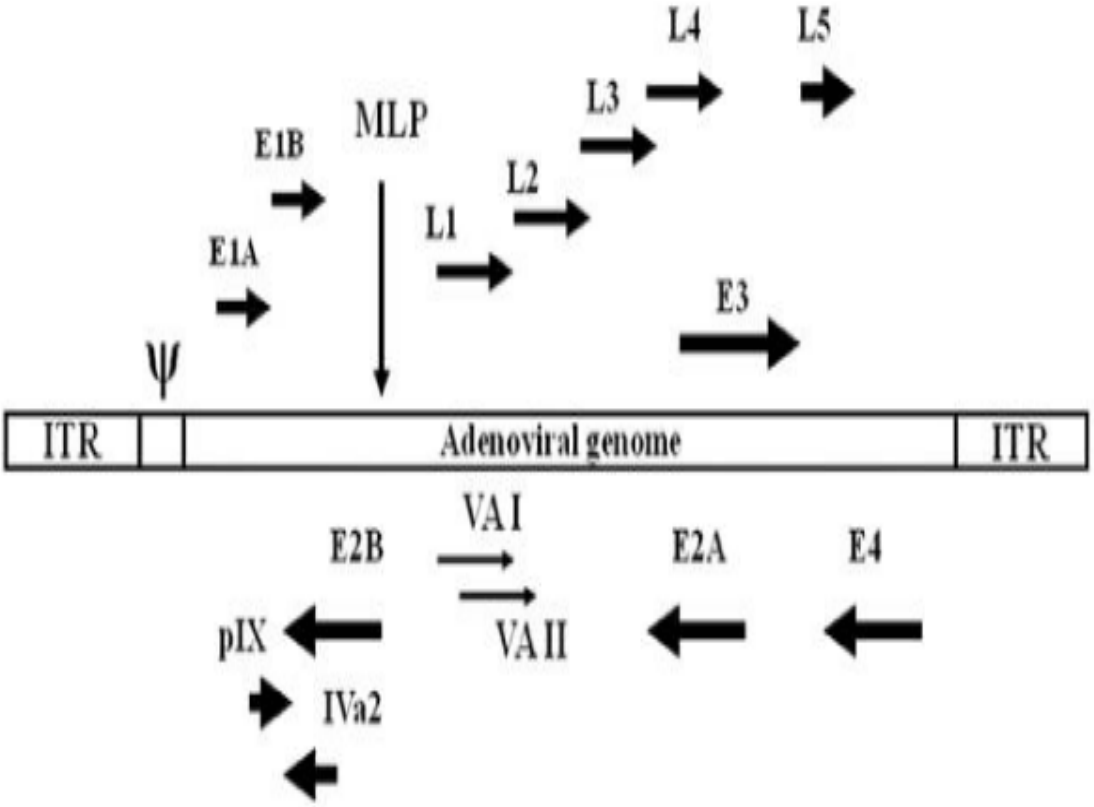

Figure 4. 3. The adenovirus genome showing the early and late genes. Arrows indicate the direction of transcription [214].

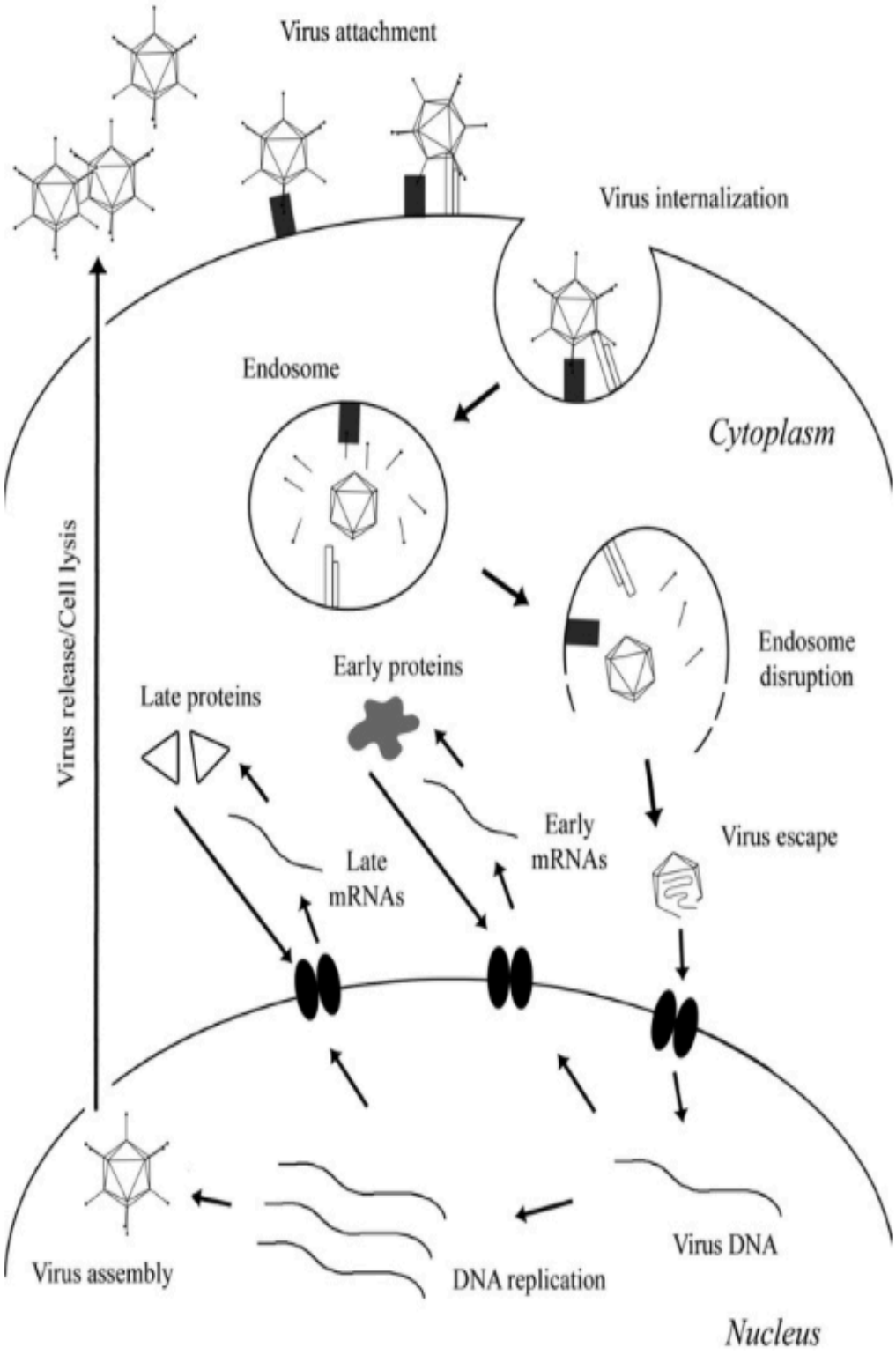

Figure 4. 4. Adenovirus Basic Replication Cycle. Adapted from Wagner et al., [215].

Table 4. 1. Representative gene therapy and virotherapy methods

Delivery vehicle	Virus type	Mode of action	Advantages	Disadvantages
Non replicating virus	Adenovirus	Cell cycle arrest	Focused action depending on the transferred gene	Minimal transduction efficiency
Replicating viruses (virotherapy)	Modified adenoviruses	Direct cell lysis by the virus	Multiply and spread to adjacent cells	Intracranial administration

E1A gene recognizes Retinablastoma (Rb) protein and binds to it. The binding results in the cell cycle to move from G0 and G1 into S phase by the release of E2F. Then, E2F activates both the E2 promoter of the adenovirus and cell cycle-regulatory genes. Cell cycle arrests do to the binding of E1B 55K protein to E2F and the inhibition of p53. A mutation of p53 is one of the most frequent genetic alterations in cancer, occurring in more than 50% of cancers [217]. E1 gene-coding region mutated adenoviruses can replicate in Rb- or p53- deficient tumor cells, while the replication of the mutated viruses is reduced in normal cells with intact pathways [218]. In most brain tumors, it has been shown that either mutation of the p53 gene or posttranslational regulations cause the inactivation of the p53 [217]. Thus, targeting the p53 or Rb pathways becomes important since these are commonly disrupted pathways in most tumors. These conditional-replicating adenoviruses could be selective for tumors.

Ad-p53, a type 5 replication-deficient human adenovirus with a region of the E1-coding gene replaced with the cDNA of the wild-type p53 gene driven by the cytomegalovirus promoter, was first used by Zhang et al., [219]. It has been shown that Ad-p53 was effective against different types of tumor including lung, head, neck and brain tumors with a minimal toxicity in Phase I clinical trials [220].

In 1966, the first generation adenovirus vectors displaying replication-deficient

adenoviruses with mutant E1 gene-coding region was constructed for the clinical trials. ONYX-015, an oncolytic Ad2/Ad5 hybrid has a deletion in the E1B 55K gene-coding region. Therefore it does not express the E1B protein that regulates the inactivation of p53, transport of the viral mRNA, inhibition of the protein synthesis of the host cell, and reduction of the replication in normal cells with intact p53 [221].

Second generation adenovirus vectors were developed to overcome the limited transgene expression capacity. These vectors have deleted the E3 region for the insertion of the transgene expression cassette of up to 7.5 kb [222].

In order to reduce the immunogenicity of adenovirus vectors, the third generation of adenovirus vector was developed. They lack viral genes, but contain the inverted terminal repeats (ITRs) and the packaging signal in order to provide more capacity for transgene expression [223]. They were tested for gene replacement therapies [224].

Moreover, adenoviruses have been also modified to increase their infectivity in cancer cells with low levels of CAR by inserting the RGD-4C peptide into the HI loop of adenoviral fiber. This regulates the binding of the virus to the cell integrins with higher affinity [225].

4.1.2.1. Adenovirus Delta-24

Oncolytic adenovirus Delta-24 (Ad-Δ24) was developed in the late 1990s by Fueyo and his colleagues [226]. Ad-Δ24 has a 24 bp deletion in the E1A gene-coding region. It is expressing a mutant E1A protein that does not bind to Rb and selectively replicates in tumor cell such as GBM with disrupted Rb pathway [226]. It has been showed that Ad-Δ24 targets the Rb pathway with more efficiency than other mutant adenoviruses such as E1B [227].

To enhance the tumor targeting efficiency, Ad-Δ24 has been improved with the RGD-4C peptide motif inserted into the adenoviral fiber, which allows the adenovirus to attach directly to integrins [225]. The use of Delta-24-RGD (Δ24RGD) used on four GBM stem cell lines and xenografts, which were derived from glioma stem cells, increased autophagic cell death in tumor cells both in *vitro* and *in vivo* studies [228, 229].

4.1.2.2. Oncolytic Viruses and 3D In Vitro Cell Culture Studies

Before the clinical applications, cell culture step is highly desirable for virus studies and for investigating the molecular biology of viral replication. Most commonly, virus studies are carried out in a two-dimensional (2D) environment as monolayer cultures [230–235]. However, several important limitations of 2D cell cultures have been recognized, such as the lack of reproducibility of the morphological and biochemical features, as well as microenvironmental conditions of the original tissues.

Studies using spheroid models, which could mimic *in vivo* characteristics of the tumors, have been reported [44, 236–239]. Adenovirus replication and virus insertion have been studied in 3D organotypic multicellular spheroid model, with both replication-deficient and replication-competent adenoviruses [240]. It has been shown that replication-deficient adenoviruses had limited success in penetrating into the spheroids, while replication-competent adenoviruses were spread into the 3D spheroids [240].

Another possible approach for developing 3D spheroids is to use 3D hydrogels. Recent studies have investigated the use of hydrogels with diverse cell types including endothelial cells, cortical neurons, astrocytes and neuronal progenitor cells [241]. Baby hamster kidney cells cultured in 3D collagens were infected with Sindbis virus and the effect of the collagen gel on the virus interaction with cells was investigated [242]. It was

demonstrated that the Sindbis virus was capable of penetrating the 3D collagen gel and infecting the cells. 3D alginate-encapsulated cells were shown to be potentially useful in viral studies [243]. 2D and 3D adenoviral transduction of human mesenchymal stem cells (hMSCs) encapsulated in alginate, agarose and fibrin hydrogels were compared [244]. They showed that within these hydrogels, 3D adenoviral transduction generated more products per cell and was more efficient than 2D transduction.

Despite all the studies, to our best knowledge, there have not been explorations in the use of the 3D PEGDA microwells for the virus therapy *in vitro*. Therefore, in this study, we fabricated PEGDA hydrogel microwells and co-cultured 3D *in vitro* U87 GBM cells with HUVEC in the microwells as we reported in our previous study. Then, we infected the 3D co-culture spheroids with Δ24RGD in order to examine the cytotoxic effect of the adenovirus at various MOIs over a period of 10 days and assess the reliability of our 3D hydrogel microwell platform in virus treatment. We subsequently compared the results obtained with our platform with those from 2D monolayer cell culture.

4.2. Results

4.2.1. Oncolytic Δ24RGD-GFP activity in 2D cell culture and 3D tumor spheroids

To examine the differences of adenoviral infectivity in 2D monolayer cultures and 3D spheroids fabricated in the PEGDA hydrogel microwell platform, we were first co-cultured GBM cells with HUVECs at a ratio of 3:1, respectively. We then infected both 2D monolayer cells and 3D tumor spheroids with three different doses of Δ24RGD. Monolayer cultures and 3D spheroids were observed for 10 days post-infection and results are shown in **Figures 4.5** and **4.6**, respectively. In 2D monolayer culture, at day 3 post-infection, cells showed continual growth when we infected them with MOIs of 10

and 50. However, they started to lose their monolayer morphology and detached from the bottom of the culture flask after infection at a MOI of 100. When the dose was increased from MOIs of 10 to 50 and 100, there was a progressive accumulation of vacuoles in the cell population. At day 10 post-infection, we observed various vacuolization in infected cells but not in uninfected control groups, which maintained monolayer cell morphology (**Figure 4.5**). With the increase of multiplicity of viral infection, the formation of vacuolization and disruption of the cellular structures were increased compared to MOIs of 10 or 50 as shown in **Figure 4.5**.

In 3D co-culture spheroids, it was observed that the edge of the uninfected control spheroids remained clear and cells continued to grow over 10 days. The Δ24RGD-infected spheroids lost their spheroid shape starting from day 3 post-infection. A distinct cytopathic effect was observed at the periphery of the spheroids after 3 days of infection. Cells were clearly observed detaching from the spheroid at day 10 post-infection (**Figure 4.6A**). The cell death was also observed in 3D co-culture spheroids. Bright field images taken with 20X magnification of fluorescence microscopy at day 10 post-infection demonstrated the increased in the vacuole formation when the multiplicity of infection was increased as shown in **Figure 4.6B**. When we used MOI of 10 of Δ24RGD, the formation of vacuoles was relatively smaller than MOIs of 50 or 100 (**Figure 4.6B**) as we expected.

After the infection with a MOI of 50, we stained cells with ethidium homodimer to detect cell death at days 1, 3 and 10. We observed GFP expression, which showed adenoviral infection of the both 2D monolayer cells and 3D co-culture spheroids, starting from Day 1 post-infection, using confocal microscopy as shown in **Figure 4.7A**.

Expression of GFP showed that Δ24RGD was successfully replicated in the co-culture spheroids and infected cells. At day 3 post-infection, cells started to die. Red dots represent death cells caused by the Δ24RGD as shown in **Figure 4.7B**. However, confocal images showed that cells were still keeping their spheroids shapes at day 3 post-infection. At day 10 post-infection, we observed an increase in the red cells that represented increased cell death induced by Δ24RGD in 3D tumor spheroids. The integrity of the spheroid was almost lost as shown in **Figure 4.7C**.

For the *in vitro* characterization of Δ24RGD on 2D monolayer cells and 3D spheroids, trypan blue staining showed a viral dose-dependent decrease in cell viabilities. **Figure 4.8A** shows Δ24RGD infection in cell cultures; Δ24RGD induced 30% to 41% and 37% to 65% cell death at the viral doses ranging from MOIs of 10 to 100 in 2D monolayer cells and 3D co-culture spheroids, respectively. When we compare multiplicity of infections of 10, 50 and 100, overall cell lysis was 1.1, 1.4 and 1.7-fold more respectively, in 3D co-culture spheroids than 2D monolayer. Our statistical analysis indicated that cell viability after 10 days of infection was significantly reduced when cells were treated with Δ24RGD for both culture types and each different dose ($p<0.01$, two-way ANOVA, n=3) as shown in **Figure 4.8A.** When we compared the differences between the two culture types, the results suggested that there is statistical significance in the cell viability between 2D monolayer and 3D spheroid culture for each of the three doses ($p<0.01$, using t-test).

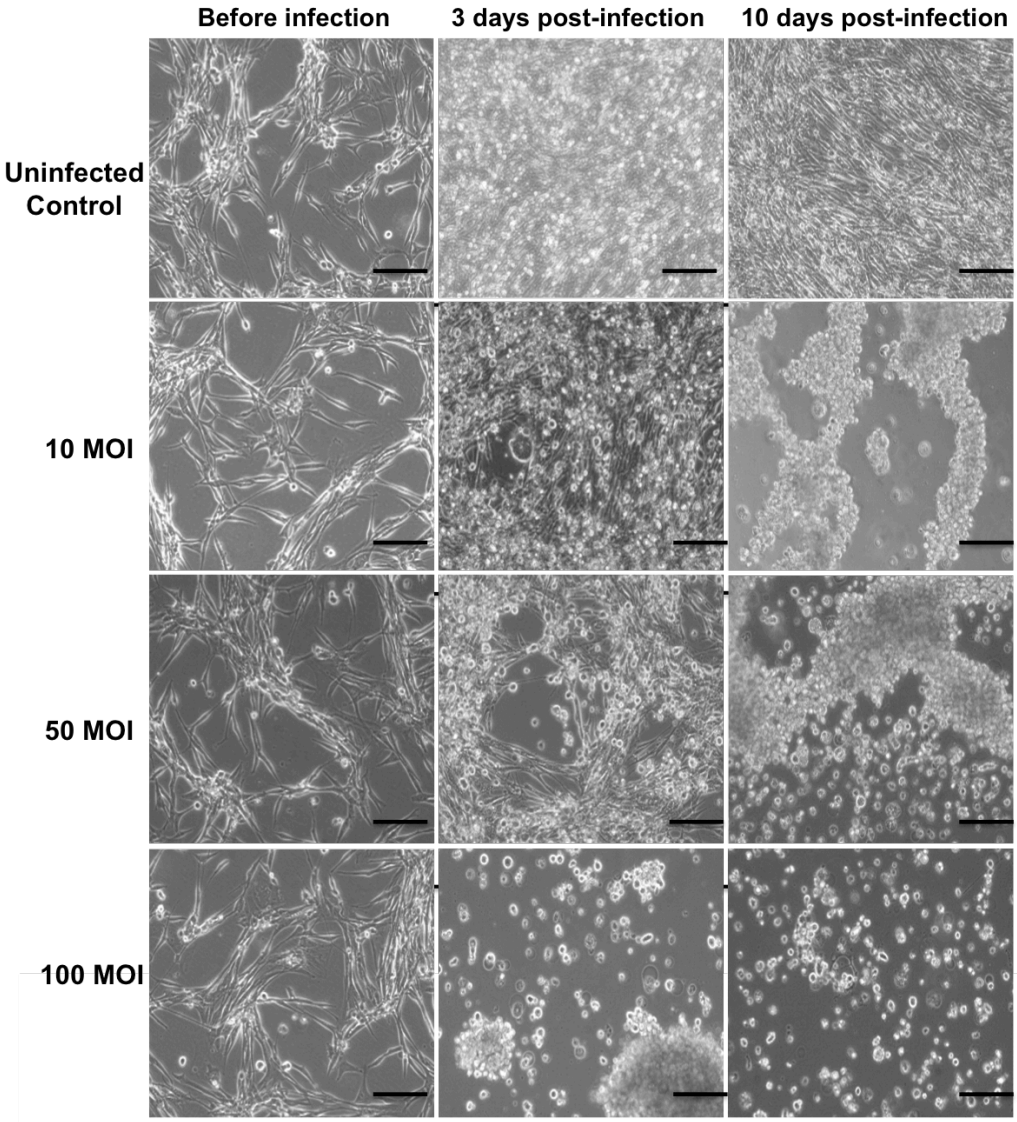

Figure 4. 5. 2D U87 and HUVEC monolayer cells infected with Δ24RGD. The images are representative views of three independent experiments. Scale bars represent 100 μm.

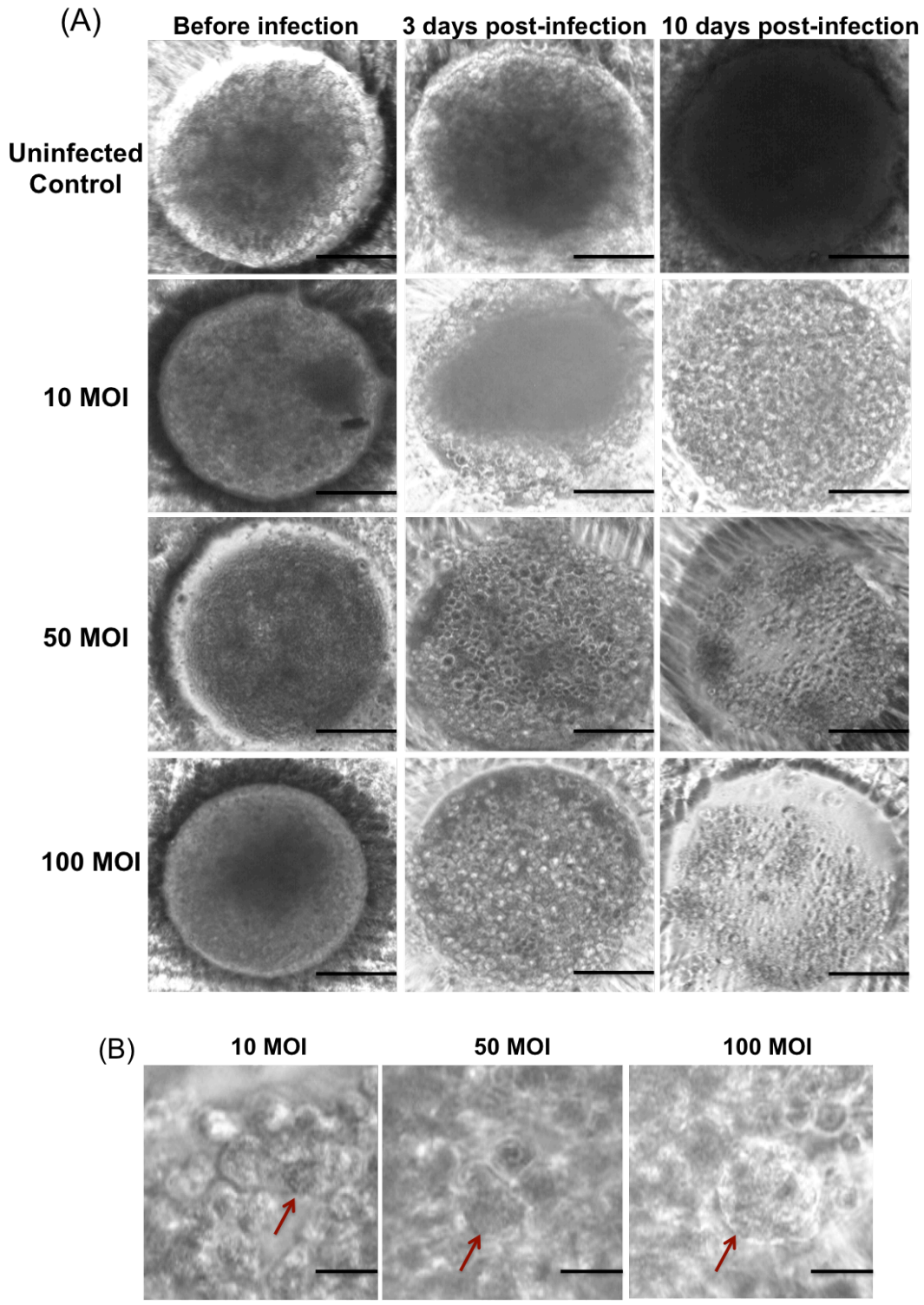

Figure 4. 6. Oncolytic activity of Δ24RGD on 3D co-culture spheroids. (A) Lysis of the 3D spheroids. Scale bars represent 200 μm. (B) At day 10 post-infection, formation of the vacuoles in the cells. Scale bars represent 40 μm.

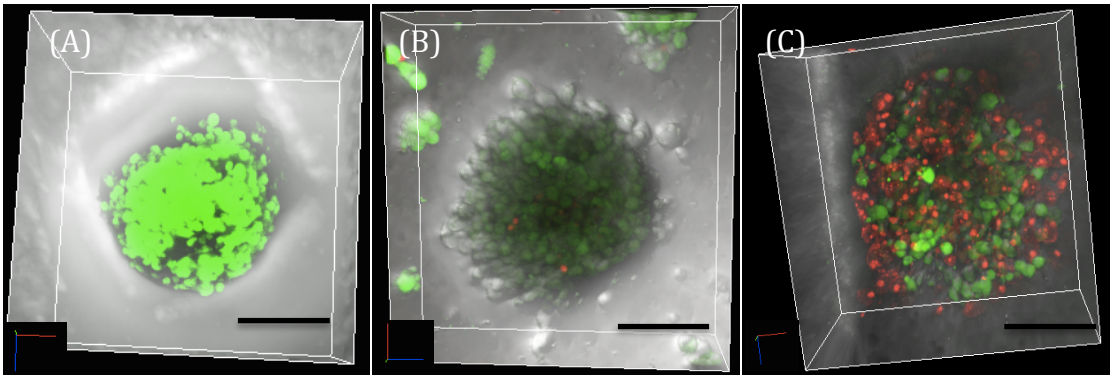

Figure 4. 7. Confocal microscopy image of Δ24RGD expressing GFP infected cells with a MOI of 50. Scale bars represent 200 μm.

Western blot analysis assessed the expression of E1A protein. Tumor spheroids were infected with a multiplicity of infection 10, 50 and 100. On day 10 post-infection, they are subjected to immunoblot analysis. Uninfected control cells were used as controls. β-actin was used as a loading control and the basal level of expression was assessed in uninfected control groups. Day 10 post-infection results confirmed that E1A was expressed in both 2D monolayer and 3D spheroid cultures. We observed that the expression of E1A was upregulated for both cell cultures when the MOI was increased comparing to uninfected control as shown in **Figure 4.8B**.

4.3. Discussion

We have previously showed that the use of PEGDA hydrogel microwells facilitated the 3D spheroid formation [133]. In this study, we used the same methods to generate 3D GBM-HUVEC co-culture spheroids. Then we investigated therapeutic effect of the replication competent Δ24RGD on 3D tumor models fabricated in the PEGDA hydrogel microwells. We also compared our results to 2D conventional models. Δ24RGD has been shown as a potential GBM therapy in preclinical studies [225, 245, 246]. Therefore, our initial reason for applying the replication-competent virus was based on the ability of the virus to penetrate into the tumor spheroids [247–250].

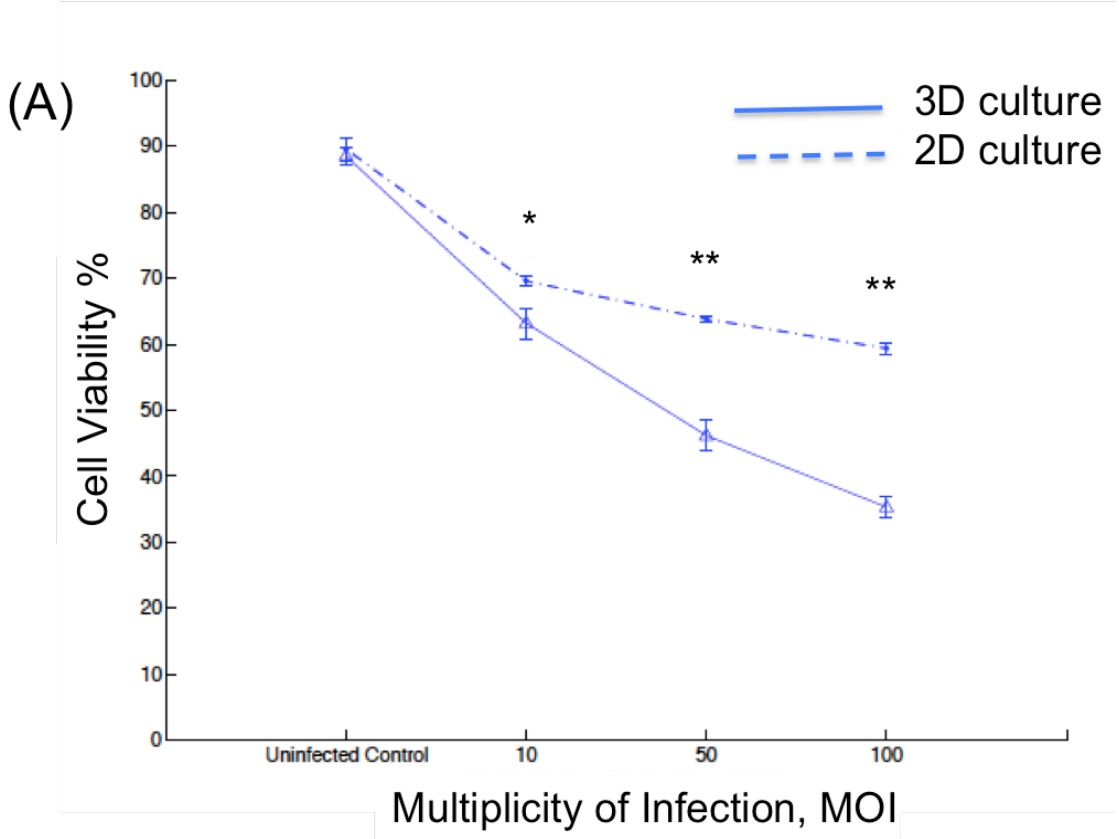

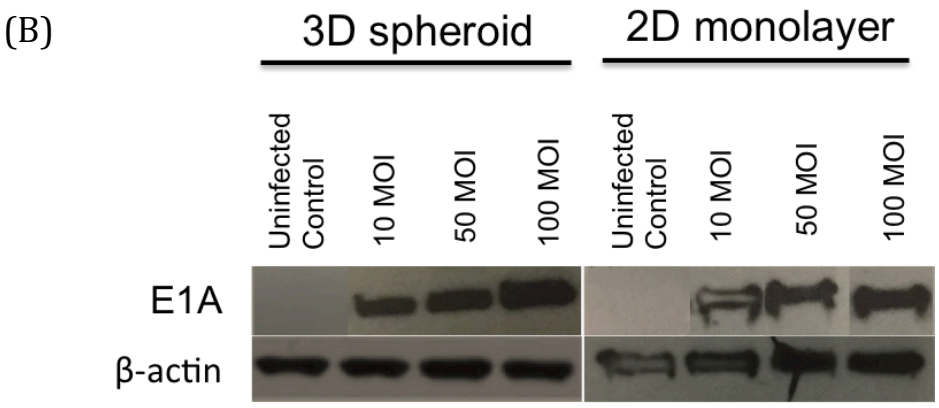

Figure 4. 8. *In vitro* characterization of Δ24RGD in 2D monolayer and 3D tumor spheroids. (A) Cell viability assay. (* denotes $p < 0.05$, ** denotes $p < 0.01$). (B) Western blot analysis of the late adenoviral protein E1A.

We demonstrated the strong replication and oncolytic potential of Δ24RGD in 3D spheroid co-culture, which was generated in hydrogel microwells. During 10 days of infection, the loss of the cell spheroid integrity was clearly observed in the microwells at

all doses (**Figures 4.6** and **4.7**). However, due to the 3D spheroid shape, it was important to determine the dose of the virus. Possibly, the dose of 10 MOI in 3D spheroids was too low to induce enough cell lysis compared to MOIs of 50 and 100 (**Figure 4.6A**). The adenovirus-induced autophagic vacuoles and their role in the cell lysis was previously documented in 2D monolayer cultures [228, 251, 252]. We showed that 3D spheroids in PEGDA hydrogel microwells were also successfully infected with Δ24RGD at all viral doses and underwent cell death (**Figure 4.6B**). We assessed expression of the green fluorescent protein and detected GFP expression in 3D co-culture spheroids as shown in **Figure 4.7**. Our results indicated successful adenoviral infection based on the intense green fluorescence from the GFP. The adenovirus-induced vacuolization, which leads to autophagic cell death was shown to be associated with the cell lysis [252]. When we used ethidium homodimer to stain the co-cultured cells infected with a MOI of 50, we observed that cells were stained. The staining of the cells' DNA was caused by the disruption in the cell membrane, which could be related to autophagic cells death (**Figure 4.7**).

To test the adenoviral therapeutic differences between 2D monolayer and 3D spheroids, we infected both types of cell cultures with Δ24RGD. In our study, Δ24RGD induces the formation of vacuoles and cell lysis in both 2D monolayer and 3D spheroids cultures, providing similar conditions in 2D and *in vivo* studies [228, 249, 253, 254]. After 10 days of infection, the viability of the spheroids significantly decreased compared to uninfected controls, when the multiplicity of infection increased, as expected for both culture types. However, under these conditions, all three dosages tested for 3D spheroids showed a significant decrease in cell viability compared to 2D monolayer culture. The

cell viability results suggested that Delta-24-RGD caused 37%, 54% and 65% cell lysis in 3D spheroids with MOIs of 10, 50 and 100 approximately respectively, significantly higher than the 31%, 36% and 41% in 2D monolayer cells as shown in **Figure 4.8A**. Expression of E1A is required for tumor-specific viral replication and production of the virus [255]. Our results suggested that the virus replication at all doses were also in complete agreement with the findings on the expression of early 1A adenoviral protein (**Figure 4.8B**).

Since solid tumors like GBM have 3D shapes *in vivo*, it is important to design 3D models that mimic the *in vivo* characteristics of the tumors and provide a suitable microenvironment for the interaction of oncolytic adenoviruses with the tumor models, which is essential for studies investigating the use of oncolytic viruses as alternative cancer treatment. Therefore, in this study we proposed a novel approach to analyze the interactions of Δ24RGD with 3D tumor spheroids generated in PEGDA hydrogel microwells. The results suggested that our hydrogel microwell platform could provide a useful 3D spheroid model to investigate the oncolytic potential of the viruses *in vitro*. We believe that this platform could provide a trustable preclinical platform for virus studies and may reduce to a certain extent the need for *in vivo* studies.

Chapter 5. Conclusion and Future Considerations

In this study, a novel 3D *in vitro* co-culture system was described for the investigation and modeling of *in vivo* environment of 3D GBM tumor cells. Their interactions with endothelial cells and adenoviruses for the tumor treatment were investigated.

We used our recently generated 3D microwell platform [133] in order to investigate the progression of 3D GBM spheroids co-cultured with endothelial cells. In our previous study we showed that *in vitro* 3D spheroids were successfully constructed in the PEGDA microwells in which we can control the spheroid's size and shape due to the cell-repellent properties of the PEG-based hydrogels [133]. 3D *in vitro* GBM spheroids generated in PEGDA hydrogel microwells showed rapid and reproducible method for the fabrication of 3D tumor spheroid models. Based on our previous results, we co-cultured 3D GBM cells with endothelial cell spheroids. We used two different ratios of GBM cells and HUVECs (1:1 and 3:1). This approach supported the idea of stimulation of endothelial cells by tumor cells at initial stages of angiogenesis [170]. Fluorescence intensity study confirmed the cellular growth of the 3D co-culture spheroids over a period of 14 days. Additionally, gene expression studies suggested that the down-regulation of the cellular adhesion molecule CD31 in HUVECs, could be related to the decreased cell-cell interaction observed in HUVEC mono-culture, which has previously reported for sub-confluent cell cultures with reduced cell-cell interaction [174–176]. The co-culture spheroids were found useful over 14 days for the high-throughput drug screening with anti-angiogenic potential in cancer research. Therefore, we then investigated therapeutic effect of the replication competent Δ24RGD on 3D tumor models fabricated in the PEGDA hydrogel microwells.

Since solid tumors like GBM have 3D shapes *in vivo*, it is important to design 3D models that mimic the *in vivo* characteristics of the tumors and provide the interaction of the oncolytic adenovirus with the tumor models for the alternative treatment. In the second part of this study, we studied the interaction of Δ24RGD on 3D tumor spheroids. We applied three different doses of Δ24RGD on 3D tumor spheroids and 2D monolayer to compare the adenoviral therapeutic differences between two cell cultures. Δ24RGD induced autophagy and cell lysis in both 2D monolayer and 3D spheroids cultures, providing similar conditions in 2D and *in vivo* studies [228, 249]. However, all three dosage showed a significant decrease in cell viability compared with 2D monolayer culture. Therefore, we believed that our hydrogel microwell platform could provide a useful 3D spheroid models to investigate the oncolytic potential of the viruses *in vitro*. We believe that this platform could provide a trustable preclinical data for virus studies that could also reduce the need for *in vivo* studies in terms of time.

Although PEGDA hydrogel microwells have been shown in this dissertation to be useful for the generation of 3D GBM tumor spheroids, several features could be improved to provide better results. In our previous study, we investigated the cellular growth over 21 days and concluded that PEGDA hydrogel microwells with different sizes (200 μm to 600 μm) and shapes (squares and rounds) were able to control the size, shape and the cellular growth of the GBM mono-cultures for long term culture [133]. In this study, we co-cultured GBM cells with endothelial cells in the 3D microwells for 21 days in order to increase the complexity of the cell culture. However in contrast to our previous study, when we used higher GBM ratio in the co-culture (GBM:HUVEC, 3:1), we observed a decrease in the cellular growth at day 21 for both mono and co-cultures.

We hypothesized that this decrease could be due to the size of the microwells that limits the growth of the 3D cell spheroids [133] or due to the high ratio of the cells, the lack of enough oxygen and nutrients in the core of the 3D spheroids could induce hypoxia in the tumor spheroids [171]. The long-term culture of high ratio cell culturing has not been successfully demonstrated in this system. Therefore, the system could be improved to maintain long-term cell viability.

We observed a decrease in the expression of CD31 in HUVEC mono-culture, although CD31 gene is known as endothelial cell adhesion molecule. The reason that causes this decrease has to be investigated more in order to provide more efficient co-culture model. Additionally, when we observed a decrease in the cellular growth at day 21, we hypothesized that the lack of enough oxygen and nutrients in the core of the 3D spheroids might induce hypoxia in the tumor spheroids [171]. Therefore, the hypoxic conditions and the difference in the HIF-1 gene expression could be investigated using quantitative real-time PCR analysis.

Related Publications

I. Yantao Fan, **Naze G. Avci**, Duong T. Nguyen, Andrei Dragomir, Yasemin M. Akay, Feng Xu, Metin Akay (2015) "Engineering a High-Throughput 3-D *In Vitro* Glioblastoma Model." *IEEE Journal of Translational Engineering in Health and Medicine*, Vol 3. doi 10.1109/JTEHM.2015.2410277.

II. **Naze G. Avci**, Fan Yantao, Andrei Dragomir, Yasemin M. Akay, Metin Akay (2015) "Investigating the Influence of HUVECs In the Formation of Glioblastoma Spheroids In High-Throughput Three-Dimensional Microwells." in submission.

III. **Naze G. Avci**, Fan Yantao, Andrei Dragomir, Yasemin M. Akay, Metin Akay (2015) "Delta-24-RGD Induced Cytotoxicity Of Glioblastoma Spheroids In Three Dimensional PEG Microwells." in submission.

References

1. Mamelak, A.N., Jacoby, D.B., "Targeted Delivery Of Antitumoral Therapy To Glioma And Other Malignancies With Synthetic Chlorotoxin (TM-601)." *Expert Opin Drug Deliv*. 2007. 4: 175–186. doi:10.1517/17425247.4.2.175

2. Goodenberger, M.L., Jenkins, R.B., "Genetics Of Adult Glioma." *Cancer Genetics.* 2012. pp. 613–621. doi:10.1016/j.cancergen.2012.10.009

3. Dolecek, T.A., Propp, J.M., Stroup, N.E., Kruchko C., "CBTRUS Statistical Report: Primary Brain And Central Nervous System Tumors Diagnosed In The United States In 2005-2009." *Neuro-Oncology*. 2012. doi:10.1093/neuonc/nos218

4. Rao, J.S., "Molecular Mechanisms Of Glioma Invasiveness: The Role Of Proteases." *Nat Rev Cancer*. 2003. 3: 489–501. doi:10.1038/nrc1121

5. Kleihues, P., Burger P.C., Scheithauer B.W., "The New WHO Classification Of Brain Tumours." *Brain Pathol.* 1993. 3: 255–268. Available: http://www.ncbi.nlm.nih.gov/pubmed/8293185

6. Ie, E.V., "The 2007 WHO ClassiWcation of Tumours of the Central Nervous System." A*cta Neuropathol*. 2007. pp. 97–109. doi:10.1007/s00401-007-0243-4

7. Louis, D.N., Ohgaki, H., Wiestler, O.D., Cavenee, W.K., Burger, P.C., Jouvet, A., "The 2007 WHO Classification Of Tumours Of The Central Nervous System." *Acta Neuropathologica*. 2007. pp. 97–109. doi:10.1007/s00401-007-0243-4

8. Brat, D.J., Prayson, R. A., Ryken, T.C., Olson, J.J., "Diagnosis Of Malignant Glioma: Role Of Neuropathology." *J Neurooncol*. 2008. 89: 287–311. doi:10.1007/s11060-008-9618-1

9. Friese, M.A., Steinle, A., Weller, M., "The Innate Immune Response In The Central Nervous System And Its Role In Glioma Immune Surveillance." *Onkologie*. 2004. pp. 487–491. doi:10.1159/000080371

10. Carolina, N., Carolina, S., "Central Brain Tumor Registry of the United States." *Brain*. 2011. pp. 1–57. Available: www.cbtrus.org

11. Furnari, F.B., Fenton, T., Bachoo, R.M., Mukasa, A., Stommel, J.M., Stegh, A., "Malignant Astrocytic Glioma: Genetics, Biology, And Paths To Treatment." *Genes and Development.* 2007. pp. 2683–2710. doi:10.1101/gad.1596707

12. Wen, P.Y., Kesari, S., "Malignant Gliomas in Adults." *N Engl J Med*. 2008. 359:492-507. doi:10.1056/NEJMra0708126

13. Howlader, N., Noone, A.M., Krapcho, M., Neyman, N., Aminou, R., Waldron, W., "SEER Cancer Statistics Review." 1975–2010, National Cancer Institute. Bethesda, MD, based on November 2012 SEER data submission, posted to the SEER web site, 2013. http//seer.cancer.gov/csr/1975_2010 (Accessed June 08, 2013). 2011.

14. Simpson, J.R., Horton, J., Scott, C., Curran, W.J., Rubin, P., Fischbach, J., "Influence Of Location And Extent Of Surgical Resection On Survival Of Patients

With Glioblastoma Multiforme: Results Of Three Consecutive Radiation Therapy Oncology Group (RTOG) Clinical Trials." *International journal of radiation oncology, biology, physics*. 1993. doi:10.1016/0360-3016(93)90203-8

15. Bozdag, S., Li, A., Riddick, G., Kotliarov, Y., Baysan, M., Iwamoto, F.M., "Age-Specific Signatures of Glioblastoma at the Genomic, Genetic, and Epigenetic Levels." *PLoS One*. 2013. 8. doi:10.1371/journal.pone.0062982

16. Thomas, A.A., Brennan, C.W., DeAngelis, L.M., Omuro, A.M., "Emerging Therapies for Glioblastoma." *JAMA Neurol*. 2014. 71: 1437. doi:10.1001/jamaneurol.2014.1701

17. Alexander, B.M., Ligon, K.L., Wen, P.Y., "Enhancing Radiation Therapy For Patients With Glioblastoma." *Expert Rev Anticancer Ther*. 2013. 13: 569–81. doi:10.1586/era.13.44

18. Lawrence, Y.R., Wang, M., Dicker, A.P., Andrews, D., Curran, W.J., Michalski, J.M., "Early Toxicity Predicts Long-Term Survival In High-Grade Glioma." *Br J Cancer*. 2011. 104: 1365–1371. doi:10.1038/bjc.2011.123

19. Malhotra, M., Prakash, S., "Targeted Drug Delivery Across Blood-Brain-Barrier Using Cell Penetrating Peptides Tagged Nanoparticles." *Current Nanoscience.* 2011. pp. 81–93. doi:10.2174/157341311794480336

20. Nagpal, S., "The Role of BCNU Polymer Wafers (Gliadel) in the Treatment of Malignant Glioma." *Neurosurgery Clinics of North America*. 2012. pp. 289–295. doi:10.1016/j.nec.2012.01.004

21. Riggs, G., "Handbook of Brain Tumor Chemotherapy." *Neurology*. 2006. pp. 1728–1728. doi:10.1212/01.wnl.0000227801.76385.fb

22. Nagasubramanian, R., Dolan, M.E., "Temozolomide: Realizing The Promise And Potential." *Current opinion in oncology*. 2003. pp. 412–418. doi:10.1097/00001622-200311000-00002

23. Hegi, M.E., Diserens, A.C., Gorlia, T., Hamou, M.F., de Tribolet, N., Weller, M., "MGMT Gene Silencing And Benefit From Temozolomide In Glioblastoma." *N Engl J Med.* 2005. 352: 997–1003. doi:10.1056/NEJMoa043331

24. Stupp, R., Hegi, M.E., Mason, W.P., van den Bent, M.J., Taphoorn, M.J., Janzer, R., "Effects Of Radiotherapy With Concomitant And Adjuvant Temozolomide Versus Radiotherapy Alone On Survival In Glioblastoma In A Randomised Phase III Study: 5-Year Analysis Of The EORTC-NCIC Trial." *Lancet Oncol*. 2009. 10: 459–466. doi:10.1016/S1470-2045(09)70025-7

25. Stupp, R., Mason, W., van den Bent, M.J., Weller, M., Fisher, B.M., Taphoorn, M.J., "Radiotherapy plus Concomitant and Adjuvant Temozolomide for Glioblastoma." *N Engl J Med*. 2005. 987–96. doi:10.1056/NEJMoa043330

26. Reardon, D.A., Rich, J.N., Friedman, H.S., Bigner, D.D., "Recent Advances In The Treatment Of Malignant Astrocytoma." *J Clin Oncol*. 2006. 24: 1253–1265. doi:10.1200/JCO.2005.04.5302

27. Ta, H.T., Dass, C.R., Dunstan, D.E., "Injectable Chitosan Hydrogels For Localised Cancer Therapy." *Journal of Controlled Release*. 2008. pp. 205–216. doi:10.1016/j.jconrel.2007.11.018

28. Ohgaki, H., Kleihues, P., "Genetic Pathways To Primary And Secondary Glioblastoma". *Am J Pathol.* 2007. 170: 1445–1453. doi:10.2353/ajpath.2007.070011

29. Watanabe, K., Tachibana, O., Sata, K., Yonekawa, Y., Kleihues, P., Ohgaki, H., "Overexpression Of The EGF Receptor And P53 Mutations Are Mutually Exclusive In The Evolution Of Primary And Secondary Glioblastomas." *Brain Pathol*. 1996. 6: 217–223; discussion 23–24. doi:10.1097/00005072-199605000-00017

30. Sturm, D., Bender, S., Jones, D.T.W., Lichter, P., Grill, J., Becher, O., "Paediatric And Adult Glioblastoma: Multiform (Epi)Genomic Culprits Emerge." *Nat Rev Cancer*. 2014. 14: 92–107. doi:10.1038/nrc3655

31. Ohgaki, H., Kleihues, P. "The Definition Of Primary And Secondary Glioblastoma." *Clinical Cancer Research*. 2013. pp. 764–772. doi:10.1158/1078-0432.CCR-12-3002

32. Mischel, P.S., Nelson, S.F., Cloughesy, T.F., "Molecular Analysis Of Glioblastoma: Pathway Profiling And Its Implications For Patient Therapy." *Cancer Biology and Therapy*. 2003. pp. 242–247. doi:10.4161/cbt.2.3.369

33. Brandes, A.A., Franceschi, E., Tosoni, A., Hegi, M.E., Stupp, R., "Epidermal Growth Factor Receptor Inhibitors In Neuro-Oncology: Hopes And Disappointments." *Clin Cancer Res*. 2008. 14: 957–960. doi:10.1158/1078-0432.CCR-07-1810

34. Koul, D., "PTEN Signaling Pathways In Glioblastoma." *Cancer Biology and Therapy*. 2008. pp. 1321–1325. doi:10.4161/cbt.7.9.6954

35. Knobbe, C.B., Merlo, A., Reifenberger, G., "PTEN Signaling In Gliomas." *Neuro Oncol*. 2002. 4: 196–211. doi:10.1093/neuonc/4.3.196

36. Weller, M., Fontana, A., Van Meir, E.G., Hadjipanayis, C.G., Norden, A.D., Shu, H.K., "Exciting New Advances in Neuro-Oncology: The Avenue to a Cure for Malignant Glioma." *Int J Oncol.* 2011. 24: 166–193. doi:10.3322/caac.20069

37. Hendriksen, E.M., Span, P.N., Schuuring, J., Peters, J.P.W., Sweep, F.C.G.J., van der Kogel, A.J., "Angiogenesis, Hypoxia And VEGF Expression During Tumour Growth In A Human Xenograft Tumour Model." *Microvasc Res*. 2009. 77: 96–103. doi:10.1016/j.mvr.2008.11.002

38. Clara, C.A., Marie, S.K.N., de Almeida, J.R.W., Wakamatsu, A., Oba-Shinjo, S.M., Uno, M., "Angiogenesis And Expression Of PDGF-C, VEGF, CD105 And

HIF-1α In Human Glioblastoma." *Neuropathology*. 2014. 34: 343–352. doi:10.1111/neup.12111

39. Semenza, G.L., "Targeting HIF-1 for Cancer Therapy." *Nat Rev Cancer.* 2003. 3: 721–732. doi:10.1038/nrc1187

40. Volpert, O. V., "Sequential Development Of An Angiogenic Phenotype By Human Fibroblasts Progressing To Tumorigenicity." *Oncogene*. 1997. 14: 1495–1502. doi:10.1038/sj.onc.1200977

41. Bergers, G., Benjamin, L.E., "Tumorigenesis And The Angiogenic Switch." *Nat Rev Cancer*. 2003. 3: 401–410. doi:10.1038/nrc1093

42. Folkman, J., "Tumor Angiogenesis: Therapeutic Implications." *N Engl J Med*. 1971. 285: 1182–1186. doi:10.1056/NEJM197111182852108

43. Bussolino, F., Mantovani, A., Persico, G., "Molecular Mechanisms Of Blood Vessel Formation." *Trends in Biochemical Sciences.* 1997. pp. 251–256. doi:10.1016/S0968-0004(97)01074-8

44. Papetti, M., Herman, I.M., "Mechanisms Of Normal And Tumor-Derived Angiogenesis." *Am J Physiol Cell Physiol*. 2002. 282: C947–C970. doi:10.1152/ajpcell.00389.2001

45. Hughes, S., Yang, H., Chan-Ling, T., "Vascularization Of The Human Fetal Retina: Roles Of Vasculogenesis And Angiogenesis." *Investig Ophthalmol Vis Sci*. 2000. 41: 1217–1228.

46. Yancopoulos, G.D., Davis, S., Gale, N.W., Rudge, J.S., Wiegand, S.J., Holash, J., "Vascular-Specific Growth Factors And Blood Vessel Formation." *Nature*. 2000. 407: 242–248. doi:10.1038/35025215

47. Carmeliet, P., "Angiogenesis In Life, Disease And Medicine." *Nature*. 2005. 438: 932–936. doi:10.1038/nature04478

48. Shibuya, M., "Vascular Endothelial Growth Factor And Its Receptor System: Physiological Functions In Angiogenesis And Pathological Roles In Various Diseases." *Journal of Biochemistry*. 2013. pp. 13–19. doi:10.1093/jb/mvs136

49. Knizetova, P., Ehrmann, J., Hlobilkova, A., Vancova, I., Kalita, O., Kolar, Z., "Autocrine Regulation Of Glioblastoma Cell Cycle Progression, Viability And Radioresistance Through The VEGF-VEGFR2 (KDR) Interplay." *Cell Cycle*. 2008. 7: 2553–2561. doi:10.4161/cc.7.16.6442

50. Gerber, H.P., McMurtrey, A., Kowalski, J., Yan, M., Keyt, B.A., Dixit, V., "Vascular Endothelial Growth Factor Regulates Endothelial Cell Survival Through The Phosphatidylinositol 3'-Kinase/Akt Signal Transduction Pathway. Requirement For Flk-1/KDR Activation." *J Biol Chem*. 1998. 273: 30336–30343. doi:10.1074/jbc.273.46.30336

51. Gomez-Manzano, C., Fueyo, J., Jiang, H., Glass, T.L., Lee, H.Y., Hu, M., "Mechanisms Underlying PTEN Regulation Of Vascular Endothelial Growth Factor And Angiogenesis." *Ann Neurol*. 2003. 53: 109–117. doi:10.1002/ana.10396

52. Ryuto, M., Ono, M., Izumi, H., Yoshida, S., Weich, H.A., Kohno, K., "Induction Of Vascular Endothelial Growth Factor By Tumor Necrosis Factor Alpha In Human Glioma Cells. Possible Roles Of SP-1." *J Biol Chem.* 1996. 271: 28220–28228.

53. Tsai, J.C., Goldman, C.K., Gillespie, G.Y., "Vascular Endothelial Growth Factor In Human Glioma Cell Lines: Induced Secretion by EGF, PDGF-BB, and bFGF." *JNeurosurg*. 1995. 82: 864–873.

54. Gerstner, E.R., Duda, D.G., di Tomaso, E., Ryg, P.A., Loeffler, J.S., Sorensen, A.G., "VEGF Inhibitors In The Treatment Of Cerebral Edema In Patients With Brain Cancer." *Nat Rev Clin Oncol.* 2009. 6: 229–236. doi:10.1038/nrclinonc.2009.14

55. Murakami, M., Simons, M., "Fibroblast Growth Factor Regulation Of Neovascularization." *Curr Opin Hematol*. 2008. 15: 215–220. doi:10.1097/MOH.0b013e3282f97d98

56. Saharinen, P., Bry, M., Alitalo, K., "How Do Angiopoietins Tie In With Vascular Endothelial Growth Factors?" *Curr Opin Hematol.* 2010. 17: 198–205. doi:10.1097/MOH.0b013e3283386673

57. Hoeben, A., Landuyt, B., Highley, M.S., Wildiers, H., Van Oosterom, A.T., De Bruijn, E.A., "Vascular Endothelial Growth Factor And Angiogenesis." *Pharmacol Rev*. 2004. 56: 549–580. doi:10.1124/pr.56.4.3.549

58. Wong, E.T., Brem, S., "Antiangiogenesis Treatment For Glioblastoma Multiforme: Challenges And Opportunities." *JNCCN J Natl Compr Cancer Netw*. 2008. 6: 515–522.

59. Hanahan, D., Weinberg, R.A., "Hallmarks Of Cancer: The Next Generation." *Cell*. 2011. pp. 646–674. doi:10.1016/j.cell.2011.02.013

60. Quail, D.F., Joyce, J.A., "Microenvironmental Regulation Of Tumor Progression And Metastasis." *Nat Med*. 2013. 19: 1423–37. doi:10.1038/nm.3394

61. Denys, H., Braems, G., Lambein, K., Pauwels, P., Hendrix, A., De Boeck, A., "The Extracellular Matrix Regulates Cancer Progression And Therapy Response: Implications For Prognosis And Treatment." *Curr Pharm Des*. 2009. 15: 1373–1384. doi:10.2174/138161209787846711

62. Joyce, J.A., Pollard, J.W., "Microenvironmental Regulation Of Metastasis." Nat Rev Cancer. 2009. 9: 239–252. doi:10.1038/nrc2618

63. Meads, M.B., Gatenby, R.A., Dalton, W.S., "Environment-Mediated Drug Resistance: A Major Contributor To Minimal Residual Disease." *Nat Rev Cancer*. 2009. 9: 665–674. doi:10.1038/nrc2714

64. Watnick, R.S., "The Role Of The Tumor Microenvironment In Regulating Angiogenesis." *Cold Spring Harb Perspect Med*. 2012. 2. doi:10.1101/cshperspect.a006676

65. Ungefroren, H., Sebens, S., Seidl, D., Lehnert, H., Hass, R., Interaction Of Tumor Cells With The Microenvironment." *Cell Communication and Signaling*. 2011. p. 18. doi:10.1186/1478-811X-9-18

66. Ricci-Vitiani, L., Pallini, R., Biffoni, M., Todaro, M., Invernici, G., Cenci, T., "Tumour Vascularization Via Endothelial Differentiation Of Glioblastoma Stem-Like Cells." *Nature*. 2010. 468: 824–828. doi:10.1038/nature10410

67. El Hallani, S., Colin, C., El Houfi, Y., Idbaih, A., Boisselier, B., Marie, Y., "Tumor and endothelial Cell Hybrids Participate In Glioblastoma Vasculature." *Biomed Res Int*. 2014. 2014. doi:10.1155/2014/827327

68. Klemm, F., "Microenvironmental Regulation Of Therapeutic Response In Cancer." *Trends Cell Biol*. 2014. 25: 198–213. doi:10.1016/j.tcb.2014.11.006

69. Fishman, A.P., "Endothelium: A Distributed Organ Of Diverse Capabilities." *Ann N Y Acad Sci*. 1982. 401: 1–8.

70. Garlanda, C., Dejana, E., "Heterogeneity of Endothelial Cells. Specific Markers." *Arterioscler Thromb Vasc Biol*. 1997. 17: 1193–1202. doi:10.1161/01.ATV.17.7.1193

71. Wallez, Y., Huber, P., "Endothelial Adherens And Tight Junctions In Vascular Homeostasis, Inflammation And Angiogenesis." *Biochimica et Biophysica Acta - Biomembranes.* 2008. pp. 794–809. doi:10.1016/j.bbamem.2007.09.003

72. Kobayashi, H., Boelte, K.C., Lin, P.C., "Endothelial Cell Adhesion Molecules And Cancer Progression." *Curr Med Chem.* 2007. 14: 377–386. doi:10.2174/092986707779941032

73. Miebach, S., Grau, S., Hummel, V., Rieckmann, P., Tonn, J.C., Goldbrunner, R.H., "Isolation And Culture Of Microvascular Endothelial Cells From Gliomas Of Different WHO Grades." *J Neurooncol.* 2006. 76: 39–48. doi:10.1007/s11060-005-3674-6

74. Bussolati, B., "Altered Angiogenesis And Survival In Human Tumor-Derived Endothelial Cells." *FASEB J*. 2003. 17: 1159–1161. doi:10.1096/fj.02-0557fje

75. Charalambous, C., Hofman, F.M., Chen, T.C., "Functional And Phenotypic Differences Between Glioblastoma Multiforme-Derived And Normal Human Brain Endothelial Cells." *J Neurosurg*. 2005. 102: 699–705. doi:10.3171/jns.2005.102.4.0699

76. Davies, D.C., "Blood-Brain Barrier Breakdown In Septic Encephalopathy And Brain Tumours." *Journal of Anatomy*. 2002. pp. 639–646. doi:10.1046/j.1469-7580.2002.00065.x

77. Aroca, F., Renaud, W., Bartoli, C., Bouvier-Labit, C., Figarella-Branger, D., "Expression Of PECAM-1/CD31 Isoforms In Human Brain Gliomas." *Journal of Neuro-Oncology*. 1999. pp. 19–25. doi:10.1023/A:1006233816724

78. DeLisser, H.M., Christofidou-Solomidou, M., Strieter, R.M., Burdick, M.D., Robinson, C.S., Wexler, R.S., "Involvement Of Endothelial PECAM-1/CD31 In Angiogenesis." *Am J Pathol*. 1997. 151: 671–677.

79. Belloni, P.N., Tressler, R.J., "Microvascular Endothelial Cell Heterogeneity: Interactions With Leukocytes And Tumor Cells." *Cancer Metastasis Rev.* 1990. 8: 353–89. Available: http://www.ncbi.nlm.nih.gov/pubmed/2182212

80. Lampugnani, M.G., Resnati, M., Raiteri, M., Pigott, R., Pisacane, A., Houen, G., "A Novel Endothelial-Specific Membrane Protein Is A Marker Of Cell-Cell Contacts." *J Cell Biol*. 1992. 118: 1511–1522. doi:10.1083/jcb.118.6.1511

81. Fackler, M.J., Civin, C.I., May, W.S., "CD34: Structure, Biology, And Clinical Utility." *Blood*. 1996. 87: 1–13.

82. Quinn, T.P., "Fetal Liver Kinase 1 Is A Receptor For Vascular Endothelial Growth Factor And Is Selectively Expressed In Vascular Endothelium." *Proc Natl Acad Sci* U S A. 1993. 90: 7533–7537.

83. Peters, K.G., De Vries, C., Williams, L.T., "Vascular Endothelial Growth Factor Receptor Expression During Embryogenesis And Tissue Repair Suggests A Role In Endothelial Differentiation And Blood Vessel Growth." *Proc Natl Acad Sci* U S A. 1993. 90: 8915–8919. Available: http://www.ncbi.nlm.nih.gov/pubmed/7692439

84. Schnürch, H., Risau, W., "Expression Of Tie-2, A Member Of A Novel Family Of Receptor Tyrosine Kinases, In The Endothelial Cell Lineage." *Development.* 1993. 119: 957–968.

85. Patan, S., "TIE1 And TIE2 Receptor Tyrosine Kinases Inversely Regulate Embryonic Angiogenesis By The Mechanism Of Intussusceptive Microvascular Growth." *Microvasc Res*. 1998. 56: 1–21. doi:10.1006/mvre.1998.2081

86. Jain, R.K., di Tomaso, E., Duda, D.G., Loeffler, J.S., Sorensen, A.G., Batchelor, T.T., "Angiogenesis In Brain Tumours." *Nat Rev Neurosci*. 2007. 8: 610–622. doi:10.1038/nrn2175

87. Ellis, L.M., Hicklin, D.J., "VEGF-Targeted Therapy: Mechanisms Of Anti-Tumour Activity." *Nat Rev Cancer.* 2008. 8: 579–591. doi:10.1038/nrc2403

88. Ferrara, N., Hillan, K.J., Gerber, H.P., Novotny, W., "Discovery And Development Of Bevacizumab, An Anti-VEGF Antibody For Treating Cancer." *Nat Rev Drug Discov*. 2004. 3: 391–400. doi:10.1038/nrd1381

89. Martínez-Murillo, R., Martínez, A., "Standardization Of An Orthotopic Mouse Brain Tumor Model Following Transplantation Of CT-2A Astrocytoma Cells." *Histol Histopathol*. 2007. 22: 1309–1326.

90. Chen, L., Zhang, Y., Yang, J., Hagan, J.P., Li, M., "Vertebrate Animal Models Of Glioma: Understanding The Mechanisms And Developing New Therapies."

Biochimica et Biophysica Acta - Reviews on Cancer. 2013. pp. 158–165. doi:10.1016/j.bbcan.2013.04.003

91. Rankin, S.L., Zhu, G., Baker, S.J., "Insights Gained from Modeling High-Grade Glioma in the Mouse." *Neuropathol Appl Neurobiol*. 2011. 38: 254–70. doi:10.1111/j.1365-2990.2011.01231.x

92. Ponten, J., "Neoplastic Human Glia Cells in Culture." *Hum Tumor Cells Vitr.* 1975. pp. 175–206.

93. Candolfi, M., Curtin, J.F., Nichols, W.S., Muhammad, A.K.M.G., King, G.D., Pluhar, G.E., "Intracranial Glioblastoma Models In Preclinical Neuro-Oncology: Neuropathological Characterization And Tumor Progression." *J Neurooncol*. 2007. 85: 133–148. doi:10.1007/s11060-007-9400-9

94. De Vries, N.A., Beijnen, J.H., van Tellingen, O., "High-Grade Glioma Mouse Models And Their Applicability For Preclinical Testing." *Cancer Treatment Reviews.* 2009. pp. 714–723. doi:10.1016/j.ctrv.2009.08.011

95. Camphausen, K., Purow, B., Sproull, M., Scott, T., Ozawa, T., Deen, D.F., "Influence of *In Vivo* Growth On Human Glioma Cell Line Gene Expression: Convergent Profiles Under Orthotopic Conditions." *Proc Natl Acad Sci U S A*. 2005. 102: 8287–8292. doi:10.1073/pnas.0502887102

96. Wen, S., Stolarov, J., Myers, M.P., Su, J.D., Wigler, M.H., Tonks, N.K., "PTEN Controls Tumor-Induced Angiogenesis." *Proc Natl Acad Sci U S A*. 2001. 98: 4622–4627. doi:10.1073/pnas.081063798

97. Jacobs, V.L., Valdes, P.A., Hickey, W.F., De Leo, J.A., Current Review Of *In Vivo* GBM Rodent Models: Emphasis On The CNS-1 Tumour Model." *ASN Neuro*. 2011. 3: e00063. doi:10.1042/AN20110014

98. Ausman, J.I., Shapiro, W.R., Rall, D.P., "Studies on the Chemotherapy of Experimental Brain Tumors : Development of an Experimental Model Studies on the Chemotherapy of Experimental Development of an Experimental Model Brain Tumors." *Cancer Res*. 1970. 30: 2394–2400.

99. Weiner, N.E., Pyles, R.B., Chalk, C.L., Balko, M.G., Miller, M.A., Dyer, C.A., "A Syngeneic Mouse Glioma Model For Study Of Glioblastoma Therapy." *J Neuropathol Exp Neurol.* 1999. 58: 54–60. doi:10.1097/00005072-199901000-00007

100. Kielian, T., Van Rooijen, N., Hickey, W.F., "MCP-1 Expression In CNS-1 Astrocytoma Cells: Implications For Macrophage Infiltration Into Tumors *In Vivo*." *J Neurooncol*. 2002. 56: 1–12. doi:10.1023/A:1014495613455

101. Aggarwal, B.B., Danda, D., Gupta, S., Gehlot, P., "Models For Prevention And Treatment Of Cancer: Problems Vs Promises." *Biochem Pharmacol*. 2009. 78: 1083–1094. doi:10.1016/j.bcp.2009.05.027

102. Hait, W.N., "Anticancer Drug Development: The Grand Challenges." *Nat Rev Drug Discov*. 2010. 9: 253–254. doi:10.1038/nrd3144

103. Bart van der Worp, H., Howells, D.W., Sena, E.S., Porritt, M.J., Rewell, S., O'Collins, V., "Can Animal Models Of Disease Reliably Inform Human Studies?" PLoS Med. 2010. 7: 1–8. doi:10.1371/journal.pmed.1000245

104. Francis, A.O., "BRAIN TUMORS." In: Masters JRW, Palsson B, editors. Human Cell Culture Vol II. New York, Boston, Dordrecht, London, Moscow: Kluwer Academic Publishers; 2002. pp. 167 – 184.

105. Li, A., Walling, J., Kotliarov, Y., Center, A., Steed, M.E., Ahn, S.J., "Genomic Changes And Gene Expression Profiles Reveal That Established Glioma Cell Lines Are Poorly Representative Of Primary Human Gliomas." *Mol Cancer Res*. 2008. 6: 21–30. doi:10.1158/1541-7786.MCR-07-0280

106. Jensen, S.S., Aaberg-jessen, C., Jakobsen, I.P., Hermansen, S.K., "THREE-DIMENSIONAL *IN VITRO* MODELS IN GLIOMA RESEARCH – FOCUS ON SPHEROIDS." In: Ghosh A, editor. GLIOMA Exploring Its Biology and Practical Relevance. 2011.

107. Abbott, A., "Cell Culture: Biology's New Dimension." *Nature*. 2003. pp. 870–872. doi:10.1038/424870a

108. Cukierman, E., Pankov, R., Stevens, D.R., Yamada, K.M., "Taking Cell-Matrix Adhesions To The Third Dimension." *Science*. 2001. 294: 1708–1712. doi:10.1126/science.1064829

109. Hirschhaeuser, F., Menne, H., Dittfeld, C., West, J., Mueller-Klieser, W., Kunz-Schughart, L.A., "Multicellular Tumor Spheroids: An Underestimated Tool Is Catching Up Again." *J Biotechnol*. 2010. 148: 3–15. doi:10.1016/j.jbiotec.2010.01.012

110. Ezhilarasan, R., Mohanam, I., Govindarajan, K., Mohanam, S., "Glioma Cells Suppress Hypoxia-Induced Endothelial Cell Apoptosis And Promote The Angiogenic Process." *Int J Oncol*. 2007. 30: 701–707.

111. Buchanan, C.F., Szot, C.S., Freeman, J.W., Rylander, M.N., "2D And 3D *In Vitro* Culture Methods To Investigate Endothelial-Cell Enhanced Tumor Angiogenesis." 2011 IEEE 37th Annual Northeast Bioengineering Conference, NEBEC 2011. 2011. doi:10.1109/NEBC.2011.5778696

112. Rape, A., Ananthanarayanan, B., Kumar, S., "Engineering Strategies To Mimic The Glioblastoma Microenvironment." *Adv Drug Deliv Rev.* Elsevier B.V.; 2014. 79-80: 172–183. doi:10.1016/j.addr.2014.08.012

113. Ghosh, S., Spagnoli, G.C., Martin, I., Ploegert, S., Demougin, P., Heberer, M., "Three-Dimensional Culture Of Melanoma Cells Profoundly Affects Gene Expression Profile: A High Density Oligonucleotide Array Study." *J Cell Physiol*. 2005. 204: 522–531. doi:10.1002/jcp.20320

114. Goodman, T.T., Ng, C.P., Pun, S.H., "3-D Tissue Culture Systems For The Evaluation And Optimization Of Nanoparticle-Based Drug Carriers." *Bioconjug Chem*. 2008. 19: 1951–1959. doi:10.1021/bc800233a

115. Lovitt, C.J., Shelper, T.B., Avery, V.M., "Advanced Cell Culture Techniques For Cancer Drug Discovery." *Biology* (Basel). 2014. 3: 345–67. doi:10.3390/biology3020345

116. Velazquez, O.C., Snyder, R., Liu, Z.J., Fairman, R.M., Herlyn, M., "Fibroblast-Dependent Differentiation Of Human Microvascular Endothelial Cells Into Capillary-Like 3-Dimensional Networks." *FASEB J.* 2002. 16: 1316–1318. doi:10.1096/fj.01-1011fje

117. Long, D.M., "Networks of the Brain." *Neurosurgery Quarterly.* 2011. p. 144. doi:10.1097/WNQ.0b013e31820f1a98

118. Lindström, S., Andersson-Svahn, H., "Miniaturization Of Biological Assays - Overview On Microwell Devices For Single-Cell Analyses." *Biochim Biophys Acta - Gen Subj.* 2011. 1810: 308–316. doi:10.1016/j.bbagen.2010.04.009

119. Pardridge, W., "CNS Drug Design Based On Principles Of Blood‐Brain Barrier Transport." *J Neurochem.* 1998. 70: 1781–1792. Available: http://onlinelibrary.wiley.com/doi/10.1046/j.1471-4159.1998.70051781.x/full

120. Habgood, M.D., Begley, D.J., Abbott, N.J., "Determinants Of Passive Drug Entry Into The Central Nervous System." *Cellular and Molecular Neurobiology*. 2000. pp. 231–253. doi:10.1023/A:1007001923498

121. Abbott, N.J., Rönnbäck, L., Hansson, E., "Astrocyte-Endothelial Interactions At The Blood-Brain Barrier." *Nat Rev Neurosci.* 2006. 7: 41–53. doi:10.1038/nrn1824

122. Bissell, M.J., Radisky, D., "Putting Tumours In Context." *Nat Rev Cancer.* 2001. 1: 46–54. doi:10.1038/35094059

123. Ong, S.M., Zhang, C., Toh, Y.C., Kim, S.H., Foo, H.L., Tan, C.H., "A Gel-Free 3D Microfluidic Cell Culture System." *Biomaterials.* 2008. 29: 3237–3244. doi:10.1016/j.biomaterials.2008.04.022

124. Li, X.J., Valadez, A.V., Zuo, P., Nie, Z., "Microfluidic 3D Cell Culture: Potential Application For Tissue-Based Bioassays." *Bioanalysis.* 2012. pp. 1509–1525. doi:10.4155/bio.12.133

125. Yuhas, J.M., Li, A.P., Martinez, A.O., Ladman, A.J., "A Simplified Method For Production And Growth Of Multicellular Tumor Spheroids." *Cancer Res.* 1977. 37: 3639–3643.

126. Mackillop, W.J., Blundell, J., Steele, P., "Short-Term Culture Of Pediatric Brain Tumors." *Childs Nerv Syst.* 1985. 1: 163–168. doi:10.1007/BF00735732

127. Bjerkvig, R., Tønnesen, A., Laerum, O.D., Backlund, E.O., "Multicellular Tumor Spheroids From Human Gliomas Maintained In Organ Culture." *J Neurosurg.* 1990. 72: 463–475. doi:10.3171/jns.1990.72.3.0463

128. Revzin, A., Russell, R.J., Yadavalli, V.K., Koh, W., Deister, C., Hile, D.D., "Fabrication of Poly (ethylene glycol) Hydrogel Microstructures Using Photolithography." *Langmuir*, 2001. pp. 5440–5447.

129. Koh, W., Revzin, A., Pishko, M.V., "Poly (ethylene glycol) Hydrogel Microstructures Encapsulating Living Cells." *Langmuir*, 2002. pp. 2459–2462.

130. Fukuda, J., Khademhosseini, A., Yeo, Y., Yang, X., Yeh, J., Eng, G., Blumling, J., Wang, C.F., Kohane, D.S., Langer, R., "Micromolding Of Photocrosslinkable Chitosan Hydrogel For Spheroid Microarray And Co-Cultures." *Biomaterials.* 2006. pp. 5259–67. doi:10.1016/j.biomaterials.2006.05.044

131. Karp, J.M., Yeh, J., Eng, G., Fukuda, J., Blumling, J., Suh, K.Y., Cheng, J., Mahdavi, A., Borenstein, J., Langer, R., Khademhosseini, A., "Controlling Size, Shape And Homogeneity Of Embryoid Bodies Using Poly(Ethylene Glycol) Microwells." *Lab Chip.* 2007. 7: 786–794. doi:10.1039/b705085m

132. Khademhosseini, A., Langer, R., "Microengineered Hydrogels For Tissue Engineering." *Biomaterials.* 2007. 28: 5087–92. doi:10.1016/j.biomaterials.2007.07.021

133. Fan, Y., Avci, N.G., Nguyen, D.T., Dragomir, A., Akay, Y.M., Xu, F., Akay, M., "Engineering a High-Throughput 3-D *In Vitro* Glioblastoma Model." *IEEE J Transl Eng Heal Med.* 2015. 3. doi:10.1109/JTEHM.2015.2410277

134. Kauzlarick, D., "FUNDAMENTALS OF MICROFABRICATION, THE SCIENCE OF MINIATURIZATION." 2nd edition [Book Review]. *IEEE Eng Med Biol Mag.* 2003. 22. doi:10.1109/MEMB.2003.1195708

135. Kunz-Schughart, L.A., Freyer, J.P., Hofstaedter, F., Ebner, R., "The Use of 3-D Cultures For High-Throughput Screening: The Multicellular Spheroid Model." *J Biomol Screen Off J Soc Biomol Screen.* 2004. 9: 273–285. doi:10.1177/1087057104265040

136. Wright, D., Rajalingam, B., Selvarasah, S., Dokmeci, M.R., Khademhosseini, A., "Generation Of Static And Dynamic Patterned Co-Cultures Using Microfabricated Parylene-C Stencils." *Lab Chip.* 2007. 7: 1272–9. doi:10.1039/b706081e

137. Kolate, A., Baradia, D., Patil, S., Vhora, I., Kore, G., Misra, A., "PEG - A Versatile Conjugating Ligand For Drugs And Drug Delivery Systems." *Journal of Controlled Release.* 2014. pp. 67–81. doi:10.1016/j.jconrel.2014.06.046

138. Li, N., Tourovskaia, A., Folch, A., "Biology On A Chip: Microfabrication For Studying The Behavior Of Cultured Cells." *Crit Rev Biomed Eng.* 2003. 31: 423–488. doi:10.1615/CritRevBiomedEng.v31.i56.20

139. El-Ali, J., Sorger, P.K., Jensen, K.F., "Cells On Chips." *Nature.* 2006. 442: 403–411. doi:10.1038/nature05063

140. Shen, C.J., Fu, J., Chen, C.S., "Patterning Cell and Tissue Function." *Cellular and Molecular Bioengineering.* 2008. pp. 15–23. doi:10.1007/s12195-008-0005-y

141. Tsang, V.L., Bhatia, S.N., "Three-Dimensional Tissue Fabrication." *Advanced Drug Delivery Reviews.* 2004. pp. 1635–1647. doi:10.1016/j.addr.2004.05.001

142. Xia, Y., Whitesides, G.M., "Soft Lithography." *Annual Review of Materials Science.* 1998. pp. 153–184. doi:10.1146/annurev.matsci.28.1.153

143. Whitesides, G.M., Ostuni, E., Takayama, S., Jiang, X., Ingber, D.E., "Soft Lithography In Biology And Biochemistry." *Annu Rev Biomed Eng.* 2001. 3: 335–373. doi:10.1146/annurev.bioeng.3.1.335

144. Duffy, D.C., McDonald, J.C., Schueller, O.J.A., Whitesides, G.M., "Rapid Prototyping Of Microfluidic Systems In Poly(Dimethylsiloxane)." *Anal Chem.* 1998. 70: 4974–4984. doi:10.1021/ac980656z

145. Gallego-Perez, D., Higuita-Castro, N., Denning, L., DeJesus, J., Dahl, K., Sarkar, A., "Microfabricated Mimics Of *In Vivo* Structural Cues For The Study Of Guided Tumor Cell Migration." *Lab on a Chip.* 2012. p. 4424. doi:10.1039/c2lc40726d

146. Delamarche, E., Bernard, A., Schmid, H., Bietsch, A., Michel, B., Biebuyck, H., "Microfluidic Networks For Chemical Patterning Of Substrates: Design And

Application To Bioassays." *J Am Chem Soc*. 1998. 120: 500–508. doi:10.1021/ja973071f

147. Kumar, A., Whitesides, G.M., "Features Of Gold Having Micrometer To Centimeter Dimensions Can Be Formed Through A Combination Of Stamping With An Elastomeric Stamp And An Alkanethiol “Ink” Followed By Chemical Etching." *Appl Phys Lett.* 1993. 63: 2002–2004. doi:10.1063/1.110628

148. Falconnet, D., Csucs, G., Grandin, H. M., Textor, M., "Surface Engineering Approaches To Micropattern Surfaces For Cell-Based Assays." *Biomaterials.* 2006. pp. 3044–3063. doi:10.1016/j.biomaterials.2005.12.024

149. Frimat, J.P., Menne, H., Michels, A., Kittel, S., Kettler, R., Borgmann, S., "Plasma Stencilling Methods For Cell Patterning." *Anal Bioanal Chem*. 2009. 395: 601–609. doi:10.1007/s00216-009-2824-7

150. Nakazawa, K., Izumi, Y., Mori, R., "Morphological And Functional Studies Of Rat Hepatocytes On A Hydrophobic Or Hydrophilic Polydimethylsiloxane Surface." *Acta Biomater.* 2009. 5: 613–620. doi:10.1016/j.actbio.2008.08.011

151. Fujioka, S., Oltea, S., Saya, H., Sudo, R., "A Microfluidic Invasion Assay for Glioma-Initiating Cells in Three-Dimensional Culture." 17th International Conference on Miniaturized Systems for Chemistry and Life Sciences. Freiburg, Germany; 2013. pp. 1075–1077.

152. Beebe, D.J., Mensing, G.A., Walker, G.M., "Physics And Applications Of Microfluidics In Biology." *Annu Rev Biomed Eng*. 2002. 4: 261–286. doi:10.1146/annurev.bioeng.4.112601.125916

153. Kim, L., Toh, Y.C., Voldman, J., Yu, H., "A Practical Guide To Microfluidic Perfusion Culture Of Adherent Mammalian Cells." *Lab Chip.* 2007. 7: 681–694. doi:10.1039/b704602b

154. Kirchauer, H., "Photolithography Simulation." PhD Thesis. TU Vienna. 1998.

155. Hennink, W., van Nostrum, C., "Novel Crosslinking Methods To Design Hydrogels." *Adv Drug Deliv Rev.* 2002. 54: 13–36. doi:10.1016/S0169-409X(01)00240-X

156. Wang, J., Heath, J., "Microfluidic Pairwise Interaction Analysis Of Glioma Cancer Cells And Modeling." University at Albany , The State University of New York , USA. 18th International Conference on Miniaturized Systems for Chemistry and Life Sciences. San Antonio; 2014. pp. 843–845.

157. Suh, K.Y., Seong, J., Khademhosseini, A., Laibinis, P.E., Langer, R., "A Simple Soft Lithographic Route To Fabrication Of Poly(Ethylene Glycol) Microstructures For Protein And Cell Patterning." *Biomaterials.* 2004. 25: 557–563. doi:10.1016/S0142-9612(03)00543-X

158. Haraldsson, K.T., Hutchison, J.B., Sebra, R.P., Good, B.T., Anseth, K.S., Bowman, C.N., "3D Polymeric Microfluidic Device Fabrication Via Contact

Liquid Photolithographic Polymerization (CLiPP)." *Sensors Actuators, B Chem*. 2006. 113: 454–460. doi:10.1016/j.snb.2005.03.096

159. Bernard, A.B., Lin, C.C., Anseth, K.S., "A Microwell Cell Culture Platform for the Aggregation of Pancreatic β-Cells." *Tissue Engineering Part C: Methods.* 2012. pp. 583–592. doi:10.1089/ten.tec.2011.0504

160. Kim, P., Yuan, A., Nam, K.H., Jiao, A., Kim, D.H., "Fabrication Of Poly(Ethylene Glycol): Gelatin Methacrylate Composite Nanostructures With Tunable Stiffness And Degradation For Vascular Tissue Engineering." *Biofabrication.* 2014. 6: 024112. doi:10.1088/1758-5082/6/2/024112

161. Cruise, G.M., Scharp, D.S., Hubbell, J.A., "Characterization Of Permeability And Network Structure Of Interfacially Photopolymerized Poly(Ethylene Glycol) Diacrylate Hydrogels." *Biomaterials.* 1998. 19: 1287–1294. doi:10.1016/S0142-9612(98)00025-8

162. Moon, J.J., Hahn, M.S., Kim, I., Nsiah, B.A., West, J.L., "Micropatterning Of Poly(Ethylene Glycol) Diacrylate Hydrogels With Biomolecules To Regulate And Guide Endothelial Morphogenesis." *Tissue Eng Part A.* 2009. 15: 579–585. doi:10.1089/ten.tea.2008.0196

163. Lutolf, M.P., Raeber, G.P., Zisch, A.H., Tirelli, N., Hubbell, J.A., "Cell-Responsive Synthetic Hydrogels." *Adv Mater.* 2003. 15: 888–892. doi:10.1002/adma.200304621

164. Holland, E.C., "Brain Tumor Animal Models: Importance And Progress." *Curr Opin Oncol.* 2001. 13: 143–147. doi:10.1097/00001622-200105000-00002

165. Rozen, S., Skaletsky, H., "Primer3 On The WWW For General Users And For Biologist Programmers." *Methods Mol Biol.* 2000. 132: 365–386. doi:10.1385/1-59259-192-2:365

166. Plate, K.H., Risau, W., "Angiogenesis In Malignant Gliomas." *Glia.* 1995. 15: 339–347. doi:10.1002/glia.440150313

167. Brown, C.K., Khodarev, N.N., Yu, J., Moo-Young, T., Labay, E., Darga, T.E., Posner, M.C., Weichselbaum, R.R., Mauceri, H.J., "Glioblastoma Cells Block Radiation-Induced Programmed Cell Death Of Endothelial Cells." *FEBS Lett.* 2004. 565: 167–170. doi:10.1016/j.febslet.2004.03.099

168. 359:492-507Shibuya, M., "Vascular Endothelial Growth Factor-Dependent And-Independent Regulation Of Angiogenesis". *Angiogenesis.* 2008. 12: 15. doi:10.5483/BMBRep.2008.41.4.278

169. Chen, Z., Htay, A., Santos, W. Dos, Gillies, G.T., Fillmore, H.L., Sholley, M.M., Broaddus, W.C., "*In Vitro* Angiogenesis By Human Umbilical Vein Endothelial Cells (HUVEC) Induced By Three-Dimensional Co-Culture With Glioblastoma Cells." *J Neurooncol.* 2009. 92: 121–128. doi:10.1007/s11060-008-9742-y

170. Khodarev, N.N., Yu, J., Labay, E., Darga, T., Brown, C.K., Mauceri, H.J., Yassari, R., Gupta, N., Weichselbaum, R.R., "Tumour-Endothelium Interactions In Co-

Culture: Coordinated Changes Of Gene Expression Profiles And Phenotypic Properties Of Endothelial Cells." *J Cell Sci.* 2003. 116: 1013–1022. doi:10.1242/jcs.00281

171. Nyga, A., Cheema, U., Loizidou, M., "3D Tumour Models: Novel *In Vitro* Approaches To Cancer Studies." *J Cell Commun Signal.* 2011. 5: 239–48. doi:10.1007/s12079-011-0132-4

172. Martínez-González, A., Calvo, G.F., Pérez-Romasanta, L.A., Pérez-García, V.M., "Hypoxic Cell Waves Around Necrotic Cores in Glioblastoma: A Biomathematical Model and Its Therapeutic Implications." *Bull Math Biol.* 2012. 74: 2875–2896. doi:10.1007/s11538-012-9786-1

173. Albelda, S.M., Oliver, P.D., Romer, L.H., Buck, C.A., "EndoCAM: A Novel Endothelial Cell-Cell Adhesion Molecule." *J Cell Biol.* 1990. 110: 1227–1237. doi:10.1083/jcb.110.4.1227

174. RayChaudhury, A., Elkins, M., Kozien, D., Nakada, M., "Regulation Of PECAM-1 In Endothelial Cells During Cell Growth And Migration." *Exp Biol Med*. 2001. 226: 686–691.

175. Lutzky, V.P., Carnevale, R.P., Alvarez, M.J., Maffia, P.C., Zittermann, S.I., Podhajcer, O.L., Issekutz, A.C., Chuluyan H.E., "Platelet-Endothelial Cell Adhesion Molecule-1 (CD31) Recycles And Induces Cell Growth Inhibition On Human Tumor Cell Lines." *J Cell Biochem.* 2006. 98: 1334–1350. doi:10.1002/jcb.20769

176. Privratsky, J.R., Newman, P.J., "PECAM-1: Regulator Of Endothelial Junctional Integrity." *Cell and Tissue Research.* 2014. pp. 1–13. doi:10.1007/s00441-013-1779-3

177. Ma, J., Waxman, D.J., "Combination Of Antiangiogenesis With Chemotherapy For More Effective Cancer Treatment." *Mol Cancer Ther.* 2008. 7: 3670–3684. doi:10.1158/1535-7163.MCT-08-0715

178. Stratmann, A., Risau, W., Plate, K.H., "Cell Type-Specific Expression Of Angiopoietin-1 And Angiopoietin-2 Suggests A Role In Glioblastoma Angiogenesis." *Am J Pathol.* 1998. 153: 1459–1466. doi:10.1016/S0002-9440(10)65733-1

179. Smadja, D.M., Bièche, I., Helley, D., Laurendeau, I., Simonin, G., Muller, L., Aiach, M., Gaussem, P., "Increased VEGFR2 Expression During Human Late Endothelial Progenitor Cells Expansion Enhances *In Vitro* Angiogenesis With Up-Regulation Of Integrin alpha (6)." *J Cell Mol Med.* 2007. 11: 1149–1161. doi:10.1111/j.1582-4934.2007.00090.x

180. Xu, C., Wu, X., Zhu, J., "VEGF Promotes Proliferation Of Human Glioblastoma Multiforme Stem-Like Cells Through VEGF Receptor 2." *Sci World J.* 2013. 2013: 417413. doi:10.1155/2013/417413

181. Yao, X., Ping, Y., Liu, Y., Chen, K., Yoshimura, T., Liu, M, Gong, W., Chen, C., Niu, Q., Guo, D., Zhang, X., Wang J.M., Bian X., "Vascular Endothelial Growth Factor Receptor 2 (VEGFR-2) Plays a Key Role in Vasculogenic Mimicry

Formation, Neovascularization and Tumor Initiation by Glioma Stem-like Cells." *PLoS One*. 2013. 8. doi:10.1371/journal.pone.0057188

182. Parsons, D.W., Jones, S., Zhang, X., Lin, J.C.H., Leary, R.J., Angenendt. P., Ankoo, P., Carter, H., Siu, I.M., Gallia, G.L., Olivi, A., McLendon, R., Rasheed, B.A., Keir, S., Nikolskaya, T., Nikolsky, Y., Busam, D.A., Tekleab, H., Diaz, L.A. Jr., Hartigan, J., Smith, D.R., Strausberg, R.L., Marie, S.K., Shinjo, S.M., Yan, H., Riggins, G.J., Bigner, D.D., Karchin, R., Papadopoulos, N., Parmigiani, G., Vogelstein, B., Velculescu, V.E., Kinzler, K.W., "An Integrated Genomic Analysis Of Human Glioblastoma Multiforme." *Science.* 2008. 321: 1807–1812. doi:10.1126/science.1164382

183. Cantley, L.C., "The Phosphoinositide 3-Kinase Pathwa.y" *Science.* 2002. 296: 1655–1657. doi:10.1126/science.296.5573.1655

184. Mizoguchi, M., Nutt, C.L., Mohapatra, G., Louis, D.N., "Genetic Alterations Of Phosphoinositide 3-Kinase Subunit Genes In Human Glioblastomas." *Brain Pathol.* 2004. 14: 372–377.

185. Verhaak, R.G.W., Hoadley, K.A., Purdom, E., Wang, V., Qi, Y., Wilkerson, M.D., Miller, C.R., Ding, L., Golub, T., Mesirov, J.P., Alexe, G., Lawrence,M., O'Kelly, M., Tamayo,P., Weir, B.A., Gabrie, S., Winckler, W., Gupta, S., Jakkula, L., Feiler, H.S., Hodgson, J.S., James, C.D, Sarkaria, J.N., Brennan, C., Kahn, A., Spellman, P.T., Wilson, R.K., Speed, T.P., Gray, J.W., Meyerson, M., Getz, G., Perou, C.M., Hayes, D.H., "Integrated Genomic Analysis Identifies Clinically

Relevant Subtypes of Glioblastoma Characterized by Abnormalities in PDGFRA, IDH1, EGFR, and NF1." *Cancer Cell.* 2010. 17: 98–110. doi:10.1016/j.ccr.2009.12.020

186. McLendon, R., Friedman, A., Bigner, D., Van Meir, E.G., Brat, D.J., Mastrogianakis, M., "Comprehensive Genomic Characterization Defines Human Glioblastoma Genes And Core Pathways." *Nature.* 2008. pp. 1061–1068. doi:10.1038/nature07385

187. Brennan, C.W., Verhaak, R.G.W., McKenna, A., Campos, B., Noushmehr, H., Salama, S.R., "The Somatic Genomic Landscape of Glioblastoma." *Cell.* 2013.155: 462–477. doi:10.1016/j.cell.2013.09.034

188. Dayanir, V., Meyer, R.D., Lashkari, K., Rahimi, N., "Identification Of Tyrosine Residues In Vascular Endothelial Growth Factor Receptor-2/FLK-1 Involved In Activation Of Phosphatidylinositol 3-Kinase And Cell Proliferation." *J Biol Chem.* 2001. 276: 17686–17692. doi:10.1074/jbc.M009128200

189. Knobbe, C.B., Reifenberger, G., "Genetic Alterations And Aberrant Expression Of Genes Related To The Phosphatidyl-Inositol-3'-Kinase/Protein Kinase B (Akt) Signal Transduction Pathway In Glioblastomas." *Brain pathology*. 2003. pp. 507–518.

190. Hamerlik, P., Lathia, J.D., Rasmussen, R., Wu, Q., Bartkova, J., Lee, M., Moudry, P., Bartek, J. Jr., Fischer, W., Lukas, J., Rich, J.N., Bartek, J., "Autocrine VEGF-VEGFR2-Neuropilin-1 Signaling Promotes Glioma Stem-Like Cell Viability And

Tumor Growth." *Journal of Experimental Medicine.* 2012. pp. 507–520. doi:10.1084/jem.20111424

191. Francescone, R., Scully, S., Bentley, B., Yan, W., Taylor, S.L., Oh, D., "Glioblastoma-Derived Tumor Cells Induce Vasculogenic Mimicry Through Flk-1 Protein Activation." *J Biol Chem.* 2012. 287: 24821–24831. doi:10.1074/jbc.M111.334540

192. Pradet-Balade, B., Boulmé, F., Beug, H., Müllner, E.W., Garcia-Sanz, J.A., "Translation Control: Bridging The Gap Between Genomics And Proteomics?" *Trends in Biochemical Sciences.* 2001. pp. 225–229. doi:10.1016/S0968-0004(00)01776-X

193. Nie, L., Wu, G., Culley, D.E., Scholten, J.C.M,. Zhang, W., "Integrative Analysis of Transcriptomic and Proteomic Data: Challenges, Solutions and Applications." *Critical Reviews in Biotechnology.* 2007. pp. 63–75. doi:10.1080/07388550701334212

194. Nagaraj, N., Wisniewski, J.R., Geiger, T., Cox, J., Kircher, M., Kelso, J., Pääbo, S., Mann, M., "Deep Proteome And Transcriptome Mapping Of A Human Cancer Cell Line." *Molecular Systems Biology.* 2011. doi:10.1038/msb.2011.81

195. Vogel, C., Marcotte, E.M., "Insights Into The Regulation Of Protein Abundance From Proteomic And Transcriptomic Analyses." *Nature Reviews Genetics.* 2012. doi:10.1038/nrg3185

196. Breitbach, C.J., Paterson, J.M., Lemay, C.G., Falls, T.J., McGuire, A., Parato, K.A., Stojdl, D.F., Daneshmand, M., Speth, K., Kirn, D., McCart, J.A., Atkins, H., Bell, J.C., "Targeted Inflammation During Oncolytic Virus Therapy Severely Compromises Tumor Blood Flow." *Mol Ther.* 2007. 15: 1686–1693. doi:10.1038/sj.mt.6300215

197. Breitbach, C.J., Arulanandam, R., De Silva, N., Thorne, S.H., Patt, R., Daneshmand, M., Moon, A., Ilkow, C., Burke, J., Hwang, T.H., Heo, J., Cho, M., Chen, H., Angarita, F.A., Addison, C., McCart, J.A., Bell, J.C., Kirn, D.H., "Oncolytic Vaccinia Virus Disrupts Tumor-Associated Vasculature In Humans." *Cancer Res.* 2013. 73: 1265–1275. doi:10.1158/0008-5472.CAN-12-2687

198. Prestwich, R.J., Harrington, K.J., Pandha, H.S., Vile, R.G., Melcher, A.A., Errington, F., "Oncolytic Viruses: A Novel Form Of Immunotherapy." *Expert Rev Anticancer Ther.* 2008. 8: 1581–1588. doi:10.1586/14737140.8.10.1581

199. Mullen, J.T., Tanabe, K.K., "Viral Oncolysis For Malignant Liver Tumors." *Ann Surg Oncol.* 2003. 10: 596–605. doi:10.1245/ASO.2003.07.020

200. Davison, A.J., Benko, M., Harrach, B., "Genetic Content And Evolution Of Adenoviruses." *Journal of General Virology.* 2003. pp. 2895–2908. doi:10.1099/vir.0.19497-0

201. Russell, W.C., "Adenoviruses: Update On Structure And Function." *J Gen Virol.* 2009. 90: 1–20. doi:10.1099/vir.0.003087-0

202. Chroboczek, J., Bieber, F., Jacrot, B., "The Sequence Of The Genome Of Adenovirus Type 5 And Its Comparison With The Genome Of Adenovirus Type 2." *Virology.* 1992. pp. 280–285. doi:10.1016/0042-6822(92)90082-Z

203. Wirth, T., Ylä-herttuala, S., "Gene Therapy of Glioblastoma Multiforme - Clinical Experience on the Use of Adenoviral Vectors." *Brain Tumors - Current and Emerging Therapeutic Strategies.* 2011.

204. Rowe, W.P., Huebner R.J., Gilmore, L.K., Parrott, R.H., Ward, T.G., "Isolation Of A Cytopathogenic Agent From Human Adenoids Undergoing Spontaneous Degeneration In Tissue Culture." *Proc Soc Exp Biol Med.* 1953. 84: 570–573. doi:10.3181/00379727-84-20714

205. Kunz, A.N., Ottolini, M., "The Role Of Adenovirus In Respiratory Tract Infections." *Curr Infect Dis Rep.* 2010. 12: 81–87. doi:10.1007/s11908-010-0084-5

206. Wickham, T.J., Mathias, P., Cheresh, D.A., Nemerow, G.R., "Integrins Alpha V Beta 3 And Alpha V Beta 5 Promote Adenovirus Internalization But Not Virus Attachment." *Cell.* 1993. 73: 309–319. doi:10.1016/0092-8674(93)90231-E

207. Glasgow, J.N., Everts, M., Curiel, D.T., "Transductional Targeting Of Adenovirus Vectors For Gene Therapy." *Cancer Gene Ther.* 2006. 13: 830–844. doi:10.1038/sj.cgt.7700928

208. Flint, J., Shenk, T., "Adenovirus E1A Protein Paradigm Viral Transactivator." *Annu Rev Genet.* 1989. 23: 141–161. doi:10.1146/annurev.genet.23.1.141

209. Hoeben, R.C., Uil, T.G., "Adenovirus DNA Replication." *Cold Spring Harbor perspectives in biology.* 2013. doi:10.1101/cshperspect.a013003

210. Singh, G., Robinson, C.M., Dehghan, S., Jones, M.S., Dyer, D.W., Seto, D., Chodosh, J., "Homologous Recombination In E3 Genes Of Human Adenovirus Species D." *J Virol.* 2013. 87: 12481–8. doi:10.1128/JVI.01927-13

211. Täuber, B., Dobner, T., "Molecular Regulation And Biological Function Of Adenovirus Early Genes: The E4 Orfs." *Gene.* 2001. 278: 1–23. doi:10.1016/S0378-1119(01)00722-3

212. White, E., "Regulation of Apoptosis by Adenovirus E1A and E1B Oncogenes." *Semin Virol.* 1998. 8: 505–513. doi:10.1006/smvy.1998.0155

213. Ziff, E.B., Evans, R.M., "Coincidence Of The Promoter And Capped 5' Terminus Of RNA From The Adenovirus 2 Major Late Transcription Unit." *Cell.* 1978. 15: 1463–1475. doi:10.1016/0092-8674(78)90070-3

214. Russell, W.C., "Update On Adenovirus And Its Vectors." *Journal of General Virology.* 2000. pp. 2573–2604. doi:10.1099/vir.0.17217-0

215. Wagner, E., Hewlett, M., Bloom, D., Camerini, D., BASIC VIROLOGY. Third edition. 2008.

216. Huebner, R.J., Smith, R.R., Rowe, W.P., Schatten, W.E., Thomas, L.B., "Studies On The Use Of Viruses In The Treatment Of Carcinoma Of The Cervix." *Cancer.* 1956. pp. 1211–1218.

217. Levine, A.J., "p53, The Cellular Gatekeeper For Growth And Division." *Cell.* 1997. pp. 323–331. doi:10.1016/S0092-8674(00)81871-1

218. Everts, B., van der Poel, H.G., "Replication-Selective Oncolytic Viruses In The Treatment Of Cancer." *Cancer Gene Ther.* 2005. 12: 141–161. doi:10.1038/sj.cgt.7700821

219. Zhang, W.W., Fang, X., Branch, C.D., Mazur, W., French, B.A., Roth, J.A., "Generation And Identification Of Recombinant Adenovirus By Liposome-Mediated Transfection And PCR Analysis." *BioTechniques.* 1993.

220. Lang, F.F., Bruner, J.M., Fuller, G.N., Aldape, K., Prados, M.D., Chang, S., Berger, M.S., McDermott, M.W., Kunwar, S.M., Junck, L.R., Chandler, W., Zwiebel, J.A., Kaplan, R.S., Yung, W.K., "Phase I Trial Of Adenovirus-Mediated P53 Gene Therapy For Recurrent Glioma: Biological And Clinical Results." *J Clin Oncol.* 2003. 21: 2508–2518.

221. Bischoff, J.R., Kirn, D.H., Williams, A., Heise, C., Horn, S., Muna, M., Ng, L., Nye, J.A., Sampson-Johannes, A., Fattaey, A., McCormick, F., "An Adenovirus Mutant That Replicates Selectively In P53-Deficient Human Tumor Cells." *Science.* 1996. 274: 373–376. doi:10.1016/S0168-9525(97)90095-0

222. Palmer, D.J., Ng, P., "Helper-Dependent Adenoviral Vectors For Gene Therapy." *Hum Gene Ther.* 2005. 16: 1–16. doi:10.1089/hum.2005.16.1

223. Alba, R., Bosch, A., Chillon, M., "Gutless Adenovirus: Last-Generation Adenovirus For Gene Therapy." *Gene Ther.* 2005. 12 Suppl 1: S18–S27. doi:10.1038/sj.gt.3302612

224. Ginn, S.L., Alexander, I.E., Edelstein, M.L., Abedi, M.R., Wixon, J., "Gene Therapy Clinical Trials Worldwide To 2012 - An Update." *Journal of Gene Medicine.* 2013. pp. 65–77. doi:10.1002/jgm.2698

225. Fueyo, J., Alemany, R., Gomez-Manzano, C., Fuller, G.N., Khan, A., Conrad, C.A., Liu, T.J., Jiang, H., Lemoine, M.G., Suzuki, K., Sawaya, R., Curiel, D.T., Yung, W.K., Lang, F.F., "Preclinical Characterization Of The Antiglioma Activity Of A Tropism-Enhanced Adenovirus Targeted To The Retinoblastoma Pathway." *J Natl Cancer Inst.* 2003. 95: 652–660.

226. Fueyo J, Gomez-Manzano C, Alemany R, Lee PS, McDonnell TJ, Mitlianga P, Shi, Y.X., Levin, V.A., Yung, W.K., Kyritsis, A.P., "A Mutant Oncolytic Adenovirus Targeting The Rb Pathway Produces Anti-Glioma Effect *In Vivo*." *Oncogene.* 2000. 19: 2–12. doi:10.1038/sj.onc.1203251

227. Jiang H, Gomez-Manzano C, Alemany R, Medrano D, Alonso M, Bekele, B.N., Lin, E., Conrad, C.C., Yung, W.K., Fueyo, J., "Comparative Effect Of Oncolytic Adenoviruses With E1A-55 Kda Or E1B-55 Kda Deletions In Malignant Gliomas." *Neoplasia.* 2005. 7: 48–56. doi:10.1593/neo.04391

228. Jiang, H., Gomez-Manzano, C., Aoki, H., Alonso, M.M., Kondo, S., McCormick, F., Xu, J., Kondo, Y., Bekele, B.N., Colman, H., Lang, F.F., Fueyo, J.,

"Examination Of The Therapeutic Potential Of Delta-24-RGD In Brain Tumor Stem Cells: Role Of Autophagic Cell Death." *J Natl Cancer Inst.* 2007. 99: 1410–1414. doi:10.1093/jnci/djm102

229. Lang, F.F., Conrad, C., Gomez-Manzano, C., Frank, T., Yung, W.K.A., Sawaya, R., Weinberg, J., Prabhu, S., Fuller, G., Aldape, K., Fueyo, J., "First-In-Human Phase I Clinical Trial Of Oncolytic Delta-24-Rgd (Dnx-2401) With Biological Endpoints." *Neuro-oncology.* 2014. 16 (suppl 3): iii39.

230. Palmer, G.D., Steinert, A., Pascher, A., Gouze, E., Gouze, J.N., Betz, O., Johnstone, B., Evans, C.H., Ghivizzani, S.C., "Gene-induced chondrogenesis of primary mesenchymal stem cells *in vitro*." *Mol Ther.* 2005. 12: 219–228. doi:10.1016/j.ymthe.2005.03.024

231. Lütschg, V., Boucke, K., Hemmi, S., Greber, U.F., "Chemotactic Antiviral Cytokines Promote Infectious Apical Entry Of Human Adenovirus Into Polarized Epithelial Cells." *Nat Commun.* 2011. 2: 391. doi:10.1038/ncomms1391

232. Leland, D.S., Ginocchio, C.C., "Role Of Cell Culture For Virus Detection In The Age Of Technology." *Clinical Microbiology Reviews.* 2007. pp. 49–78. doi:10.1128/CMR.00002-06

233. Zachos, T., Diggs, A., Weisbrode, S., Bartlett, J., Bertone, A., "Mesenchymal Stem Cell-Mediated Gene Delivery Of Bone Morphogenetic Protein-2 In An Articular Fracture Model." *Mol Ther*. 2007. 15: 1543–1550. doi:10.1038/sj.mt.6300192

234. Sonabend, A.M., Ulasov, I.V., Tyler, M.A., Rivera, A.A., Mathis, J.M., Lesniak, M.S., "Mesenchymal Stem Cells Effectively Deliver An Oncolytic Adenovirus To Intracranial Glioma." *Stem Cells.* 2008. 26: 831–841. doi:10.1634/stemcells.2007-0758

235. de Jonge, J., Berghauser Pont, L.M., Idema, S., Kloezeman, J.J., Noske, D., Dirven, C.M., Lamfers, M.L., "Therapeutic Concentrations Of Anti-Epileptic Drugs Do Not Inhibit The Activity Of The Oncolytic Adenovirus Delta24-RGD In Malignant Glioma." *J Gene Med.* 2013. 15: 134–141. doi:10.1002/jgm.2703

236. Lamfers, M.L.M., Hemminki, A., "Multicellular Tumor Spheroids In Gene Therapy And Oncolytic Virus Therapy." *Curr Opin Mol Ther*. 2004. 6: 403–411.

237. Lamfers, M.L.M., Grill, J, Dirven, C.M.F., Van Beusechem, V.W, Geoerger, B., Van Den, B.J., Alemany, R., Fueyo, J., Curiel, D.T., Vassal, G., Pinedo, H.M., Vandertop, W.P., Gerritsen, W.R., "Potential of the Conditionally Replicative Adenovirus Ad5-Δ24RGD in the Treatment of Malignant Gliomas and Its Enhanced Effect with Radiotherapy." *Cancer Res.* 2002. 62: 5736 – 5742.

238. Lamfers, M.L.M., Idema, S., Bosscher, L., Heukelom, S., Moeniralm, S., van der Meulen-Muileman, I.H., "Differential effects of combined Ad5- delta 24RGD and radiation therapy in *in vitro* versus *in vivo* models of malignant glioma." *Clin Cancer Res.* 2007. 13: 7451–7458. doi:10.1158/1078-0432.CCR-07-1265

239. Sutherland, R.M., "Cell And Environment Interactions In Tumor Microregions: The Multicell Spheroid Model." *Science.* 1988. 240: 177–184. doi:10.1126/science.2451290

240. Grill, J., Lamfers, M.L.M., Van Beusechem, V.W., Dirven, C.M., Pherai, D.S., Kater, G.M., Van der Valk, P., Vogels R., Vandertop W.P., Pinedo, H.M., Curiel, D.T., Gerritsen, W.R., "The Organotypic Multicellular Spheroid Is A Relevant Three-Dimensional Model To Study Adenovirus Replication and Penetration in Human Tumors *in Vitro*." *Molecular Therapy.* 2002. 6: 609 – 614.

241. Edelman, D.B., Keefer, E.W., "A Cultural Renaissance: *In Vitro* Cell Biology Embraces Three-Dimensional Context." *Experimental Neurology.* 2005. pp. 1–6. doi:10.1016/j.expneurol.2004.10.005

242. Thach, D.C., Stenger, D.A., "Effects Of Collagen Matrix On Sindbis Virus Infection Of BHK Cells." *J Virol Methods.* 2003. 109: 153–160. doi:10.1016/S0166-0934(03)00066-1

243. Tran, N.M., Dufresne, M., Duverlie, G., Castelain, S., Défarge, C., Paullier, P., Legallais, C., "An Appropriate Selection of a 3D Alginate Culture Model for Hepatic Huh-7 Cell Line Encapsulation Intended for Viral Studies." *Tissue Engineering Part A.* 2012. p. 121001062427004. doi:10.1089/ten.tea.2012.0139

244. Neumann, A.J,. Schroeder, J., Alini, M., Archer, C.W., Stoddart, M.J., "Enhanced Adenovirus Transduction Of Hmscs Using 3D Hydrogel Cell Carriers." *Mol Biotechnol.* 2013. 53: 207–216. doi:10.1007/s12033-012-9522-y

245. Witlox, A.M., Van Beusechem, V.W., Molenaar, B., Bras, H., Schaap, G.R., Alemany, R., Curiel, D.T., Pinedo, H.M., Wuisman, P.I., Gerritsen, W.R., "Conditionally Replicative Adenovirus with Tropism Expanded towards Integrins Inhibits Osteosarcoma Tumor Growth *in Vitro* and *in Vivo*." *Clin Cancer Res.* 2004. 10: 61–67. doi:10.1158/1078-0432.CCR-0609-03

246. Suzuki, K., Fueyo, J., Krasnykh, V., Reynolds, P.N., Curiel, D.T., Alemany, R.A., "Conditionally Replicative Adenovirus With Enhanced Infectivity Shows Improved Oncolytic Potency." *Clin Cancer Res.* 2001;7: 120–126.

247. Lam, J.T., Hemminki, A., Kanerva, A., Lee, K.B., Blackwell, J.L., Desmond, R., Siegal, G.P., Curiel, D.T., "A Three-Dimensional Assay For Measurement Of Viral-Induced Oncolysis." *Cancer Gene Ther.* 2007. 14: 421–430. doi:10.1038/sj.cgt.7701028

248. Suzuki, K., Fueyo, J., Krasnykh, V., Reynolds, P.N., Curiel, D.T., Alemany, R.A., "Conditionally Replicative Adenovirus with Enhanced Infectivity Shows Improved Oncolytic Potency A Conditionally Replicative Adenovirus with Enhanced Infectivity Shows Improved Oncolytic Potency." *Clin Cancer Res.* 1. 2001. pp. 120–126.

249. Jiang, H., Clise-Dwyer, K., Ruisaard, K.E., Fan, X., Tian, W., Gumin, J., Lamfers, M.L., Kleijn, A., Lang, F.F., Yung, W.K.A., Vence, L.M, Gomez-Manzano, C., Fueyo, J., "Delta-24-RGD Oncolytic Adenovirus Elicits Anti-Glioma Immunity In An Immunocompetent Mouse Model." *PLoS One.* 2014. 9: e97407.

doi:10.1371/journal.pone.0097407

250. Jiang, H., Conrad, C., Fueyo, J., Gomez-Manzano, C., Liu, T-J., "Oncolytic Adenoviruses For Malignant Glioma Therapy." *Front Biosci.* 2003. 8: d577–d588. doi:10.2741/923

251. Ito, H., Aoki, H., Kühnel, F., Kondo, Y., Kubicka, S., Wirth, T., Iwado, E., Iwamaru, A., Fujiwara, K., Hess, K.R., Lang, F.F., Sawaya, R., Kondo, S., "Autophagic Cell Death Of Malignant Glioma Cells Induced By A Conditionally Replicating Adenovirus." *J Natl Cancer Inst.* 2006. 98: 625–636. doi:10.1093/jnci/djj161

252. Jiang, H., White, E.J., Ríos-Vicil, C.I., Xu, J., Gomez-Manzano, C., Fueyo, J., "Human Adenovirus Type 5 Induces Cell Lysis Through Autophagy And Autophagy-Triggered Caspase Activity." *J Virol.* 2011. 85: 4720–9. doi:10.1128/JVI.02032-10

253. Alonso, M.M., Jiang, H., Yokoyama, T., Xu, J., Bekele, N.B., Lang, F.F., Kondo, S., Gomez-Manzano, C., Fueyo, J., "Delta-24-RGD In Combination With RAD001 Induces Enhanced Anti-Glioma Effect Via Autophagic Cell Death." *Mol Ther.* 2008. 16: 487–93. doi:10.1038/sj.mt.6300400

254. Ulasov, I.V., Tyler, M.A., Rivera, A.A., Nettlebeck, D.M., Douglas, J.T., Lesniak, M.S., "Evaluation Of E1A Double Mutant Oncolytic Adenovectors In Anti-Glioma Gene Therapy." *J Med Virol.* 2008. 80: 1595–1603. doi:10.1002/jmv.21264

255. Wohlfahrt, M.E., Beard, B.C., Lieber, A., Kiem, H.P., "A Capsid-Modified, Conditionally Replicating Oncolytic Adenovirus Vector Expressing TRAIL Leads To Enhanced Cancer Cell Killing In Human Glioblastoma Models." *Cancer Res.* 2007. 67: 8783–8790. doi:10.1158/0008-5472.CAN-07-0357